U.PORTO

FEUP FACULDADE DE ENGENHARIA
UNIVERSIDADE DO PORTO

INFLUENCE OF THE FOUNDATION GEOTECHNICAL CHARACTERISTICS ON THE STRUCTURAL BEHAVIOR OF RIGID PAVEMENTS

ISRAEL ENRIQUE PERTUZ RODRÍGUEZ

Dissertação submetida para satisfação parcial dos requisitos do grau de

MESTRE EM ENGENHARIA CIVIL — ESPECIALIZAÇÃO EM GEOTECNIA

Orientador: Professor Doutor Eduardo Fortunato

JUNHO DE 2017

MESTRADO INTEGRADO EM ENGENHARIA CIVIL 2015/2016

DEPARTAMENTO DE ENGENHARIA CIVIL Tel. +351-22-508 1901

Fax +351-22-508 1446

✉ miec@fe.up.pt

Editado por

FACULDADE DE ENGENHARIA DA UNIVERSIDADE DO PORTO

Rua Dr. Roberto Frias 4200-465 PORTO

Portugal

Tel. +351-22-508 1400

Fax +351-22-508 1440

✉ feup@fe.up.pt

http://www.fe.up.pt

Reproduções parciais deste documento serão autorizadas na condição que seja mencionado o Autor e feita referência a *Mestrado Integrado em Engenharia Civil - 2015/2016 - Departamento de Engenharia Civil, Faculdade de Engenharia da Universidade do Porto, Porto, Portugal, 2016*.

As opiniões e informações incluídas neste documento representam unicamente o ponto de vista do respetivo Autor, não podendo o Editor aceitar qualquer responsabilidade legal ou outra em relação a erros ou omissões que possam existir.

Este documento foi produzido a partir de versão eletrónica fornecida pelo respetivo Autor.

To my family

“No llores porque acabó, sonríe porque aconteció”

Gabriel García Márquez

ACKNOWLEDGMENTS

The accomplishment of this thesis was only possible due to the contribution of some people. To all who have accompanied me during the last semester, I express my sincere gratitude. I present my special thanks:

- First of all, to Prof. Dr. Eduardo Fortunato. For the availability and for all the help, providing me with the necessary resources and his knowledge on the topic. Specially for the very quickly reply in the moments I need his advices.
- To the Civil Engineering Department of FEUP, especially to the professors associated to the specialization in geotechnics for the constant support and their incredible talent to engage all students.
- To all the friends who accompanied me over these two years, for all the affection, friendship and motivation. To the friends who I had the opportunity to meet in these five months in Aachen, that were undoubtedly important in this experience;
- To the "GeoGalera", for all the affection, patience and constant support over the last year and for accepted me and integrated me as one of them;
- Finally, I would like to thank to those whom I owe more than I deserve, my family. To my mother, Merce, for being the engine of my life, for her love and affection. To my father, Placido, the best father I could have, for all his support. To my brothers and sisters, for the unconditionally love.

ABSTRACT

Rigid pavements are structure systems consisting of Portland Cement Concrete (PCC) slabs supported on a foundation. Since one of the most key factor affecting the performance of the rigid pavements are the geotechnical characteristics of the foundation, this study focuses on the structural response analysis of rigid pavement, when they are loaded statically, as function of the foundation conditions. The finite element software EverFE is used to carry out the numerical simulation.

A parametric study of the foundation is carried out. The study is divided in three parts, it the first part a sensitive analysis the subgrade k-value on the thickness design is conducted using both the PCA method and the AASHTO method, in the second part a sensitive analysis the compound k-value (depending on the subgrade k-value and the base or stabilized subgrade k-value) on the thickness design is conducted using the AASHTO method. In this section five different type of support (non-stabilized base, cement stabilized subgrade, lime stabilized subgrade, cement treated base, and lean concrete base) are studied. Finally, the third part consists of the numerical simulation of several slab thickness designs discussed in the second part.

The results of the first 2 parts of this study suggest that the k-value has a significant role on the slab thickness design and therefore the geotechnical characteristics of the foundation is also involved in the mechanical response of the rigid pavements. It was found that low elastic modulus values of the base or stabilized subgrade might conduct to failure of the slabs when they are loaded at a critical position in the fatigue analysis. Further research on the characterization of the k-value and its influence on the design and performance of rigid pavement is suggested

KEYWORDS: rigid pavement, geotechnical parameters, slab thickness design, finite element method.

RESUMO

Os pavimentos rígidos são um sistema composto de lajes de betão de Cimento Portland (PCC) suportado sobre uma fundação. Considerando que um dos fatores que afetam o desempenho dos pavimentos rígidos são as características geotécnicas da fundação, o objetivo desta tese é a analise da resposta mecânica do pavimento rígido, quando carregado estaticamente, em função das condições da fundação. O programa de elementos finitos EverFE é usado para realizar a simulação numérica.

Foi realizado um estudo paramétrico relacionado com as características da fundação. Esse estudo foi dividido em três partes. Na primeira parte foi feita uma análise de sensibilidade relativa à influência do valor de k da fundação na determinação da espessura da laje, utilizando tanto o método da "Portland Cement Association" (PCA) como o método da AASHTO. Na segunda parte, é conduzida uma análise de sensibilidade do valor k composto (que depende do valor k da fundação e do valor k da base ou fundação estabilizada) sobre o calculo da espessura com o método da AASHTO, incluindo cinco tipos diferentes de camada de apoio (base não estabilizada, fundação estabilizada com cimento, fundação estabilizada com cal, base tratada com cimento, e base de betão pobre). Finalmente, na terceira parte são simulados alguns dos pavimentos estudados na segunda parte.

Os resultados das duas primeiras partes do estudo sugerem que o valor k tem um papel importante no projeto da espessura da laje e, portanto, as características geotécnicas da fundação também estão envolvidas na resposta mecânica dos pavimentos rígidos. Verificou-se também que um módulo de elasticidade da camada de apoio baixo, poderia conduzir a falha das lajes quando são carregadas numa posição crítica na análise de fadiga. Conclui-se que é necessário desenvolver mais estudos no sentido de caracterizar adequadamente o valor de k em função do tipo de solos e avaliar com maior rigor a sua influência no projeto e desempenho de pavimentos rígidos.

PALAVRAS-CHAVE: pavimentos rígidos, parâmetros geotécnicos, dimensionamento da espessura da laje, método dos elementos finitos.

TABLE OF CONTENTS

ACKNOWLEDGMENTS i
ABSTRACT iii
RESUMO v
1. INTRODUCTION 1
2. STATE OF ART OF RIGID PAVEMENTS 3
2.1. ROMAN ROADS 3
2.2. TELFORD AND MACADAM 4
2.3. EARLY PORTLAND CEMENT CONCRETE PAVEMENTS 5
2.4. PORTLAND CEMENT CONCRETE PAVEMENTS IN THE PRESENT 6
3. CONCEPTION OF REGID PAVEMENT 9
3.1. MATERIALS 9
3.1.1. AGGREGATES 9
3.1.1.1. Physical properties 10
3.1.1.2. Chemical properties 12
3.1.2. PORTLAND CEMENT 12
3.1.2.1. Chemical properties 13
3.1.2.2. Physical properties 14
3.1.3. MIXING AND CURING WATER 16
3.1.3.1. Mixing water 17
3.1.3.2. Curing water 18
3.1.4. ADDITIVES 19
3.1.5. JOINT AND CRACK SEALANT PRODUCTS 21
3.1.5.1. Hot Pour Liquid 22
3.1.5.2. Preformed Compression 22
3.1.5.3. Silicone 22
3.1.5.4. Backer Rods 23
3.2. RIGID PAVEMENT TYPES 23
3.2.1. JOINTED PLANE CONCRETE PAVEMENTS (JPCP) 24
3.2.2. JOINTED REINFORCED CONCRETE PAVEMENT (JRCP) 24
3.2.3. CONTINUOUS REINFORCED CONCRETE PAVEMENTS (CRCP) 24
3.2.4. PRE-STRESSED CONCRETE PAVEMENTS (PCP) 25

3.3. BASE AND SUBBASE 25
3.3.1. DESIGN OF BASE AND SUBBASE FOR RIGID PAVEMENTS 26
3.3.1.1. Non-stabilized base 27
3.3.1.2. Stabilized base 28
3.4. THICKNESS DESIGN 29
3.4.1. GENERAL DESIGN FACTOR 29
3.4.1.1. Traffic and Loading 29
3.4.1.2. Environment 30
3.4.1.3. Design Material parameters 32
3.4.1.4. Failure Criteria 33
3.4.1.5. Reliability 33
3.4.2. PCA DESIGN METHOD 34
3.4.2.1. Design factors 34
3.4.2.2. Design criteria 44
3.4.3. AASHTO DESIGN METHOD 60
3.4.3.1. Design equations 60
3.4.3.2. Design Variables 63
4. INFLUENCE OF THE FOUNDATION ON THE SLAB THICKNESS DESIGN-NUMERICAL SIMULATION 75
4.1. PARAMETRIC STUDY WITH THE PCA AND AASHTO METHOD 75
4.1.1. GENERAL ASPECTS 75
4.1.2. PCA METHOD 76
4.1.3. AASHTO METHOD 80
4.1.4. COMPARISON OF RESULTS OBTAINED WITH PCA- AND AASHTO METHOD 81
4.1.5. INFLUENCE OF THE BASE OR STABILIZED SUBGRADE ON THE AASHTO METHOD THICKNESS DESIGN 82
4.2. EVERFE SOFTWARE 88
4.2.1. BASIC FINITE-ELEMENT DISCRETIZATION 88
4.2.1.1. Model boundary conditions 88
4.2.1.2. Modeling of the slab, base and sub-base layers 89
4.2.1.3. Modeling of the dense liquid foundation 89
4.2.2. SLAB-BASE INTERFACE 89
4.2.3. DOWELS AND TIES MODELLING 90
4.2.4. AGGREGATE INTERLOCK MODELLING 91
4.2.5. AXLE LOADS AND THERMAL EFFECTS 92
4.2.5.1. Axle Loads 92

4.2.5.2. Thermal and Shrinkage Effects 92
4.2.6. SIMULATION OF THE MECHANICAL RESPONSE OF RIGID PAVEMENTS USING EVERFE 93
4.2.6.1. Model 93
4.2.6.2. Visualization of the results 99
4.2.6.3. Analysis of the results 104

5. CONCLUSION AND FURTHER WORK 109

5.1. CONCLUSION 109
5.2. FURTHER WORK 110

BIBLIOGRAPHY 112

ANNEX A 113

A.1. PCA THICKNESS DESIGN 113
A.2. AASHTO THICKNESS DESIGN PARAMETERS 130

ANNEX B 136

B.1. SIMULATION RESULTS 135

LIST OF FIGURES

Figure 2.1 - Illustration of Roman pavement structure near Radstock, England [13] 4

Figure 2.2 - Telford pavement section [13] 4

Figure 2.3 - Macadam pavement section [13].....5

Figure 2.4 Early pavement thickness trends [13].....6

Figure 2.5 PJCP layer configuration [14] 6

Figure 3.1 - Representative Gradation Specifications for Aggregate Courses from the 1996 FHWA (adapted from [13]).....10

Figure 3.2 - Typical shape factors for liquid sealants [23].....21

Figure 3.3 - Type of pavements: 1) jointed plain concrete pavement (JPCP), 2) jointed reinforced concrete pavement (JRCP), 3) continuous reinforced concrete pavement (CRCP), and 4) prestressed concrete pavement (PCP) [15]. 24

Figure 3.4 - Pumping of rigid pavement [15].....26

Figure 3.5 - Wheel configurations for typical semitrailer units (1 ft = 0.305 m) [15].....29

Figure 3.6 - Dimension of tire contact area, a) real contact area, b) equivalent contact area [15] 30

Figure 3.7 - Slab curling and warping, a) downward, b) upward [24].....31

Figure 3.8 - Determination of freezing index [15].....32

Figure 3.9 - Flexural strength, age and design relationships [6] 35

Figure 3.10 - Plate loading test scheme [15].....36

Figure 3.11 - Approximate interrelationships of soil classifications and bearing values (adapted from [6]) 37

Figure 3.12 - Percentage of trucks in right lane of multilane divided highway [6].....41

Figure 3.13 - Critical loading position for fatigue analysis [15].....44

Figure 3.14 - Equivalent edge stress factor depends on the percent of trucks at edge [15] 46

Figure 3.15 - Fatigue analysis-allowable load repetitions based on stress ratio factor (with and without concrete shoulder) [15].....47

Figure 3.16 - Axle-load position for critical pavement deflection [15].....50

Figure 3.17 - Erosion analysis-allowable load repetitions based on erosion factor (without concrete shoulder) [15].....52

Figure 3.18 - Erosion analysis-allowable load repetitions based on erosion factor (with concrete shoulder) [15].....53

Figure 3.19 - Allowable ADTT, Axle-Load Category 2* - Pavements with Doweled Joints [15] 58

Figure 3.20 - Allowable ADTT, Axle-Load Category 2* - Pavements with Aggregate-Interlock Joints [15] 59

Figure 3.21 - Design chart for composite concrete pavement (lean concrete subbase) [15]..... 60

Figure 3.22 - Environmental serviceability loss versus time for a specific location [15]..... 68

Figure 3.23 - Chart for estimating the modulus of subgrade reaction (1in=25.4mm, 1 psi=6.9kPa, 1 pci=271.3kN/m^3) [15] 70

Figure 3.24 - Chart for modifying modulus of subgrade reaction due to rigid foundation near surface (1 ft = 0 .305 m, 1 psi = 6.9 kPa, 1 pci = 271 .3 kN/m3) [15] 71

Figure 3.25 - Correction of effective modulus of subgrade reaction due to loss of foundation support [15] 72

Figure 4.1 – Slab supported directly on the subgrade..... 76

Figure 4.2 - User interface of the AASHTO 93 equation solver [13]. 81

Figure 4.3 - Influence of the subgrade k-value on the thickness design 82

Figure 4.4 - Scheme of the original layer configuration..... 82

Figure 4.5 - Scheme of the simplified layer configuration 83

Figure 4.6 - calculation of the compound k-value (app available on [23])..... 84

Figure 4.7 - Non-stabilized base with shoulder 85

Figure 4.8 - Non-stabilized base without shoulder 85

Figure 4.9 - Cement stabilized subgrade with shoulder 85

Figure 4.10 - Cement stabilized subgrade without shoulder 85

Figure 4.11 - Lime stabilized subgrade with shoulder 86

Figure 4.12 - Lime stabilized subgrade without shoulder 86

Figure 4.13 - Cement treated base with shoulder 86

Figure 4.14 - Cement treated base without shoulder 86

Figure 4.15 - Lean concrete base with shoulder 87

Figure 4.16 - Lean concrete base without shoulder 87

Figure 4.17 - Basic Finite-Element Discretization [25] 88

Figure 4.18 - Modeling Separation and Shear Transfer at the Slab-Base Interface [25] 90

Figure 4.19 - Dowel Element [25] 90

Figure 4.20 - Dowel Modeling [25]..... 91

Figure 4.21 - Geometry panel: k-value = 20MPa/m, with shoulder, 100mm base. 94

Figure 4.22 - Geometry panel: k-value = 20MPa/m, with shoulder, 200mm base. 94

Figure 4.23 - Geometry panel: k-value = 20MPa/m, without shoulder, 100mm base. 95

Figure 4.24 - Geometry panel: k-value = 20MPa/m, without shoulder, 200mm base. 95

Figure 4.25 - Slab, Dowels and Ties material subpanel. 96

Figure 4.26 - Foundation material parameters subpanel. 96

Figure 4.27 - Loading panel 97

Figure 4.28 - Linear model for dowel and aggregate interlock.....98

Figure 4.29 - Meshing: a) geometry discretization with shoulder, b) meshing panel geometry with shoulder, c) geometry discretization without shoulder, d) meshing panel geometry without shoulder. .99

Figure 4.30 - Non-stabilized (100mm, with shoulder) base results data: a) principal stress values per slabs, b) maximum stress value at the slab bottom, c) maximum stress value at the bottom of the base, d) minimum stress value at the bottom of the base, e) dowel maximum shear force, f) deformed slabs. 100

Figure 4.31 - Non-stabilized (200mm, with shoulder) base results data: a) principal stress values per slabs, b) maximum stress value at the slab bottom, c) maximum stress value at the bottom of the base, d) minimum stress value at the bottom of the base, e) dowel maximum shear force, f) deformed slabs. 101

Figure 4.32 - Non-stabilized (100mm, without shoulder) base results data: a) principal stress values per slabs, b) maximum stress value at the slab bottom, c) maximum stress value at the bottom of the base, d) minimum stress value at the bottom of the base, e) dowel maximum shear force, f) deformed slabs. 102

Figure 4.33 - Non-stabilized (200mm, without shoulder) base results data: a) principal stress values per slabs, b) maximum stress value at the slab bottom, c) maximum stress value at the bottom of the base, d) minimum stress value at the bottom of the base, e) dowel maximum shear force, f) deformed slabs. 103

Figure 4.34 - Maximum stress value for 100mm base or stabilized subgrade (with shoulder).....104

Figure 4.35 - Maximum stress value for 200mm base or stabilized subgrade (with shoulder).....105

Figure 4.36 - Maximum stress value for 100mm base or stabilized subgrade (without shoulder).....106

Figure 4.37 - Maximum stress value for 200mm base or stabilized subgrade (without shoulder).....106

LIST OF TABLES

Table 3.1 - Main Constituents in a Typical Portland Cement [13] 13

Table 3.2 - Basic types of Portland cement [13] 14

Table 3.3 - Tolerable Concentrations of Impurities in Concrete Mixing Water [22] 18

Table 3.4 - Gradation requirements for soil-aggregate materials (AASHTO M 147) [1]. 28

Table 3.5 - Effect of Untreated Subbase on k Values [15] 37

Table 3.6 - Design k Values for Cement-Treated Subbase [15] 38

Table 3.7 - Percentages of Four-Tire Single Units and Trucks (ADTT) on Various Highway Systems [6] 40

Table 3.8 - Yearly Rates of Traffic Growth and Corresponding Projection Factors* [15] 42

Table 3.9 – Example of Axle-Load Data [6] 43

Table 3.10 - Equivalent Stress-Concrete Shoulder (Single Axle/Tandem Axle/Tridem Axle) 48

Table 3.11 - Equivalent Stress-Concrete Shoulder (Single Axle/Tandem Axle/Tridem Axle) 48

Table 3.12 - Equivalent Stress-No Concrete Shoulder (Single Axle/Tandem Axle/Tridem Axle) 49

Table 3.13 - Equivalent Stress-No Concrete Shoulder (Single Axle/Tandem Axle/Tridem Axle) 49

Table 3.14 - Erosion Factors-Doweled Joints, Concrete Shoulder (Single Axle/Tandem Axle/Tridem Axle) 54

Table 3.15 - Erosion Factors-Doweled Joints, Concrete Shoulder (Single Axle/Tandem Axle/Tridem Axle) 54

Table 3.16 - Erosion Factors-Doweled Joints, No Concrete Shoulder (Single Axle/Tandem Axle/Tridem Axle) 55

Table 3.17 - Erosion Factors-Doweled Joints, No Concrete Shoulder (Single Axle/Tandem Axle/Tridem Axle) 55

Table 3.18 - Axle-Load Categories [15] 56

Table 3.19 - Subgrade Soil Types and Approximate k Values [15] 57

Table 3.20 - Length of Analysis Period [15] 64

Table 3.21 - Lane Distribution Factor [15] 65

Table 3.22 - Total Growth Factor [15] 66

Table 3.23 - Suggested Levels of Reliability for Various Functional Classifications [15] 67

Table 3.24 - Computation of the effective modulus of subgrade reaction [15]**Erro! Marcador não definido.**

Table 3.25 -Typical Ranges of LS Factors for Several Types of Materials [15] 72

Table 3.26 - Recommended Load Transfer Coefficient for Various Pavement Types and Design Conditions [15] 73

Table 3.27 - Recommended Values of Drainage Coefficients $C\ d$ for Rigid Pavements [15] 74

Table 4.1 - Concrete slab data 75

Table 4.2 – Typical geotechnical values for common types of Soil (NCHRP 1-37A, 2004, adapted from [14]) 76

Table 4.3 – Design data for the AASHTO 80

Table 4.4 – Base and stabilized subgrade data (after AASHTO 93, adapted from [15]) 83

Table 4.5 –Slab thickness design for simulation 93

Table 4.6 - Dowels and ties parameters 98

Table 4.7 - Model discretization 98

LIST OF SYMBOLS

A_C = Tire area of contact (m2)

L = Tire Length (m)

W = Tire Width (m)

MR = Flexural strength modulus (MPa)

$K =$ Constants

$f(c)' =$ Compressive strength (MPa)

$k - value$ = Modulus of subgrade reaction (MPa/m)

P = Pressure on the plate test (N/m2)

$\delta =$ Deflection of plate (mm)

$ESAL$ = Equivalent single axle loads

$(ADT)_0 =$ Average daily traffic at the start of the design period

T = Design period (years

$T_f =$ Number of 80-kN single-axle load applications per truck.

ADTT = Average Daily Truck Traffic

G = Growth Factor (%)

D = Truck Directional Distribution (%)

LSF = Load Safety Factors

$D_r =$ Accumulated damage ratio

N_i = Allowable number of repetitions

p_t = Serviceability at end of time t

$L_1 =$ Load on one single axle or a set of tandem axles (kip)

L_2 = Axle code (1 for single axle, 2 for tandem axle)

$D =$ Slab thickness (inches)

W_{t18} = Number of 18-kip

E_c = Modulus of elasticity of concrete (GPa)

S_c = Modulus of rupture of concre (MPa),

J = Load transfer coefficient

C_d = Drainage coefficient

σ = Maximum tensile stress in concrete (psi)

$Z_R S_o$ = Reliability

M_R = Resilient modulus (psi)

1

INTRODUCTION

During several centuries, pavement engineering has attempted to develop construction techniques, design and analysis methods to improve the mechanical response, durability and functionality of pavements. Rigid pavements, also called cement concrete pavement or simply concrete pavement, are structure systems consisting of Portland Cement Concrete (PCC) slabs supported on a foundation. This foundation can be either selected material layers or, if it has good load bearing capacity, the compacted subgrade [1]. The PCC slabs, as well as the foundation are subjected to stresses induced by external forces, such as traffic loading and environmental conditions, that influence significantly the performance of the structure system. Furthermore, the performance also depends on the characteristics of the slabs and on the foundation and the interaction between them. For a better understanding of the factors affecting the rigid pavements performance numerous studies have been carried out using Finite Element Analysis (FEA) where it is difficult to conduct laboratory and field testing [2].

FEA has been successfully used for many researchers to study the curling stresses [3, 4], slab-foundation interaction [5], load transfer mechanism [6], dowels-slabs interaction [7-10], thermal gradient and shrinkage effects [3, 11, 12], among others. The computational tools based on the finite element method, specifically developed for pavement analysis and design, e.g., ILLI-SLAB, WESLIQID, KENSLAB, are typically two-dimensional representation of the real structure. Nowadays, the new analysis models and the computational facilities improvements permit to develop more powerful and capable three-dimensional (3D) nonlinear dynamic analysis of the pavement structures. Nevertheless, 3D general purpose –and commercial- software, e.g., ABAQUS, ANSYS or DINA3D, demand much computational effort, as well as time for developing a structural model. In the past two decades, the usage of EverFE2 has significantly increased due to its free distribution, user-friendly interface and versatility. Although the studies, using EverFE2, suggest good accordance with experimental studies, further research is needed [7, 8].

EVERFE2 is a 3D finite element software, for Jointed Plain Concrete Pavements (JPCP), developed by professor Bill Davids at the University of Maine. EVERFE2 allows to simulate i) up to nine slab/shoulder units and three elastic base layers, ii) linear and nonlinear aggregates interlock and dowel load transfer, and iv) nonlinear materials. Moreover, recent versions of the program, like EVERFE2.24, include advanced capabilities for modeling tied adjacent slabs and shoulders, nonlinear thermal gradients, and simulation of an extended dowel-slab interaction model and expanded library axle loads, as well as the slab-base interaction [7]. One of the main feature of this program is the capability for

modelling slab-base interaction, which can be analyzed as bounded or unbounded. This interaction impacts significantly the slabs stresses, such as the thermal curling and thermal contraction or expansion that produce additional bending stresses and compressive or tensile stresses, respectively [5].

Rigid pavement design, in addition to the bearing capacity of the PCC slab, relies on the uniformity of support provided by the base layers. This uniformity is mainly altered by three causes: pumping of the fine particles, frost heave and soil expansion [1]. Since one of the most key factors affecting the performance of the rigid pavements are the geotechnical characteristics of the foundation, this study focuses on the structural response of rigid pavement analysis, when they are loaded by vehicles, as function of the foundation conditions. The numerical simulation is carry out with the finite element software EverFE version 2.24.

The remainder part of this study is organized in 5 chapters, as follows:

Chapter 2: the state-of-the-art of rigid pavements. It is presented an introduction of the beginnings and evolution of rigid pavements since the Romans until the modern times.

Chapter 3: conception of rigid pavements. In this chapter are discussed important topics, such as the constituent materials of the slab concrete and sealants, types of rigid pavements, and the base and subbase materials. Finally, details on the design methods PCA and AASHTO as presented.

Chapter 4: influence of the foundation support on the slab thickness design-numerical simulation. The chapter is divided in three parts, in the first part the influence of the reaction subgrade modulus on the slab thickness design is studied using the PCA and AASHTO methods. The second part presents the impact of the base or stabilized subgrade on the slab thickness design using the AASHTO method. In las part, the numerical simulation of several slab thickness is carry out using EverFE.

Chapter 5: conclusions and further works. Conclusions of the analysis of results from the chapter 4 are summarized. Finally, ideas for further research are presented.

2

STATE OF THE ART OF PAVEMENTS

Design, construction and performance of pavement evolution should provide perspective on present and future practice. In this section, an introduction of the past and present of rigid pavement is presented. It will start with the Romans, then the Macadam and Telford. Then the evolution, focused on the U.S.A. and U.K., of the first 150 years of Portland concrete pavement is summarized. Finally, a brief view of the concrete pavement practices around the world is discussed [13].

2.1. ROMAN ROADS

The credits for the construction and maintenance of the first road system are given to the Carthaginians (about 600 B.C.) It is suggested that the Romans took up the practice of a military road system from the Carthaginians after destroying Carthage in 146 B.C. It is estimated that the Romans built about 87,000 km of roads within their empire.

There is no record of traditional roads in the U.K. prior to the Romans. The main Roman roads in the U.K. were for military purpose, i.e., connected camps which were about 30 km apart. These roads were for foot soldiers, the roads were straight, but virtually without regard to grade. They generated high noise levels, were rough and labor intensive (slave and “statue” labor often used).

Figure 2.1 shows the Roman design for their primary U.K. roads generally consisted of four layers [13]:

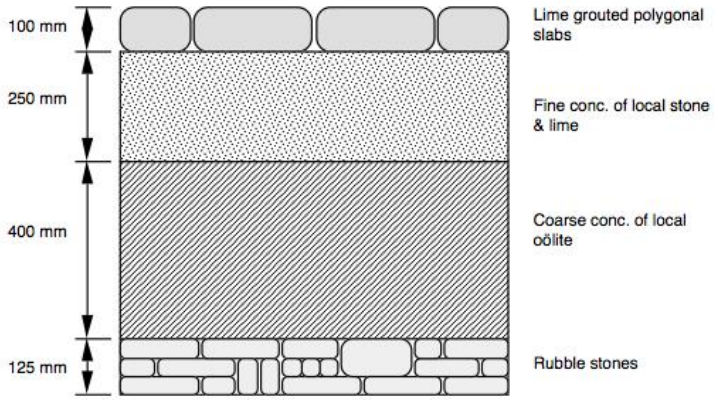

Figure 2.1 - Illustration of Roman pavement structure near Radstock, England [13]

Roman road construction was expensive. Updated construction estimates of the Appian Way in Italy are about $2,000,000 per km [13].

2.2. TELFORD AND MACADAM

2.2.1. TELFORD

Telford attempted, where possible, to build roads on relatively flat grades to reduce the number of horses needed to haul cargo. Further, the pavement section was about 350 to 450 mm in depth and generally specified in three layers. The bottom layer, which makes the Telford design unique, was comprised of 100 mm stones wide and 75 to 180 mm in depth. On top of this were placed two layers of stones of 65 mm maximum size (about 150 to 250 mm total thickness) followed by a wearing course of gravel about 40 mm thick. It was estimated that this system would support a load corresponding to 88 N/mm [13]. Figure 2.2 shows the Telford pavement section.

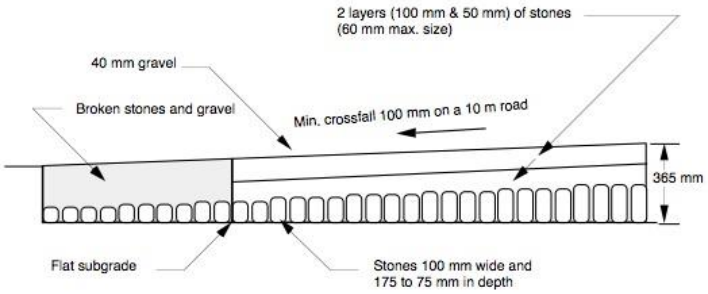

Figure 2.2 - Telford pavement section [13]

2.2.2. MACADAM

Most of the “paved” U.K. roads in early 1800s were composed of rounded gravel. John Macadam used a sloped subgrade surface to improve drainage (unlike Telford who used a flat subgrade surface) on which he placed angular aggregate because he knew angular aggregate over a well-compacted subgrade would perform better. The hand-broken aggregates had a maximum size of 75 mm and they were placed in two layers for a total depth of about 200 mm. On top of this, about 50 mm thick with a maximum aggregate size of 25 mm wearing course was placed. Macadam’s reason for the 25-mm maximum

aggregate size was to provide a "smooth" ride for wagon wheels. Thus, the total depth of a typical Macadam pavement was about 250 mm. Figure 2.3 shows the Macadam pavement section [13].

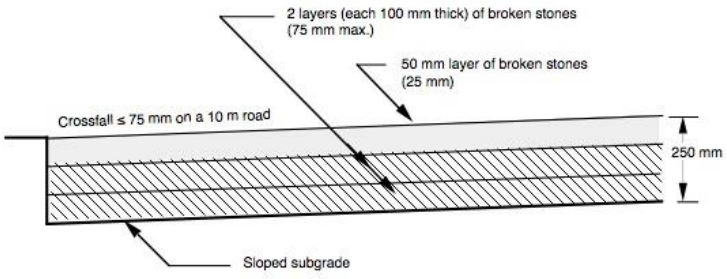

Figure 2.3 - Macadam pavement section [13]

The term "macadam" is also used to indicate "broken stone" pavement. Macadam realized that the layers of broken stone would eventually become "bound" together by fines generated by traffic. With the introduction of the rock crusher, large mounds of stone dust and screenings were generated. This resulted in use of such fines resulting in the more traditional dense graded base materials which in turn produced pavement thicknesses as thin as 100 to 150 mm [13].

By 1850, about 2,200 km of macadam type pavements were in use in the urban areas of the UK. The first macadam pavement in the U.S. was constructed in Maryland in 1823 [13].

2.3. Early Portland Cement Concrete Pavements

Portland cement concrete (PCC) was not used as a pavement wearing course until after about 1910, but it was regularly used as a stiff base to support other wearing courses such as wooden bricks, cobble stones, etc. [13].

PCC was first used as a base for other wearing courses in London in 1872 and in New York in 1888 (base for stone surfacing). According to Collins and Hart (1936), the first use of PCC as a wearing course was in Edinburgh, U.K., in 1872 and Grenoble, France, in 1876; however, one source stated that the first PCC pavement was placed in Inverness, Scotland, in 1865. The first PCC pavement in the U.S. was constructed in 1891 in Bellefontaine, Ohio. This pavement was only 3.0 m wide and 67.1 m long. In 1909, in Wayne County, Michigan, a PCC highway system was constructed [13].

By the 1930s, several PCC pavement design features began to evolve. The first evolution was the reduction of the slab thickness. The typical slab thicknesses were about 200 mm with several states using a thickened edge design (maximum of about 225 mm). The second improvement was the joints design. It became clear that longitudinal joints should be used every 3.0 to 3.7 m and transverse contraction joints the same for a better control of cracks [13].

Pavement structures decrease from about 0.9 m for Roman designs to 350 to 450 mm for Telford designs, to about 250 mm for Macadam designs, to 100 mm at about the turn of the century, as Figure 2.4 shows. Naturally, the thinnest pavements were not always used [13]. The reduction of the slab thickness was possible due to the a better understanding of the material and pavement structures behavior.

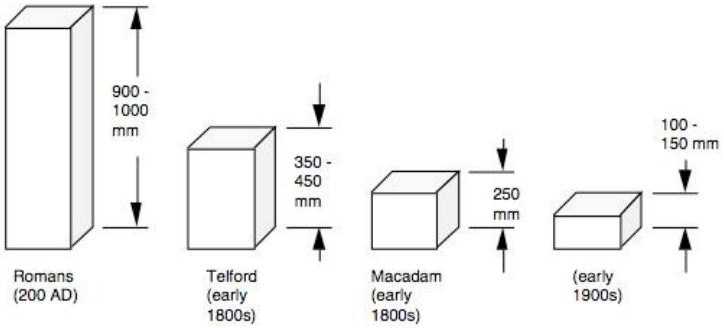

Figure 2.4 - Early pavement thickness trends [13]

Up to the early 1900s, the design emphasis was placed on the use of fixed standards occasionally modified for local soil conditions. Further, the need for more durable pavements was mandated by the changing vehicle fleet [13].

2.4. Portland Cement Concrete Pavements In The Present

In the present, the pavement structure has, basically, three components. A slab manufactured with PCC, which is supported by the foundation consisting of a base and occasionally a subbase, and a prepared subgrade. See Figure 2.5.

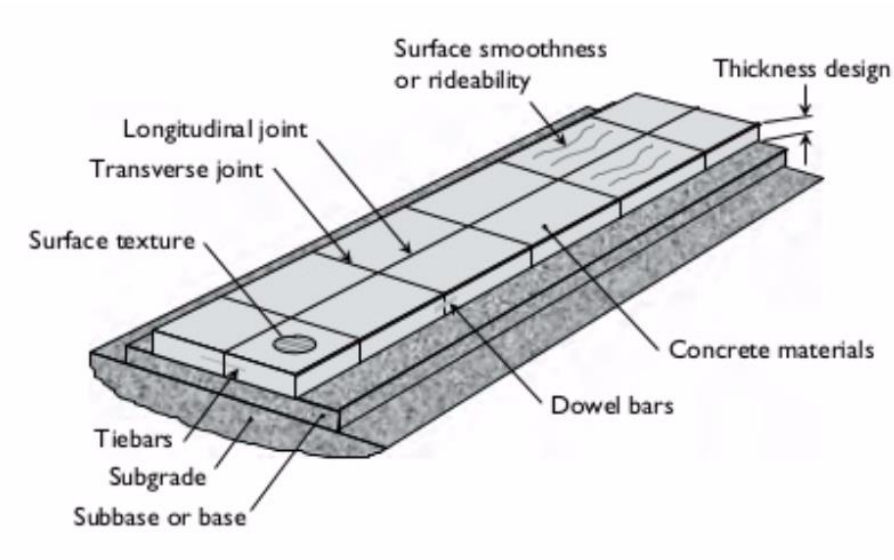

Figure 2.5 - JPCP layer configuration [14]

The pavement design of the slab concrete focuses on the estimation of the thickness requirements. The properties of the concrete and foundation layers, as well as external factors such as traffic loads and climate, are the input data in the design method. Details on material properties, rigid pavement types, foundation configuration, and thickness design are discussed in the next chapter.

A brief introduction of the design methods used in different continents is presented as follows.

2.4.1. NORTH AMERICA

There are several types of models and methods used for the design of rigid pavements in the United States. Nowadays, the AASHTO Method, which is based on the empirical equations obtained from the AASHO Road Test with further modifications based on theory and experience, is the most used method. A survey conducted in 1994 and 1995 showed that most state highway agencies used some version of the AASHTO pavement design procedures for rigid pavements. About 84% used either the 1972 or 1986/1993 AASHTO design procedures for rigid pavement design, about 4% used the PCA method, and the remaining 12% used their own design procedures [15]. In Canada, the PCA method is recommended and widely used.

As far as the author knows, there is not an official survey in the last decade. However, considering the information available on the homepage of the departments of transportation (DOTs) of several states, the percentages presented above remain. The material specifications are presented in the AASHTO and ASTM standards. Details on the PCA and AASHTO methods are discussed in Section 3.4.2. and Section 3.4.3., respectively.

In the last decade, AASHTO released a new version of the AASHTO pavement design procedures for rigid pavements, but it has not been widely implemented.

2.4.2. SOUTH AMERICA

Rigid pavements arrived at Latin America in the 1920s, after sixty years of the first rigid pavement. The pavement technology was at an intermediate state, it was not as advanced as current pavement design and construction process, but it was better than the first pavements designs. When the rigid pavements arrived at Latin America, there was already concrete production equipment, paver equipment and surface finishing techniques [16].

After 150 years, rigid pavements became durable, comfortable, economic and environmental friendly. The type of pavement most used are Jointed Plane Concrete Pavement (JPCP) and Jointed Reinforced Concrete Pavement (JRCP). The design and performance analysis methods most used are the PCA 84 and AASHTO method. Many of the department of transportation do not specify a design method, thus the design method became an extra variable [16].

The material specifications are based on the AASHTO and ASTM standards, but each country has a national guide that adjust the standards to the local materials and scenarios.

2.4.3. EUROPE

In several European countries such as Portugal and Spain, flexible pavements are more widely used as compared to rigid pavements. Most of the structure are selected from a catalog created by each transportation agency. As far as the author knows, there is not any European Standard (EN) for the design and performance analysis of rigid pavement. However, in the last decade it was created the European Concrete Paving Association (EUPAVE) with the objective of promoting cement and concrete application in transport infrastructure [17].

In 1991, the TC 227 was created by CEN (the European Standardization Committee) to prepare standards on road materials. Due to the great diversity of materials for pavements, five Working Groups were created inside TC 227 [18]:

- WG1: Bituminous materials,
- WG2: Surface dressings and slurry surfacing,
- WG3: Materials for concrete roads, including joint fillers and sealants,
- WG4: Hydraulic bound mixtures and unbound mixtures including byproducts and waste materials,
- WG5: Surface characteristics.

To prepare the relevant standards, the following Task Groups were created:

- TG1: Functional and performance requirements Convener,
- TG2: Materials for concrete pavements excluding joint fillers and sealants Convener,
- TG3: Joint fillers and sealants", divided into three Subtask Groups:
  1. TG3A: Hot applied joint sealants Convener,
  2. TG3B: Cold applied sealants Convener,
  3. TG3C: Preformed joint seals Convener.

Concerning the specifications for concrete pavements, they have been divided into three parts:

1. Specifications for concrete and its constituents and other products used for concrete roads,
2. Functional requirements for the constructed pavement,
3. Specifications for dowels.

Details on the task of each subgroup can be found on the paper published by C. Jofré [18].

2.4.4. AUSTRALIA

In 2004, Austroads released a revision of the 1992 Guide for concrete pavement design based on the PCA method. The Guide provides a mechanistic procedure for calculating the required concrete slab thickness for JPCP, JRCP, Continuous Reinforced Concrete Pavement (CRCP) and Steel Fiber Concrete Pavement (SRCP).

The method considers a variety of inputs such as design traffic, subgrade CBR, base thickness and type, project design reliability, concrete flexural strength, axle group distribution and provision of dowels and shoulders. The thickness calculated with this method is based on the cumulative damage due to fatigue of the concrete slab and erosion of subbase and subgrade materials [19].

Since the Austroads Guide for concrete pavement design is based on the PCA method, specific information will be omitted in this document. Details on the Austroads Guide for concrete pavement design can be found in the *Organisation of Australasian road transport and traffic agencies* homepage [20].

3

CONCEPTION AND DESIGN OF RIGID PAVEMENTS

There are three main groups of pavement typologies: flexible, rigid and semi-rigid pavements. The decision of which type of pavement fulfill better the requirements is made according to many factors, basically technical and economic factors. There are certain conditions that suggest the usage of a specific type of pavement. In the case of rigid pavements, the traffic, the materials, the constructive method, the foundation, and the thickness, among others, are critical issues to consider.

In this chapter, a brief introduction of the rigid pavement conception is presented. The material specifications for the slabs and foundation layers, the type of rigid pavement and joins, the type of base, are discussed. Examples of thickness design are presented at the end of the chapter.

3.1. MATERIALS

The pavement system consists of layer constituted by material with certain specifications. These specifications vary significantly according with the geotechnical characteristics of the subgrade, environmental conditions of the region, the period of design, and the stress state due to the traffic load. In this section, the materials used to construct the surface slab are discussed. The materials specifications for dowel and ties, and foundation are presented in the two subsequent sections.

3.1.1. AGGREGATES

Aggregates are mineral materials such as sand, gravel, and crushed stone used with asphalt or hydraulic cement to form asphalt concrete or Portland cement concrete, respectively. In the last decades, the recycling of old concrete allows to use crushed concrete particle as part of the aggregate amount in new pavements. The percentage of aggregates, by volume, of cement concrete is about 80%. Aggregates are also used for base and subbase layers for pavements typologies.

The aggregates used in the hydraulic concrete manufacturing have specific characteristics. The aggregates, for the concrete pavement, should have higher tensile strength, lower volumetric changes, low cracking susceptibility, fatigue resistance and durability. The main aspects to be considered in the aggregate test characterization are described below [13, 21].

3.1.1.1. Physical properties

Aggregate physical properties are very important in the production of PCC, and even as base or subbase material, because they affect directly the aggregate performance. In this study only two American standard test procedures, the American Society for Testing and Materials (ASTM) and the American Association of State Highway and Transportation Officials (AASHTO), are referenced. The most common measured physical properties are [13]:

a) Gradation and Size

Gradation is an important concern in PCC mix design and most agencies specify allowable aggregate gradations. Gradation helps to determine durability, porosity, workability, cement and water content, strength, and shrinkage. Size is also very important because large maximum sizes may not fit between reinforcement bar openings. Because the lower water-cement ratio of the large maximum size, the PCC strength generally increases (ASTM C 125). Figure 3.1 shows some Representative Gradation Specifications for Aggregate Courses from the 1996 FHWA Standard Specifications for Construction of Roads and Bridges on Federal Highway Projects (FP-96).

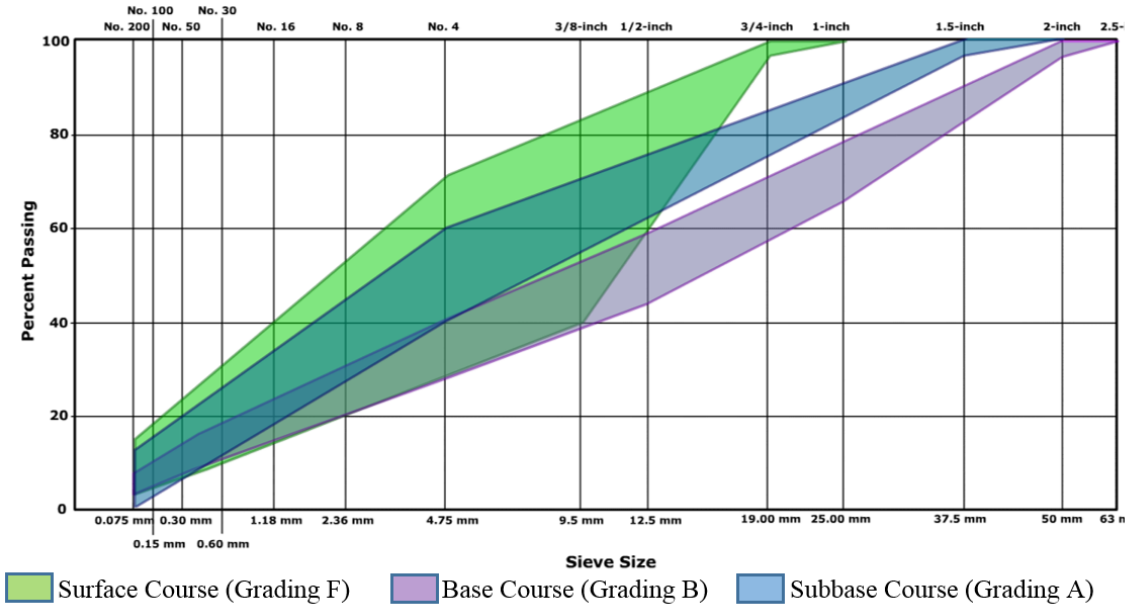

Figure 3.1 - Representative Gradation Specifications for Aggregate Courses from the 1996 FHWA (adapted from [13])

b) Toughness and Abrasion Resistance

Aggregates should be hard enough to resist crushing, degradation and disintegration from manufacturing, stockpiling, production, placing, and compaction. They must be able to transmit loads from the exterior to the underlying layers. Aggregates can cause structural failure and loss of skid resistance if they are not resistant to abrasion and polishing. The standard Los Angeles abrasion test is [13]:

- AASHTO T 96 or ASTM C 131: Resistance to Degradation of Small-Size Coarse Aggregate by Abrasion and Impact in the Los Angeles Machine

c) Durability and Soundness

The terms given to the weathering resistance characteristics of aggregates are durability and soundness. To avoid premature pavement distresses, aggregates must be resistant to breakdown and disintegration from wetting/drying and freezing/thawing cycles. The soundness test determines a resistance to disintegration of aggregates. Standard test procedures [13]:

- AASHTO T 104 and ASTM C 88: Soundness of Aggregate by Use of Sodium Sulfate or Magnesium Sulfate.

d) Particle Shape and Surface Texture

For proper compaction, deformation resistance, and workability, aggregate particle shape and surface should be studied. Since aggregates in PCC are used as a less expensive high-strength material to occupy volume, workability is the major issue regarding particle shape. Rounded particles are desirable for PCC because of their better workability (although particle smoothness will not appreciably affect strength) [6]. Rough-surfaced particles provide more area to which the cement paste can bond. The most popular tests used to identify and quantify aggregate particle shape and surface texture are [13]:

- Particle index (ASTM D 3398: Index of Aggregate Particle Shape and Texture),
- Percent fractured face (or coarse aggregate angularity) (AASHTO TP 61: Determining the Percentage of Fracture in Coarse Aggregate; ASTM D 5821: Determining the Percentage of Fractured Particles in Coarse Aggregate),
- Fine aggregate angularity (AASHTO T 304 or ASTM C 1252: Uncompact Void Content of Fine Aggregate), and
- Flat and elongated particles (ASTM D 4791: Flat Particles, Elongated Particles, or Flat and Elongated Particles in Coarse Aggregates)

e) Specific gravity and absorption

Specific gravity is a measure of a material's density as compared to the density of water at 23°C. Therefore, by definition, water at a temperature of 23°C has a specific gravity of 1. Absorption is a measure of the amount of water that an aggregate can absorb into its pore structure. Both measurements, specific gravity and absorption, are determined in the same test. The standard fine and course aggregate specific gravity and absorption test are [13]:

- AASHTO T 84 and ASTM C 128: Specific Gravity and Absorption of Fine Aggregate
- AASHTO T 85 and ASTM C 127: Specific Gravity and Absorption of Coarse Aggregate

f) Cleanliness and Deleterious Materials

The presence of vegetation, clay lumps, excess dust, and soft particles must be removed, or limited to low quantities, from the aggregates because they can cause a loss of structural support or prevents binder-aggregate bonding. Standard test procedures [13]:

- AASHTO T 112 and ASTM C 142: Clay Lumps and Friable Particles in Aggregate.

g) Moisture Content

Aggregates moisture content affects the water content of the manufactured PCC, and consequently the water-cement ratio, because aggregates are generally not dried before the production. The water content also affects aggregate proportioning because it contributes to aggregate weight. Typical moisture tests are [13]:

- ASTM C 70: Surface Moisture in Fine Aggregate
- AASHTO T 85 and ASTM C 127: Specific Gravity and Absorption of Coarse Aggregate
- AASHTO T 84 and ASTM C 128: Specific Gravity and Absorption of Fine Aggregate
- AASHTO T 255: Total Evaporable Moisture Content of Aggregate by Drying
- ASTM C 566: Total Moisture Content of Aggregate by Drying.

3.1.1.2. Chemical properties

The aggregate expansion, caused by the reaction of reactive silica in the aggregates with cement paste alkalis, can cause cracking, surface pop-outs and spalling. Therefore, chemical properties are commonly measured.

The typical chemical properties that are measured for aggregates is the Alkali-Aggregate Reaction. It is the expansion reaction in the PCC between the alkali contained in the cement paste and elements within an aggregate. Alkali-silica is the most common reaction, which occurs in most PCC. It can result in map or pattern cracking, surface pop-outs and spalling if it is severe enough.

These are not the only chemical and physical properties of aggregates but rather the most commonly measured. Tests used to quantify these properties are largely empirical [13].

3.1.2. Portland Cement

Portland cement is the binding agent in the Portland cement concrete (PCC). It is a hydraulic cement that hardens into a solid mass when mixed with water. As a construction material, it has been used for over 175 years and its behavior is empirically well understood. However, chemically, Portland cement is a complex substance whose mechanisms and interactions have yet to be fully defined. The definition provided by ASTM C 125 and the Portland Cement Association (PCA) is the following [13]:

- Hydraulic cement: An inorganic material or a mixture of inorganic materials that sets and develops strength by chemical reaction with water by formation of hydrates.
- Portland cement: A hydraulic cement composed primarily of hydraulic calcium silicates.

Nowadays, Portland cement is the most used construction material in the world with about 1.72 billion tons produced per year. The largest sole use of Portland cement and PCC in the United states is the construction of rigid pavements [13].

A brief description of the Portland cement properties, taken from [13], is presented.

3.1.2.1. Chemical properties

Chemical properties of Portland cement determine its physical properties and how it cures. For a better understanding of how and why Portland cement behaves as it does, a basic knowledge of Portland cement chemistry is important. In this section, it is briefly described the basic chemical composition of a typical Portland cement and how it hydrates.

a) Basic Composition

Table 3.1 shows the main chemical compound constituents of Portland cement.

Table 3.1 - Main Constituents in a Typical Portland Cement [13]

Chemical Name	Chemical Formula	Shorthand Notation	Percent by Weight
Tricalcium Silicate	$3CaO \times SiO_2$	C_3S	50
Dicalcium Silicate	$2CaO \times SiO_2$	C_2S	25
Tricalcium Aluminate	$3CaO \times Al_2O_3$	C_3A	12
Tetracalcium Aluminoferrite	$4CaO \times Al_2O_3 \times Fe_2O_3$	C_4AF	8
Gypsum	$CaSO_4 \times H_2O$	CSH_2	3.5
Others			1.5

b) Hydration

The chemical compound constituents of Portland cement undergo a series of chemical reaction, when mixed with water, which cause its hardening. The chemical reactions with water, which occur at different time and rate, are called hydration. The results of these reactions determine how Portland cement hardens and gains strength.

- Tricalcium silicate (C_3S): hydrates and hardens rapidly and is largely responsible for initial set and early strength. Portland cements with higher percentages of C3S will exhibit higher early strength.
- Dicalcium silicate (C_2S): hydrates and hardens slowly and is largely responsible for strength increases beyond one week.
- Tricalcium aluminate (C_3A): hydrates and hardens the quickest. Liberates a large amount of heat almost immediately and contributes somewhat to early strength. Gypsum is added to Portland cement to retard C_3A hydration. Without gypsum, C_3A hydration would cause Portland cement to set almost immediately after adding water.
- Tetracalcium aluminoferrite (C_4AF). Hydrates rapidly but contributes very little to strength. Its use allows lower kiln temperatures in Portland cement manufacturing.

c) Types of Portland Cement in USA

In the U.S., AASHTO M 85 and ASTM C 150, Standard Specification for Portland cement, recognize eight basic types of Portland cement. However, other types of Portland cement can be manufactured

adjusting the amount of the constituent chemical compounds. The basic types of Portland cement are presented in the table below.

Table 3.2 - Basic types of Portland cement [13]

Type	Name	Purpose
I	Normal	General-purpose cement suitable for most purposes.
IA	Normal-Air Entraining	An air-entraining modification of Type I.
II	Moderate Sulfate Resistance	Used as a precaution against moderate sulfate attack. It will usually generate less heat at a slower rate than Type I cement.
IIA	Moderate Sulfate Resistance- Air Entraining	An air-entraining modification of Type II.
III	High Early Strength	Used when high early strength is needed. It has more C3S than Type I cement and has been ground finer to provide a higher surface-to-volume ratio, both of which speed hydration. Strength gain is double that of Type I cement in the first 24 hours.
IIIA	High Early Strength- Air Entraining	An air-entraining modification of Type III.
IV	Low Heat of Hydration	Used when hydration heat must be minimized in large volume applications such as gravity dams. Contains about half the C3S and C3A and double the C2S of Type I cement.
V	High Sulfate Resistance	Used as a precaution against severe sulfate action – principally where soils or groundwater have a high sulfate content. It gains strength at a slower rate than Type I cement. High sulfate resistance is attributable to low C3A content.

3.1.2.2. Physical properties

For quality control purposes, Portland cements are commonly characterized by their physical properties. This section lists the more common U.S. Portland cement physical properties that are tested. Specification values, where given, are taken from ASTM C 150, *Standard Specification for Portland Cement*.

These properties only include Portland cement and water (neat cement pastes). Neat cement pastes are typically difficult to handle and test and thus they introduce more variability into the results. Cements may also perform differently when used in a mixture of cement, water and sand (mortar). However, if the sand is not carefully specified in a mortar test, the results may not be transferable.

a) Fineness

Particle size of Portland cement affects hydration rate and thus the rate of strength gain. The smaller the particle size, the greater the surface area-to-volume ratio, and thus, the more area available for water-

cement interaction per unit volume. The effects of greater fineness on strength are generally seen during the first seven days [13].

The following standard test methods are used to determine the Portland cement fineness:

- AASHTO T 98 and ASTM C 115: Fineness of Portland Cement by the Turbidimeter,
- AASHTO T 128 and ASTM C 184: Fineness of Hydraulic Cement by the 150-mm (No. 100) and 75-mm (No. 200) Sieves,
- AASHTO T 153 and ASTM C 204: Fineness of Hydraulic Cement by Air Permeability Apparatus,
- AASHTO T 192 and ASTM C 430: Fineness of Hydraulic Cement by the 45-mm (No. 325) Sieve.

b) Soundness

In this context, soundness refers to the ability to retain its volume after setting without delayed destructive expansion when the cement paste is hardened. Free lime (CaO) or magnesia (MgO) cause this destructive expansion. For this reason, most specification limit magnesia content and expansion. The typical expansion test places a small sample of cement paste into a high-pressure steam vessel (autoclave).

The autoclave is slowly brought to 2.03 MPa, then kept at that pressure for 3 hours. The change in specimen length due to its time in the autoclave is measured and reported as a percentage. ASTM C 150, Standard Specification for Portland cement specifies a maximum autoclave expansion of 0.80 percent for all Portland cement types. Standard Test Methods:

- AASHTO T 107 and ASTM C 151: Autoclave Expansion of Portland Cement

c) Setting Time

Several factors, such as cement fineness, water-cement ratio, chemical content, affect the cement paste setting time. For construction purposes, the initial set must not be too soon and the final set must not be too late. Additionally, setting times can give some indication of if a cement is undergoing normal hydration. Normally, two setting times are defined:

- Initial set: occurs when the paste begins to stiffen considerably.
- Final set: occurs when the cement has hardened to the point at which it can sustain some load.

These times are arbitrary points used to characterize cement and they are not tied to the setting time of concrete. The following tests are used to characterize the cement setting time:

- AASHTO T 131 and ASTM C 191: Time of Setting of Hydraulic Cement by Vicat Needle,
- AASHTO T 154: Time of Setting of Hydraulic Cement by Gillmore Needles,
- ASTM C 266: Time of Setting of Hydraulic-Cement Paste by Gillmore Needles.
-

d) Strength

Cement paste strength is defined in three ways, compressive, tensile, and flexural. These strengths are affected by factors such as water-cement ratio, cement-fine aggregate ratio, type and grading of fine aggregate, manner of mixing and molding specimens, curing conditions, size and shape of specimen, moisture content at time of test, loading conditions and age. Typically, times are 1 day, 3 days, 7 days, 28 days and 90 days. It is important to keep in mind that cement mortar strength is not directly related to concrete strength. But it is typically used as a quality control measure. Strength tests are done on cement mortars and not on cement pastes.

The following are the standard test methods used to characterize the cement paste strength:

- Portland Cement Compressive Strength
  - AASHTO T 106 and ASTM C 109: Compressive Strength of Hydraulic Cement Mortars (Using 50-mm or 2-in. Cube Specimens),
  - ASTM C 349: Compressive Strength of Hydraulic Cement Mortars (Using Portions of Prisms Broken in Flexure).
- Portland Cement Tensile Strength
  - AASHTO T 198 and ASTM C 496: Splitting Tensile Strength of Cylindrical Concrete Specimens
- Portland Cement Flexural Strength
  - AASHTO T 97 and ASTM C 78: Flexural Strength of Concrete (Using Simple Beam with Third-Point Loading)
  - AASHTO T 177 and ASTM C 293: Flexural Strength of Concrete (Using Simple Beam with Center-Point Loading)

e) Specific Gravity

Specific gravity is used in mixture proportioning calculations. The specific gravity of Portland cement is generally around 3.15 and Portland-pozzolan cements may have specific gravities near 2.90. Standard Test Methods:

- AASHTO T 133 and ASTM C 188: Density of Hydraulic Cement.

f) Heat of Hydration

When the Portland cement and the water react, it is generated a heat called heat of hydration. In massive concrete structures such as gravity dams, hydration heat is produced faster than it can be dissipated, it may cause undesirable stresses as the concrete cools to ambient temperature. Standard Test Methods:

- ASTM C 186: Heat of Hydration of Hydraulic Cement

3.1.3. Mixing and curing Water

Mixing and curing water can be from various sources, but it should be free of substances that affect negatively the setting process of the concrete. Guidance on mixing water quality is available using

AASTHO Designation T26 and ASTM C 94, Specification C 1602/C 1602M is cited for water requirements.

In this section, some mixing and curing water specifications are presented [22].

3.1.3.1. Mixing water

The water quality, when it is questionable, can be clarified by comparing compressive strength and times of setting of specimens made with water in question and with distilled or 100% potable water used as reference. ASTM C 1602/C 1602M requires compressive strength to be minimum of 90% of the specimen made with the reference water. And the time of setting in the test mortar should not be more than one hour quicker nor more than one and a half hour slower than the setting when distilled or 100% potable water is used.

The same process of validation of the quality of water applies to the use of groundwater and wash water from the mixer washout operations for mixing water. Groundwater should be carefully used because of the solids in the water. The density of the water is used as an indicator.

a) Effects of Impurities in Mixing Water

This subject has been extensively studied. Some of the more significant conclusion based on the study conducted by Abrams, with over 6000 mortar and concrete specimens representing 68 water samples, are as follows [22]:

- The time of setting of Portland cement mixtures containing impure mixing waters were about the same as those observed with the use of clean fresh waters with only a few exceptions.
- None of the waters caused unsoundness of the neat Portland cement pat when tested over boiling water.
- Most of the samples gave satisfactory results in concrete because the quantities of injurious impurities were quite small.
- The quality of mixing water is best measured by the ratio of 28-day concrete or mortar strength to that of similar mixtures made with pure water.
- Neither odor nor color is an indication of quality of water for mixing concrete.
- The next samples were found to be unsuitable for mixing concrete because they presented a strength ratio of 85% as compared to that observed with pure water: acid water, discharge from galvanizing plants, water containing over 3% of sodium chloride or 3.5% of sulfates, and water containing sugar or similar compounds.
- Based on the minimum strength ratio of 85%, the following waters were found to be suitable for mixing concrete: bog and marsh water, water with a maximum concentration of 1% SO_4, seawater (not for reinforcement concrete), alkali water with a maximum of 0.15% Na_2SO_4 or NaCl, water from coal and gypsum mines, and wastewater from breweries, gas plants, and paint and soap factories.

Table 3.3 shows the tolerable concentrations of impurities, including the limit for suspended particles, in concrete mixing water according with the requirement of the U.S.

Table 3.3 - Tolerable Concentrations of Impurities in Concrete Mixing Water [22]

impurity	Maximum tolerable Concentration
Sodium and potassium carbonates and bicarbonates	1000 ppm
Sodium chloride	20000 ppm
Sodium sulfate	10000 ppm
Calcium and magnesium bicarbonates	400 ppm of bicarbonate ion
Calcium chloride	2% by mass, of cement in plain concrete
Iron salts	40000 ppm
Sodium iodate, phosphate, arsenate, and borate	500 ppm
Sodium sulfide	100 ppm
Hydrochloric and sulfuric acids	10000 ppm
Sodium hydroxide	0.5 % by mass of cement if set not affected
Salt and suspended particles	2000 ppm

b) Use of Seawater in Mixing Concrete

There are several studies that support the use of seawater. Abram study states that seawater with maximum concentration salts on the order of 3.5% does not appreciable reduce the strength of concrete, although it may lead to corrosion of reinforcement. There are other references in the literature that indicate that salt water has been used in mixing plain concrete without incurring in trouble at later periods.

Extreme caution is urged when mixing water for reinforced concrete is selected. If water contains salts, the residual salts in the concrete when combined with air and moisture will result in some corrosion.

3.1.3.2. Curing water

The suitability of water for curing concrete is defined by two aspects: the first one is the possibility it would cause staining because of the impurities. The second one is that it might contain aggressive impurities that would can attack or causing deterioration of the concrete, but it is unlikely.

The most common cause of staining is usually a relatively high concentration of iron or organic matter in the water. However, low concentration of these impurities, especially if concrete is subjected to prolonged wetting by runoff of curing water from other portions of the structure, may cause staining.

The Corps of Engineer´s Standard Practice for Concrete gives a test procedure, such as Designation CRD-C 401 to conduct performance- type test, to evaluate the organic impurities effect on the concrete. The Corps of Engineer´s Standard Practice for Concrete states that there must be no permanent staining of surface where appearance is important [13].

3.1.4. ADDITIVES

Additives, also called admixtures, are ingredients added to alter a specific PCC property such as workability, setting time, strength or durability. They are usually classified according to the desired effect they have on the concrete. A general list of the most commonly used additives is presented as follows [13].

a) Accelerators

Effect: accelerate setting and early strength development.

Material: calcium chloride, triethanolamine, sodium thiocyanate, calcium formate, calcium nitrite, calcium nitrate.

b) Air detainers

Effect: decrease air content

Material: tributyl phosphate, dibutyl phthalate, octyl alcohol, water-insoluble esters of carbonic and boic acid, silicones.

c) Air-entraining

Effect: improve durability in environments of freeze-thaw, deicers, sulfate and alkali reactivity and improve workability.

Material: salts of wood resins, lignin, petroleum acids, proteinaceous material or sulfonated hydrocarbons; some synthetic detergents; Fatty and resinous acids and their salts; Alkylbenzene sulfonates.

d) Alkali-reactivity reducers

Effect: reduce alkali-reactivity expansion

Material: pozzolans, blast-furnace slag, salts of lithium and barium, air-entraining agents.

e) Bonding

Effect: increase bond strength

Material: rubber, polyvinyl chloride, polyvinyl acetate, acrylics, butadiene styrene copolymers.

f) Corrosion inhibitors

*Effect: r*educe steel corrosion activity in a chloride environment

*Material: c*alcium nitrite, sodium nitrite, sodium benzoate, certain phosphates or fluorosilicates, fluroaluminates.

g) Damp proofing

Effect: retard moisture penetration into dry PCC
Material: soaps of calcium or ammonium stearate or oleate; butyl stearate; petroleum products.

h) Cementitious Minerals

Effect: hydraulic properties; Partial cement replacement
Material: ground granulated blast-furnace slag; natural cement; hydraulic hydrated lime.

i) Natural pozzolans

Effect: pozzolonic activity; improve workability, plasticity, sulfate resistance; reduce alkali reactivity, permeability, heat of hydration; partial cement replacement; filler
Material: diatomaceous earth, opaline cherts, clays, shales, volcanic tuffs, pumicites; fly ash (classes C and F); silica fume.

j) Inert minerals

Effect: improve workability; filler
Material: marble, dolomite, quartz, granite.

k) Permeability reducers

Effect: reduce permeability
Material: silica fume, fly ash, ground slag, natural pozzolans, water reducers, latex.

l) Pumping aids

Effect: improve pumpability
Material: organic and synthetic polymers; organic flocculents; organic emulsions of paraffin, coal tar, asphalt, acrylics; bentonite and pyrogenic silicas; natural pozzolans; fly ash; hydrated lime

m) Retarders

Effect: retard setting time
Material: lignin, borax, sugars, tartaric acid and salts.

n) Superplasticizers (high-range water reducers)

Effect: reduce water-cement ratio by a minimum of 12%; Increase workability at low water-cement ratios
Material: sulfonated melamine formaldehyde condensates; sulfonated naphthalene formaldehyde condensates; lignosulfonates.

o) Water reducer

Effect: reduce water demand by a minimum of 5%

Material: lignosulfonates; Hydroxylated carboxylic acids; Carbohydrates.

p) Workability agents

Effect: improve workability
Material: air-entraining admixtures; cementitious materials, natural pozzolans and inert minerals (except silica fume).

3.1.5. JOINT AND CRACK SEALANT PRODUCTS

Sealant products are used in joints and cracks to minimize infiltration of surface water and incompressible material into the joint system or cracks. In the case of joint sealants, they can also reduce dowel bar corrosion by reducing entrance of chemicals. Figure 3.2 shows the typical shape factors for liquid sealants.

Long-standing practice has been to seal all concrete pavement joints. However, there are some case where joints do not require to be sealed. Joint sealing may be omitted in newly constructed, doweled concrete pavement and some specialty concrete pavement types where erosion of the subbase is not of concern (e.g., undoweled bonded concrete overlays of asphalt pavements), but any previously sealed joint should be resealed as necessary during concrete pavement preservation activities [23].

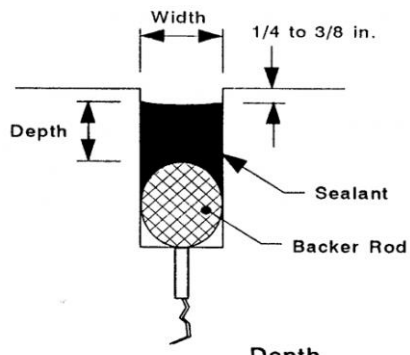

$$\text{Shape Factor} = \frac{\text{Depth}}{\text{Width}}$$

Liquid Sealant Type	Typical Shape Factor
Hot-Pour	1.0
Silicone	0.5

Figure 3.2 - Typical shape factors for liquid sealants [23]

There are many liquid and preformed sealant products. Liquid sealants depend on long term adhesion to the joint face for successful sealing. Preformed compression seals depend on lateral rebound for long-term success. Sealant properties necessary for long-term performance depend on the specific application and the climatic environment of the installation. Properties to consider include [23]:

- Elasticity: The ability of a sealant to return to its original size when stretched or compressed.
- Modulus: The change in internal stresses in a sealant while being stretched and compressed over a range of temperatures (stiffness of material). A low modulus is desirable and is particularly important in cold weather climates.
- Adhesion: The ability of a sealant to adhere to concrete. Initial adhesion and long-term adhesion are equally important. (Not applicable to compression seals.)
- Cohesion: Ability of a sealant to resist tearing from tensile stresses. (Not applicable to compression seals.)

- Compatibility: Relative reaction of the sealant to materials which it contacts (such as backer rods and other sealants).
- Weatherability: Ability of a sealant to resist deterioration when exposed to the elements (primarily ultra violet sun rays and ozone).
- Jet Fuel Resistance: Ability of a sealant to resist degradation in contact with jet fuel. Some material swelling may occur in contact with jet fuel. Upon evaporation, the sealant material must return to original shape and maintain adherence to the reservoir walls.

The three most used sealants, i.e., hot-pour seals, compression seals, and silicone seals, are discussed as follows [23]:

3.1.5.1. Hot Pour Liquid

Hot pour liquid sealants were the first type used for concrete pavement. Manufacturers have improved their characteristics over many years and now they provide low modulus materials with better elasticity. The temperature requires for proper application go from 177 to 200 °C. Most manufactures require melting the material in a double boiler. The inside melting vat is surrounded by a vat of oil. An agitator in the melting vat helps distribute the heat evenly.

Some hot-pour sealants contain poly-vinyl chloride (PVC) plastic with coal tar. These sealants are extremely tacky and most are resistant to jet fuel. The PVC coal tar sealants require heating to only about 120°C for installation [23].

3.1.5.2. Preformed Compression

Compression seals differ from liquid sealants because they are manufactured ready for installation and they do not require field heating, mixing or curing.

Preformed compression seals are in compression throughout their life, unlike liquid sealants that experience both compression and tension. Therefore, their success depends solely on the lateral pressure exerted by the seal. Neoprene, which is the principle compound in compression seals, is a synthetic rubber which provides excellent rebound pressure under compression. The seals consist of a series of webs. The webs provide the outward force which holds the sealant against the reservoir walls.

Sizing compression seals is very important. Joint opening may become too wide at low temperatures if a compression seal is undersized, the seal will lose contact with the reservoir walls and loosen. Also, expansion/isolation joints in the pavement may allow any contraction joints within about 30 m to open too wide. Manufacturers provide seals of various nominal widths and depths. The appropriate sealant width is greater than the maximum (coldest weather) joint reservoir width [23].

3.1.5.3. Silicone

Silicone sealants are a field-poured liquid with a base ingredient of silicone polymer. They are installed in an analogous way to hot pour materials. Silicone sealants, which are a single component that requires no mixing or heating, come prepackaged and ready for immediate application.

Most silicone sealants develop a low elastic modulus which allows good extension and compression recovery. Typical low modulus silicones can undergo at least 100% extension and 50% compression without detriment. They require about 30 minutes curing time before opening to traffic and developing sufficient adhesion. However, the amount of time may differ depending on the manufacturer and environmental conditions [23].

3.1.5.4. Backer Rods

Backer rods prevent liquid sealant from flowing out of the bottom of a joint and adhering to the reservoir bottom. As shown in Figure 3.2, backer rods also help to define the shape factor and optimize the quantity of sealant used. The following considerations are recommended for various materials [23]:

- Polyethylene Foam: It is a closed-cell foam that does not absorb water and is moderately compressible. It is better suited for cold-pour sealants since it may melt in con-tact with hot-pour materials.
- Crosslinked Polyethylene Foam: It is a closed-cell foam that is compatible with hot-pour sealants. It will not absorb water and is moderately compressible.
- Polyurethane Foam: This open-cell foam absorbs water, but does not melt when used with hot-pour materials. It is very compressible, and commonly used with hot-pour sealants.

Backer rod size depends on the joint or crack reservoir width. Backer rods are compressed about 25 percent to assure they stay at the desired depth in reservoir.

3.2. RIGID PAVEMENT TYPES

There are several types of pavements, but the most widely used is the jointed plain concrete pavement (JPCP). Other typologies include jointed reinforced concrete pavement (JRCP), continuous reinforced concrete pavement (CRCP), and prestressed concrete pavement (PCP). Except for PCP with lateral pre-stressing, a longitudinal joint should be installed between two traffic lanes to prevent longitudinal cracking. Figure 3.3 shows the major characteristics of these four types of pavements [15].

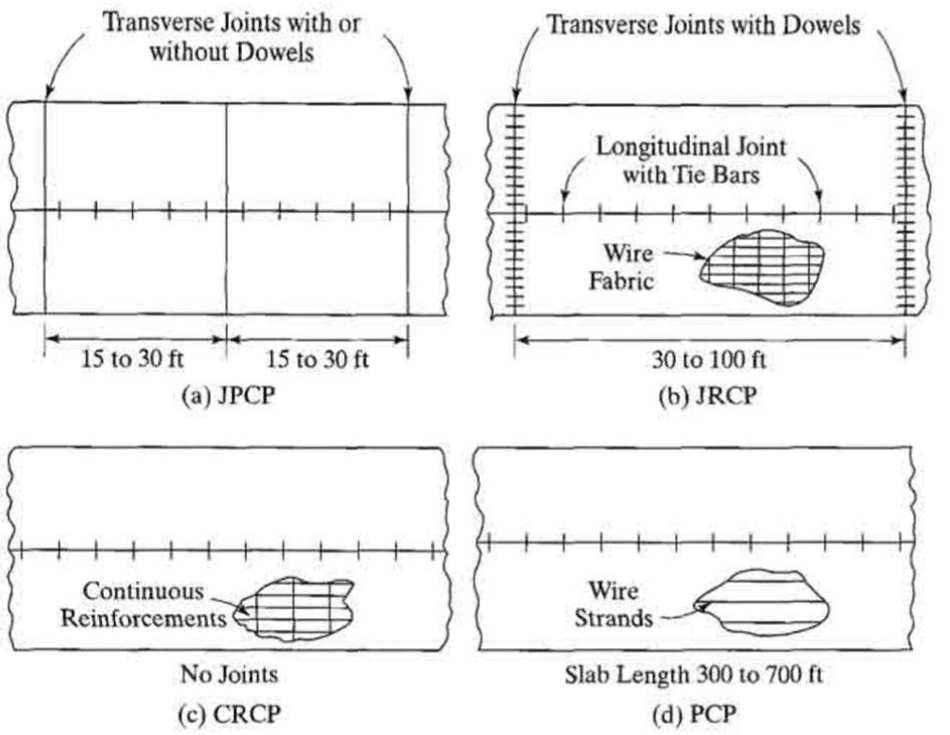

Figure 3.3 - Type of pavements: 1) jointed plain concrete pavement (JPCP), 2) jointed reinforced concrete pavement (JRCP), 3) continuous reinforced concrete pavement (CRCP), and 4) prestressed concrete pavement (PCP) [15].

3.2.1. JOINTED PLANE CONCRETE PAVEMENTS (JPCP)

JPCP are pavements constructed with contraction joints. The load transfer across the joints is solved using aggregate interlocks or dowels. The joints are constructed relative close, e.g., 6.1 m for doweled joints and 4.6 m for undoweled joints. The joint spacing depends on type of aggregate, climate, and prior experience. It is important to know that as the joint spacing increases, the aggregate interlock decreases, and there is also an increased risk of cracking [15].

3.2.2. JOINTED REINFORCED CONCRETE PAVEMENT (JRCP)

JRCP is a pavement constructed using steel reinforcements in the form of wire mesh or deformed bars. The reinforcement does not increase the structural capacity of pavements but allow the use of longer joint spacing. The amount of steel in JRCP increases with the increase in joint spacing and is designed to hold the slab together after cracking. Because of the longer panel length, which vary from 9.1 to 30 m, dowels are required for load transfer across the joints [15].

3.2.3. CONTINUOUS REINFORCED CONCRETE PAVEMENTS (CRCP)

It was originally reasoned that joints were the weak spots in rigid pavements and that the elimination of joints would decrease the thickness of pavement required. The first experimental use of CRCP was in 1921 on Columbia Pike near Washington, D.C. After the experience obtained in more than 12 states, the thickness of CRCP has been empirically reduced by 25 to 50 mm, or arbitrarily taken as 70 to 80% of the conventional pavement [15].

The distress that occurs most frequently in CRCP is punch-out at the pavement edge. There is no reason to use a thinner CRCP if failures occur at the pavement edge instead of at the joint. The formation of transverse cracks at relatively close intervals is a distinctive characteristic of CRCP. These cracks are held tightly by the reinforcements and should be of no concern if they are uniformly spaced [15].

Methods of design, such as the PCA method, have a section to calculate the amount of reinforcement required, in addition to the basic thickness design. The 1986 AASHTO design guide suggests using the same equation or monograph for determining the thickness of JRCP and CRCP. However, the recommended load transfer coefficients for CRCP are slightly smaller than those for JPCP or JRCP and so result in a slightly smaller thickness of CRCP. The amount of longitudinal reinforcing steel should be designed to control the spacing and width of cracks and the maximum stress in the steel [15].

3.2.4. Pre-stressed Concrete Pavements (PCP)

The first known prestressed highway pavement in the United States was a 91 m pavement in Delaware built in 1971. The prestressed concrete pavements have less probability of cracking and fewer transverse joints and therefore result in less maintenance and longer pavement life [15].

The modulus of rupture of the concrete governs the slab thickness required. The value varies with the tensile strength of the concrete. The pre-application of a compressive stress to the concrete greatly reduces the tensile stress caused by the traffic loads and thus decreases the thickness of concrete required [15].

Prestressed concrete has been used more frequently for airport pavements than for highway pavements because the saving in thickness for airport pavements is much greater than that for highway pavements. The thickness of prestressed highway pavements has generally been selected as the minimum necessary to provide sufficient cover for the pre-stressing steel. Prestressed concrete pavements are still at the experimental stage, and their design arises primarily from the application of experience and engineering judgment [15].

3.3. Base And Subbase

In the early days of rigid pavement construction, concrete slabs were placed directly on top of the subgrade without any base or subbase layers. Then, in 1940, the U.S. Army Corps of Engineers were assigned the responsibility for the design and construction of military airfields to support new heavy bomber aircraft. This pivotal work on rigid pavement design led to a much better understanding of the importance of the bases and subbases., specially, their uniformity, and degree of compaction. Some of the findings of this study based on H.M. Westergaard's work are presented bellow [1]:

The importance of the bases for the PCC was one of the most important findings during the implementation of the new design procedure. Pumping of the subgrade, through the joints and cracks in the PCC pavement, due to the increase of traffic load, volume and speed was observed. Pumping started a progressive damage process, which start by the loss of support and resulted in an increase in other distresses such as faulting, roughness, and corner breaks. To overcome the pumping problem, a sand layer was specified. This filter layer also acted as a "subgrade improvement" layer, contributing not only to the reduction in pumping but also to the strength of the pavement and its constructability.

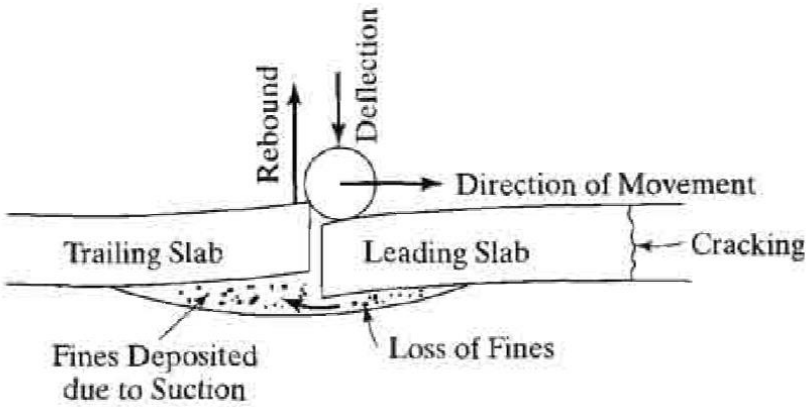

Figure 3.4 - Pumping of rigid pavement [15]

Rigid pavement design relies on the structural carrying capacity of the PCC and on the uniformity of support provided by the base layers. In most rigid pavement designs, increasing slightly the slab thickness is more economical than structurally increasing the thickness of the base layer to achieve the necessary structural capacity, because the PCC design thickness is relatively insensitive to the foundation strength.

The key characteristic of a superior quality rigid pavement foundation is the provision of uniform support that is free of any abrupt spatial and material changes, instead of the strength of the support. The three major causes of a non-uniform foundation are: a) Pumping of the fine particles, b) frost heave and c) soil expansion.

a) Pumping

The main causes are heavy axles, poor load transfer, e.g., no doweled joints, presence of water between pavement and subgrade and fine-grained subgrade or erodible base/subbase materials.

b) Frost heave

It typically occurs in frost-susceptible soils, in the present of water and freezing temperatures penetrating the soil.

c) Soil expansion

Expansive soil such as the American Association of State Highway and Transportation Officials (AASHTO) classification A-6 or A-7 soil groups or the Unified Soil Classification System CH, MH, and OH soils. As well as degree of moisture change within the soil.

3.3.1. Design of base and subbase for rigid pavements

The vertical stress providing support to the PCC pavement is assumed to be directly proportional to the vertical deflection of the slab in the Westergaard design equations. In the conceptual model, the foundation is considered as a spring- or dense liquid subgrade, which is commonly quantified by the modulus of subgrade reaction (known as the k-value). The k-value is determined by dividing the load, the one applied to generate the deflection, by the volume of the deflection basin. A stronger support to the PCC can be provided placing a base or subbase and then a composite k-value should be used. Since this value is not significant in the slab thickness design, an exact k-value is not required.

The satisfactory performance of the rigid pavement is not guaranteed by constructing a stronger and stiffer base layer. The reduction of strains in the slabs and the load transfer improvement is obtained

with a reasonable strength of the support the foundation. In contrast, a very stiff base increases the stresses and deflections due to the curling and warping caused by the environment loads. It means, using a base too stiff may eventually cause cracks to develop in the slabs, especially when the concrete is relatively young.

The thickness of the subbase is governed by subgrade type, depth of frost penetration, and availability of water near the subgrade. On the other hand, base thickness generally depends on the degree of support required for the construction equipment and type and condition of the underlying subgrade. The base width is usually wider than the edge of the slabs to accommodate the paving equipment [1].

3.3.1.1. Non-stabilized base

Non-stabilized bases and subbases, also called as granular bases, do not have any bounding material. The desired characteristics of these layers are governed by the gradation of the aggregates. They can be dense-graded aggregate base or open-graded aggregate drainage layer.

An adequate base design and construction guarantees an excellent field performance at a lower cost than stabilized bases. Non-stabilized bases can be constructed with several materials, such as crushed stone, sand-gravels, sands, and a variety of waste and byproducts. The requirements that the materials should meet are presented in the AASHTO M 147. Where the amount of fines is the most important criterion for preventing pumping, base erosion, and frost action. In general, the materials for non-stabilized base should meet the following criteria [1]:

- Less than 10 percent passing No. 200 sieve.
- Plasticity index of 6 or less and liquid limit of 25 or less.
- Maximum particle size not exceeding one third of layer thickness.
- Los Angeles (L.A.) abrasion resistance (AASHTO T 96) of 50 percent or less.

The AASHTO M 147 gradations shown in Table 3.4 were developed for both asphalt and concrete pavements, and the standard facilitates a rather wide range of gradations. All the gradations except gradations A and C allow more than 15 percent passing the No. 200 sieve. Therefore, to utilize gradations B, D, E, and F, the requirement for percent passing the No. 200 sieve should be adjusted to limit the amount of fines.

Table 3.4 - Gradation requirements for soil-aggregate materials (AASHTO M 147) [1].

Percent Passing	Sieve Designation					
Inch	Gradation A*	Gradation B	Gradation C	Gradation D	Gradation E	Gradation F
2 in.	100	100	-	-	-	-
1 in.	75-95	100	100	100	100	100
¾ in.	30-65	40-75	50-85	60-100	-	-
No. 4	25-55	30-60	35-65	50-85	55-100	70-100
No. 10	15-40	20-45	25-50	40-70	40-100	55-100
No. 40	8-20	15-30	15-30	25-45	20-50	30-70
No. 200	2-8	5-20	5-15	5-15	6-20	8-25

3.3.1.2. Stabilized base

Stabilized bases are constructed using a bounding material, typically cement or asphalt. The concrete or asphalt paving equipment used in the construction allows to achieve a smooth surface. The stabilized bases contribute to achieving an elevated level of smoothness for concrete pavements as well. The stabilized bases are divided in two groups, a) the cement-stabilized bases and b) the asphalt-stabilized bases:

a) Cement-stabilized bases:
   - Cement-treated base
     For cement-treated bases, which typically contain 2 to 5 percent cement, the material requirements may be relaxed to allow up to 35 percent passing the No. 200 sieve and a plasticity index of 10, i.e., requirements less restricted as compared as those for non-stabilized bases. Granular soils with plasticity index of 10 or less (more specifically, AASHTO classification A-1, A-3, A-2-4, and A-2-5 soils) may be used for these base types

   - Lean concrete base
     Another treated base is the lean concrete base, which contains more cement than cement-treated base but less than conventional concrete. It could be possible the use of locally available, lower quality aggregates that do not meet the requirements for non-stabilized base or conventional concrete due to the increased cement content.
   - Cement-treated open-graded drainage layer
     It has very little aggregate passing the No. 200 sieve. Cement-treated open-graded drainage layers are typically produced with a water-to-cement ratio of 0.37.

b) Asphalt-stabilized bases, can be asphalt dense-graded base, asphalt-treated base and asphalt-treated open-graded drainage layer. Asphalt-treated bases have a lower grade asphalt binder than normal asphalt concrete. The material requirements are like the existing requirements for asphalt surfaces. However, it is important to use durable aggregates to obtain satisfactory pavement performance.

3.4. THICKNESS DESIGN

3.4.1. GENERAL DESIGN FACTOR

Design factors can be divided into four broad categories: traffic and loading, environment, materials, and failure criteria. The factors, adapted from [15], to be considered in each category are discussed in the next subsections.

3.4.1.1. Traffic and Loading

The traffic and loading to be considered include axle loads, the number of load repetitions, tire-contact areas, and vehicle speeds.

a) Axle Loads

The traffic is characterized by the type of vehicle and the axles. There are several configurations depending on the vehicle, but usually there are catalogs for purpose design. Figure 3.5 shows the wheel spacing for a typical semitrailer consisting of single axle with single tires, single axle with dual tires, and tandem axles with dual tires. Exist also special heavy-duty haul trucks with different configuration, usually with tridem axles.

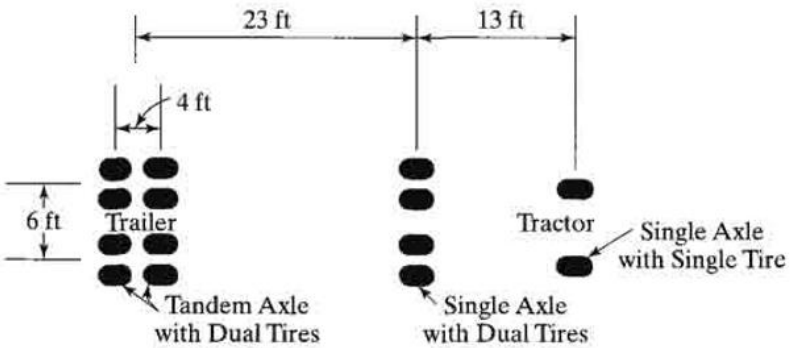

Figure 3.5 - Wheel configurations for typical semitrailer units [15]

In the pavement design the spacing between axles has no effect because the wheels are so far apart that their effects in term of stresses and strain should be considered independently. The consideration of multiple axles is not a simple matter, unless an equivalent single-axle load is used. If each axle is treated independently and considered as one repetition the design is too conservative. On the other hand, the design may be unsafe if the tandem and tridem axles are treated as a group and considered as one repetition.

b) Number of Repetitions

The method of dividing axle loads into several groups has been used frequently for the design of rigid pavements, as illustrated by the PCA method in Section 3.4.2. In early years, this method was tedious, but with the use of a high-speed computer, it is no problem to consider the number of load repetitions for each axle load and evaluate its damage.

Another simplified and widely accepted procedure is to develop equivalent factors and convert each load group into an equivalent 80 kN (18 kip) single-axle load, instead of analyzing the stresses and

strains due to each axle-load group. This procedure is used by the Asphalt Institute method, for flexible pavement, and the AASHTO method.

c) Contact Area

In the mechanistic method of design, it is necessary to know the contact area between tire and pavement, so the axle load can be assumed to be uniformly distributed over the contact area.

The size of contact area depends on the tire pressure. In pavement design, the contact pressure is generally assumed to be equal to the tire pressure. Assuming the tire pressure as the contact pressure is safer because heavier axle loads have higher tire pressures and more destructive effects on pavements. Heavier axle loads are always applied on dual tires. Figure 3.6 (a) shows the approximate shape of contact area for each tire used previously by PCA (1966) [6], which is composed of a rectangle and two semicircles. By assuming length L and width $0.6L$, the area of contact is given by

$$A_C = \pi(0.3L)^2 + (0.4L)(0.6L) = 0.5227L^2 \text{ or} \tag{3.1}$$

$$L = \sqrt{\frac{A_c}{0.5227}} \tag{3.2}$$

Where: A_C is the contact area, which can be obtained by dividing the load on each tire by the tire pressure. Figure 3.6 (b) shows the contact area used by the current PCA (1984) method, which is based on the finite element procedure. In this method, a rectangular area is assumed with length $0.8712L$ and width $0.6L$, which has the same area of $0.5227L^2$.

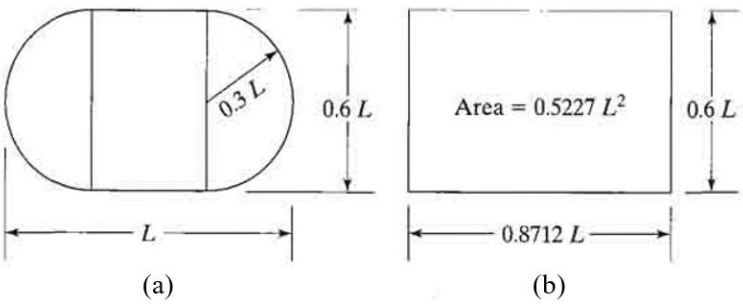

Figure 3.6 - Dimension of tire contact area, a) real contact area, b) equivalent contact area [15]

3.4.1.2. Environment

The temperature and precipitation are environmental factors that influence pavement design, both affecting the elastic moduli of the constituent layers. In the mechanistic-empirical method of design, each year can be divided into several periods, each having a distinct set of layer moduli. The damage during each period is evaluated and summed throughout the year to determine the design life.

a) Temperature

The temperature gradient in concrete pavements affects not only the curling stress but also the slab–subgrade contact. The slab curls down during the day, when the temperature at top is higher than that at bottom, so that its interior may not be in contact with the subgrade. At night in contrast, when the temperature at top is lower than that at bottom, the slab curls upward so that its edge and corner may be

out of contact with the subgrade. The stresses in the slab will be affected by loss of subgrade contact due to wheel loads. The temperature gradient also determines the joint and crack openings and affects the efficiency of load transfer.

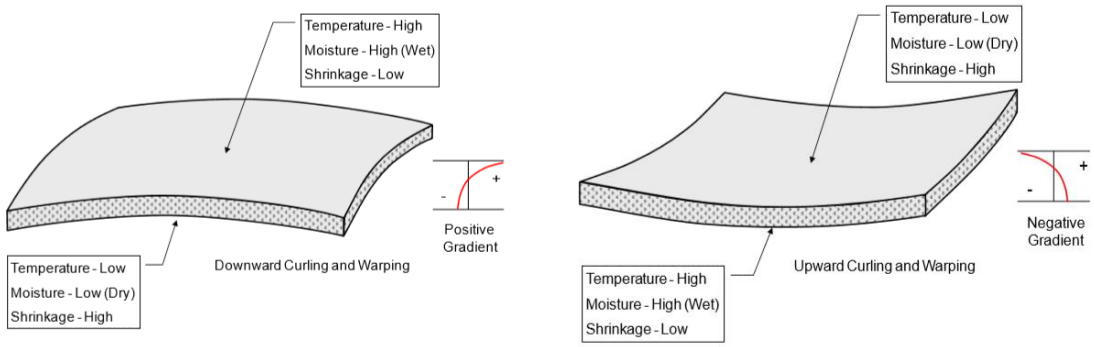

Figure 3.7 - Slab curling and warping, a) downward, b) upward [24]

Frost penetration is another effect of temperature on pavement design in cold climate. It results in a stronger subgrade in the winter but a much weaker subgrade in the spring. It is desirable to protect the subgrade by using non-frost-susceptible materials within the zone of frost penetration. The spring breakup period is the most critical because it is when the ice melts and the subgrade is in a saturated condition. If frost-susceptible materials are used, the design method should take into consideration the weakening of the subgrade during spring break-up.

The frost severity can be expressed as a freezing index in terms of degree days. A negative one-degree day represents one day with a mean air temperature one degree below freezing; a positive one-degree day indicates one day with a mean air temperature one degree above freezing. The mean air temperature for a given day is the average of high and low temperatures during that day. As shown in figure 3.8, the difference between the maximum and minimum points on the curve during one year is called the freezing index for that year. The freezing index has been correlated with the depth of frost penetration and can be used as a factor of pavement design and evaluation.

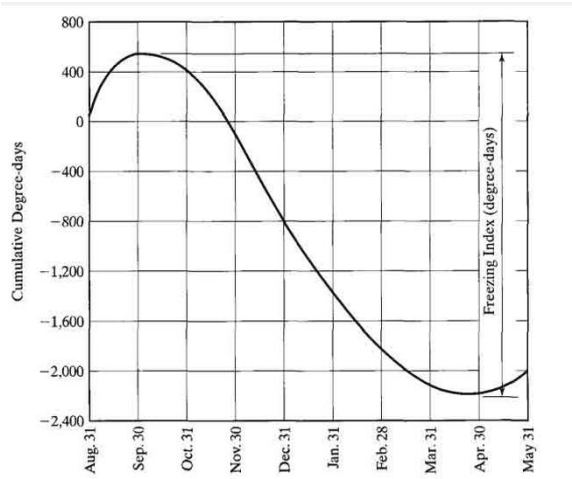

Figure 3.8 - Determination of freezing index [15]

b) Precipitation

The quantity of surface water infiltration and the location of the phreatic level is affected by the precipitation from rain and snow. The detrimental effects of water can be mitigated using an effective drainage system. The water table should be kept at least 1 m below the pavement surface. In seasonal frost areas, the depth from the pavement surface to the groundwater table should be much greater.

Smaller elastic moduli must be selected for the component layers if proper drainage cannot be provided. However, this measure might not solve the problem, because poor drainage could still incur damages other than the lack of shear strength, such as the pumping and the loss of support.

3.4.1.3. Design Material parameters

Material properties must be specified to determine the pavement responses, such as stresses, strains, and displacements in the critical components in the mechanistic-empirical methods of design. These responses are then used with the failure criteria to predict whether failures will occur or the probability that failures will occur.

The general material properties for both flexible and rigid pavements that should be specified are:

a) When pavements are considered as linear elastic, the elastic moduli and Poisson ratios of the subgrade and each component layer must be specified. The Poisson ratios have relatively small effects on pavement responses, so their values can be reasonably assumed.

b) If the elastic modulus of a material varies with the time of loading, the resilient modulus, which is the elastic modulus under repeated loads, must be selected in accordance with a load duration corresponding to the vehicle speed.

c) When a material is considered nonlinear elastic, the constitutive equation relating the resilient modulus to the state of stresses must be provided.

For rigid pavements, the following properties may be specified:

a) The modulus of subgrade reaction k for rigid pavements on liquid foundations, must be specified.
b) The coefficient of thermal expansion of the concrete must be specified to consider the effect of temperature curling.

c) If other distresses, such as faulting caused by excessive bearing stress on dowel bars, are used as a basis for design, appropriate properties, such as the diameter and spacing of dowels, must be specified.

3.4.1.4. Failure Criteria

The failure of rigid pavement can be evaluated according to failure criteria, such as fatigue, erosion or faulting. Fatigue cracking has long been considered the major or only criterion for rigid pavement design. Pumping or erosion has been considered basically since 1984 in the PCA method. Other criteria under consideration include faulting and joint deterioration of JPCP and JRCP and edge punch-out of CRCP. A brief description of these criteria is presented below.

a) Fatigue Cracking Model

It is most likely caused by the edge stress at the mid-slab. The stress ratio between flexural tensile stress and the concrete modulus of rupture determine the allowable number of load repetitions to cause fatigue cracking. The total number of load repetitions must be reduced to an equivalent number of edge loads because the design is based on the edge loading and only a small portion of the traffic loads is applied at the pavement edge. Details on this criterion are discussed in Section 3.4.2.

b) Pumping or Erosion

The resilient deformation under repeated wheel loads will cause pumping of the slabs. Consequently, corner deflections have been used in the latest version of the PCA method (PCA, 1984) [6] as an erosion criterion in addition to the fatigue criterion. The applicability of the PCA method is quite limited because it is based on the results of the AASHO Road Test, which employed a highly erodible subbase. Pumping is caused by many other factors, such as types of subbase and subgrade, precipitation, and drainage, so a more rational method for analyzing pumping is needed.

c) Other Criteria

Other major types of distress in rigid pavements include faulting, spalling, and joint deterioration. These distresses are difficult to analyze mechanistically, and a significant effort has been made recently in developing regression models to predict them. These empirical models are applicable only under the conditions from which the models were derived.

3.4.1.5. Reliability

Probabilistic approaches based on the reliability are used to predict the distresses, since they at the end of a design period varies a lot, depending on the variability of predicted traffic and the quality control on materials and construction. If Present Serviceability Index (PSI) is used as a failure criterion, the reliability of the design, or the probability that the PSI is greater than the terminal serviceability index, can be determined by assuming the PSI at the end of a design period to be a normal distribution with a mean and a standard deviation.

3.4.2. PCA DESIGN METHOD

The Portland Cement Association's (PCA) thickness-design procedure for rigid pavement is one of the most used design methods, especially in American continent. It was published in 1984 and the procedure can be applied to JPCP, JRCP, and CRCP [6]. The design tables and charts were developed applying some design criteria to critical stresses and deflections obtained from finite element program JSLAB. The design criteria are based on general pavement design, performance, and research experience, including relationships to performance of pavements in the AASHO Road Test and to studies of pavement faulting. Design problems can be worked out by hand with tables and charts computer program available from PCA [15].

The thickness design criteria are based, mainly, in general pavement performance experience. However, if local performance experience suggests more favorable or adverse conditions, the design criteria can be modified. Some local factors can be climate, soil, drainage conditions, and future design innovations [6].

The design factors, design procedure and other relevant aspects are discussed in this section.

3.4.2.1. Design factors

After deciding the type of concrete, type of base if needed, and the type of shoulder, the thickness design is governed by four design factors: a) concrete modulus of rupture, b) subgrade and subbase support, c) design period, and d) traffic. These factors are discussed in more retails bellow [6]:

a) Concrete Modulus of Rupture

Flexural strength of concrete is considered in the design procedure for fatigue criterion, which controls cracking of the pavement under repetitive trucks loading. Compressive and flexural stresses are both produced the bending of a rigid pavement under axle loads. Flexural strength is determined at 28 days by the method specified by ASTM in "C78-84 Standard Test Method for Flexural Strength of Concrete Using Simple Beam with Third Point Loading."

If compressive strength tests are used to evaluate the quality of the concrete, the relationship between the flexural strength and the compressive strength should be determined for the mix design under consideration. An approximate relationship between flexural and compressive strength is

$$MR = K\sqrt{f(c)'} \tag{3.3}$$

where: MR is the flexural strength, in MPa, for third-point loading, K is a constant, usually between 0.7 (for rounded aggregates) and 0.8 (for crashed aggregates), and $f(c)'$ is the compressive strength, in MPa.

Figure 3.9 shows a relationship between flexural strength and age of the concrete.

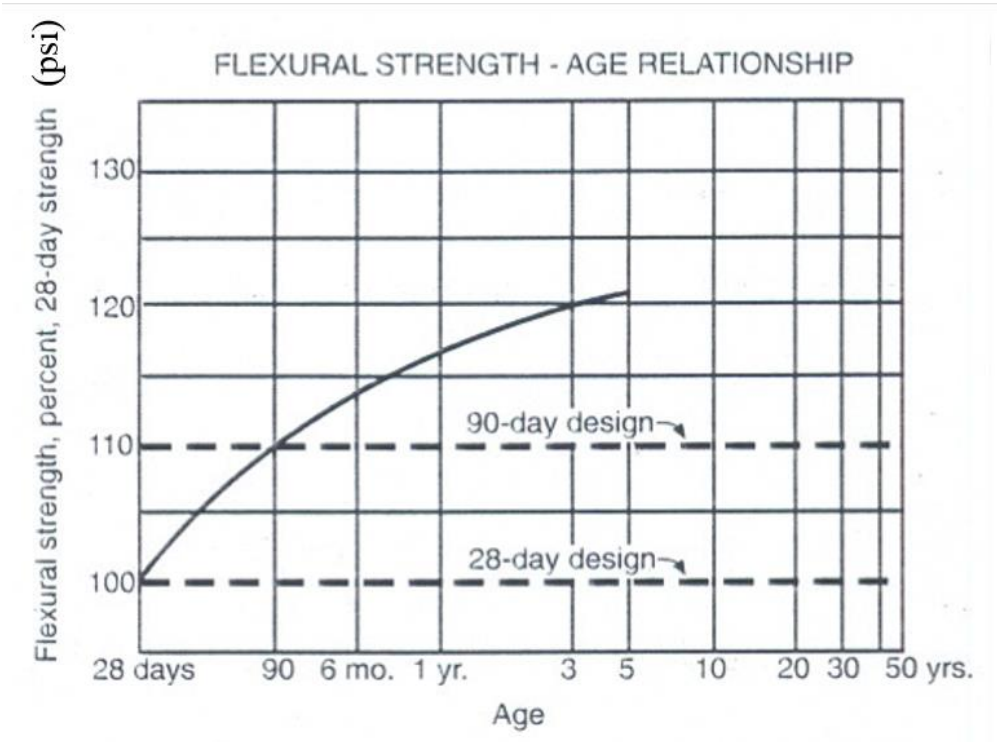

Figure 3.9 - Flexural strength, age and design relationships [6]

The variations in modulus of rupture have far greater effect on thickness design than do the usual variations in other material properties, so it is recommended that the modulus of rupture be reduced by one coefficient of variation. A coefficient of variation of 15 %, which represents good to fair quality control, was assumed and was incorporated into the design charts and tables, as well as the effect of strength gain after 28 days.

b) Subgrade and Subbase Support

The support given to concrete pavement by the subbase and subgrade is the second factor in thickness design. The support is defined in term of Westergaard modulus of subgrade reaction (k). The PCA method does not consider the variation of k values over the year. The contention is that the reduced subgrade support during thaw periods has very little or no effect on the required thickness of concrete pavements, as evidenced by the results of AASHO Road Test. This is true because the brief periods when k values are low during spring thaws are more than offset by the longer freezing periods when k values are much higher than the design value. To avoid the tedious methods to design for seasonal variations in k values, i.e., normal summer- or fall weather k values, can be used as reasonable mean values for design purposes. The k value is given by

$$k = \frac{P}{\delta} \tag{3.4}$$

where P is the pressure on the plate, in newtons per square meter on a loaded area (760 mm- diameter plate), and δ is the deflection of plate in millimeters for that load. The k value is expressed as megapascals per meter (MPa/m) or as pounds per cubic inch (pci).

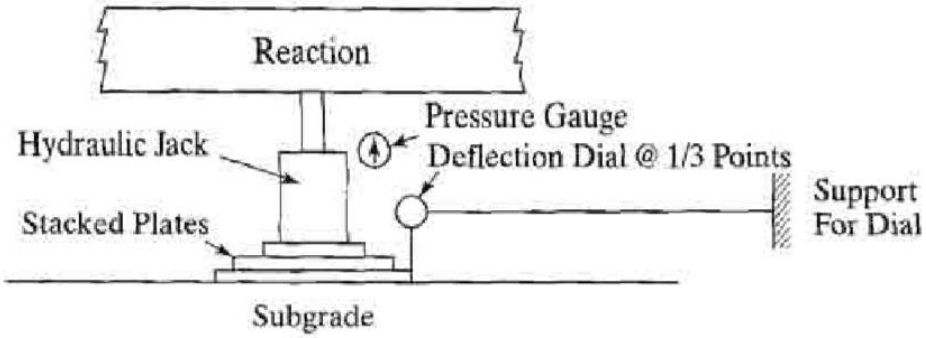

Figure 3.10 - Plate loading test scheme [15]

Since the plate-loading test is time consuming and expensive, the k value is generally estimated by correlation to simpler tests such as the Californian Bearing Ratio (CBR) or R-value tests. For designing purpose the k value estimated is valid, because the variation of k values does not appreciable affect the pavement thickness. There are several relationships between the soil classification, CBR and the subgrade reaction k, as shown in the Figure 3.11.

It is not economical to use untreated subbases for the sole purpose of increasing k values. However, there are many reasons to use subbases. Where a subbase is used, there will be an increase in k that should be considered in the thickness design. Table 3.5 and Table 3.6 show design k values for untreated and cement-treated subbases, respectively.

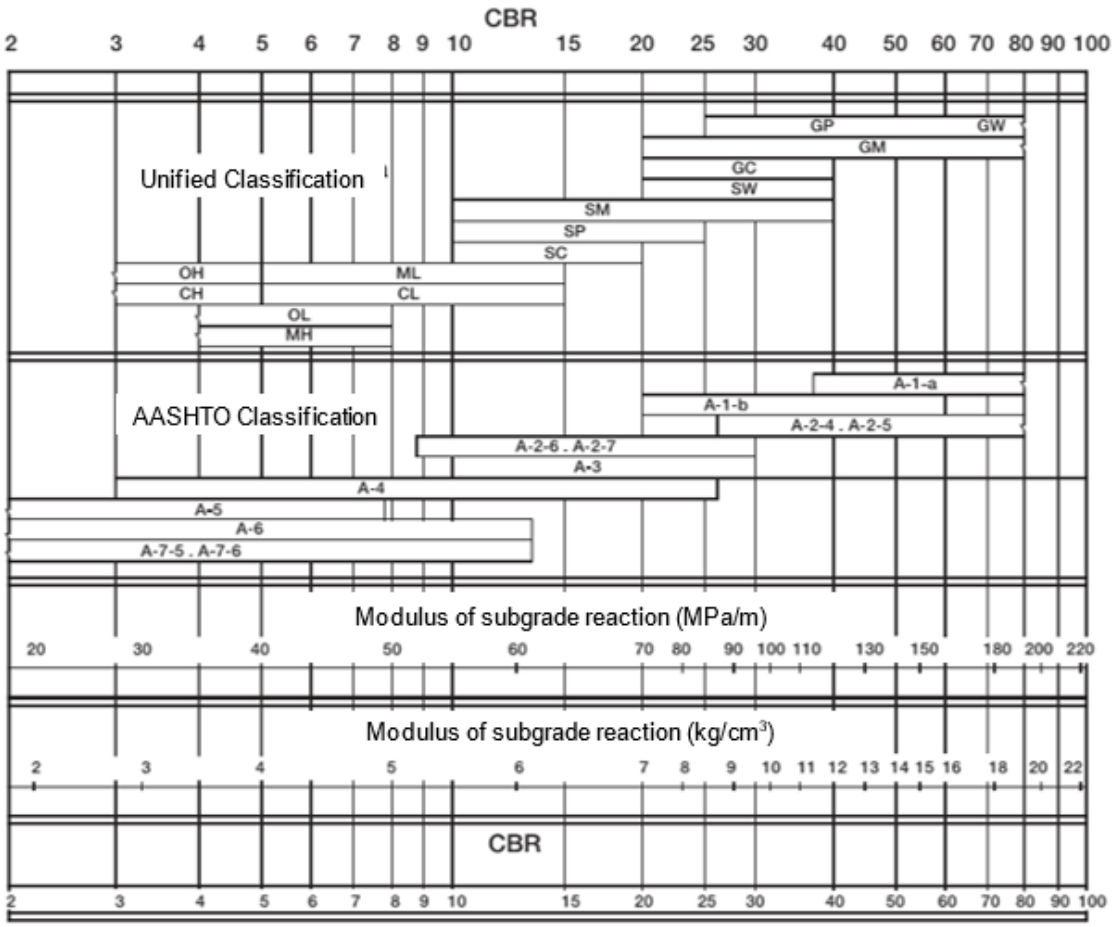

Figure 3.11 - Approximate interrelationships of soil classifications and bearing values (adapted from [6])

Table 3.5 - Effect of Untreated Subbase on k Values [15]

Subgrade k value		Subbase k value							
		100 mm		150 mm		225 mm		300 mm	
MPa/m	pci	MPa/m	pci	MPa/m	pci	MPa/m	pci	MPa/m	pci
20	73	23	85	26	96	32	117	38	140
40	147	45	165	49	180	57	210	66	245
60	220	65	235	66	245	76	280	90	330
80	295	87	320	90	330	100	370	117	430

Table 3.6 - Design k Values for Cement-Treated Subbase [15]

Subgrade k value		Subbase k value							
		100 mm		150 mm		225 mm		300 mm	
MPa/m	pci	MPa/m	pci	MPa/m	pci	MPa/m	pci	MPa/m	pci
20	73	60	220	80	300	105	400	135	500
40	147	100	370	130	500	185	680	230	850
60	220	140	520	190	700	245	900	-	-

c) Design Period

The term design period is used in this method rather than pavement life, which is not subject to precise definition. Design period is more nearly synonymous with the term traffic analysis period. Because traffic probably cannot be predicted with much accuracy for a longer period, a design period of 20 years has commonly been used in pavement design.

The design period selected affects the thickness design since it determines how many years, and thus how many trucks, the pavement must serve. Economic analysis of pavement costs and service provided throughout the entire period are commonly the selection criteria of the design period.

d) Traffic

The last factor considered in the PCA thickness design method is the traffic, which has a significant impact on the thickness. The number and weight of heavy axle loads expected during the design life. They are estimated from the average daily traffic (ADT) in both directions, all vehicles, the average daily truck traffic in both directions (ADTT), and the axle load of trucks. Information on ADT is obtained from special traffic counts or from traffic-volume maps. This ADT is called current or present ADT. The design ADT is then estimated by any method to estimate a reasonable expected traffic during the design life.

The initial traffic on the design lane is obtained multiplying the initial daily traffic, which is in two directions over all traffic lanes, by the directional and lane distribution factors. The traffic to be used for design is the average traffic during the design period, so the initial traffic must be multiplied by a growth factor. Then the total number of repetitions to be used in design ith load group is given by:

$$n_i = (n_0)_i(G)(D)(L)(365)(Y) \tag{3.5}$$

where $(n_0)_i$ is the initial number of repetitions per day for the ith load group, G is the growth factor, D is the directional distribution factor, which is usually assumed to be 0.5 unless the traffic in two directions is different, L is the lane distribution factor which varies with the volume of traffic and the number of lanes, and Y is the design period in years.

If the design is based on the equivalent 80 kN single-axle load (ESAL), the equivalent axle load for the design lane is given by

$$ESAL = \left(\sum_{i=1}^{m} p_i F_i\right)(ADT)_0(T)(A)(G)(D)(L)(365)(Y) \tag{3.6}$$

where p_i is the percentage of total repetitions for the ith load group, F_i is the equivalent axle load factor (EALF) for the ith load group, $(ADT)_0$ is the average daily traffic at the start of the design period, T is the percentage of trucks in the ADT, and A is the average number of axles per truck. It is convenient to combine the first and fourth terms in the equation above to form the new term called truck factor T_f:

$$T_f = \left(\sum_{i=1}^{m} p_i F_i\right)(A) \tag{3.7}$$

T_f is the number of 80-kN single-axle load applications per truck. Thus, the equation for calculating the ESAL becomes

$$ESAL = (ADT)_0(T)(T_f)(G)(D)(L)(365)(Y) \tag{3.8}$$

- Average Daily Truck Traffic (ADTT)

  The ADTT is needed in the design procedure. It can be expressed as a percentage of the ADT or as an actual value. The ADTT value includes only trucks with 6 tires or more.

  The data can be provided by the actual traffic counts on the existing roadway where the pavement is to be constructed or on nearby highways with similar travel patterns. These data are then used to determine the percentage relationship between ADTT and ADT. Surveys conducted by the highway departments can also provide ADTT percentages and other essential traffic data. For example, a highway department loadometer table for a Midwestern state yields the following vehicle count for a loadometer station on their interstate rural system (Adapted from [6]):

All vehicles-ADTT	9490
Trucks:	
All single units and combinations	1650
Panels and pickups	350
Other fur-tire single units	75

  Therefore, for this station:

$$ADTT = \frac{1650 - 350 - 75}{9490} \times 100 = 13\%$$

As mentioned above, the ADTT value includes only trucks with 6 tires or more. For this reason, in the numerator panels and pickups and other four-tire single units are subtracted. This ADTT percentage would be appropriate for design of project where factors influencing the growth and composition of traffic are like those at this loadodometer station.

The National Truck Characteristics Report is another source of information on ADTT. Table 3.7 shows the percentages of four-tire single units and trucks on the major highway system in the Unite State. However, the percentages in the table are only suitable for design of projects where ADTT percentages are also about average because the values are average computed from many projects in all sections of the Unite State.

Table 3.7 - Percentages of Four-Tire Single Units and Trucks (ADTT) on Various Highway Systems [6]

Highway system	Rural average daily traffic			Urban average daily traffic		
	2-axle, 4-tire single units	Trucks (ADTT)	Total of both	2-axle, 4-tire single units	Trucks (ADTT)	Total of both
Interstate	14	21	35	8	16	24
Other federal-aid primary	16	13	29	17	9	26
Federal-aid secondary	10	15	25	14	8	22

For facilities of four lanes or more, the ADTT is adjusted using Figure 3.12.

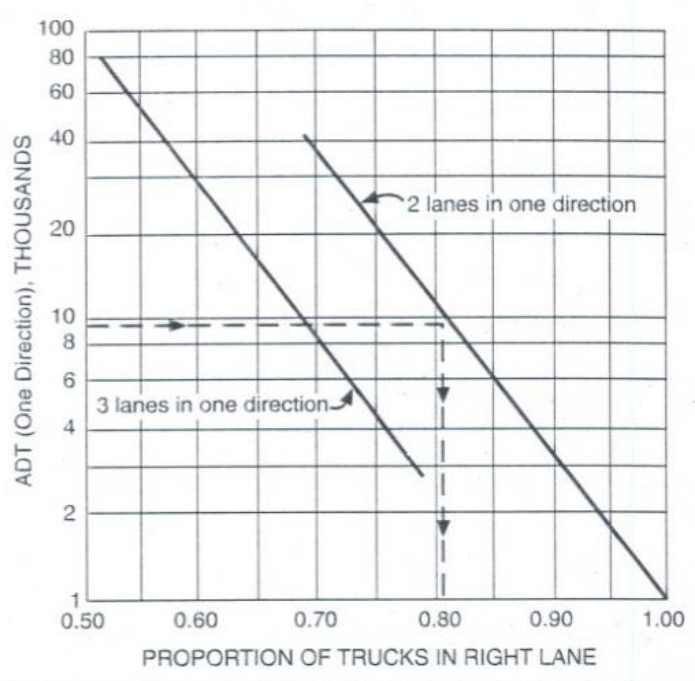

Figure 3.12 - Percentage of trucks in right lane of multilane divided highway [6]

- Growth Factor (G)

One way to project the growth factor is to assume a yearly rate of traffic growth and use the average traffic at the start and end of the design period as the design traffic. The PCA (1984) [6] applies the traffic at the middle of the design period as the design traffic:

$$G = (1 + r)^{0.5Y} \tag{3.9}$$

The four factors that influence yearly growth rates and traffic projections are the attracted or diverted traffic, the normal traffic growth, the generated traffic, and the development traffic. The combined effects will cause annual growth rates of about 2% to 6%. Table 3.8 shows the projection factors for 20 and 40 years. Where there are some questions about the rate of growth, it is recommended to use a high rate. Especially on intercity routes and on urban projects where a high rate of urban growth may cause a higher than expected rate of traffic growth.

Table 3.8 - Yearly Rates of Traffic Growth and Corresponding Projection Factors [15]

Annual growth rate (%)	20-Year design period	40-Year design period
1.00	1.10	1.20
1.50	1.20	1.30
2.00	1.20	1.50
2.50	1.30	1.60
3.00	1.30	1.80
3.50	1.40	2.00
4.00	1.50	2.20
4.50	1.60	2.40
5.00	1.60	2.70
5.50	1.70	2.90
6.00	1.80	3.20

- Truck Directional Distribution (D)

  In most design problems, it is assumed that pavement in each direction carries half of the total ADTT, i.e., a 50-50 distribution. This may not be true where many of the trucks may be hauling full loads in one direction and returning empty in the other direction. An adjustment should be made if these exceptional cases are presented.

- Axle-Load Distribution

  Data on the axle load distribution of truck traffic is needed to compute the number of single and tandem axles of various weights expected during the design period.

  These data can be obtained from one of the three ways: i) special traffic studies to establish the loadometer data for the specific project, ii) data from the provincial highway department´s loadometer station representing truck weights and types that are expected to be like the project under design, and iii) using an alternative procedure when axle-load distribution data are not available.

  The use of axle-load data is presented in Table 3.9. The data has been grouped by 8.8 kN and 17.6 kN increments for single- and tandem-axle, respectively.

Table 3.9 – Example of Axle-Load Data [6]

Axle load, kN (1)	Axles per 1000 trucks (2)	Axles per 1000 trucks (adjusted) (3)	Axles in design period (4)
Single axles			
125-133	0.28	0.58	6310
115-125	0.65	1.35	14690
107-115	1.33	2.77	30140
97.8-107	2.84	5.92	64410
88.8-97.8	4.72	9.83	106900
80.0-88.8	10.40	21.67	235800
71.1-80.0	13.56	28.24	307200
62.2-71.1	18.64	38.83	422500
53.3-62.2	25.89	53.94	586900
44.4-53.3	81.05	168.85	1837000
Tandem axles			
213-231	0.94	1.96	21320
195-213	1.89	3.94	42870
178-195	5.51	11.48	124900
160-178	16.45	34.27	372900
142-160	39.08	81.42	885800
125-142	41.06	85.54	930700
107-125	73.07	152.23	1656000
88.8-107	43.45	90.52	984900
71.1-88.8	54.15	112.81	1227000
53.3-71.1	59.85	124.69	1356000

Columns 1 and 2 derived from loadometer W-4 Table. This table also shows 13,215 total trucks counted with 6,918 two-axle, four-tire trucks (52%). Column 3: Column 2 values adjusted tor two-axle, four-tire trucks; equal lo Column 2/ (1-52/100). Column 4 = Column 3 x (trucks in design period)/1000. See sample problem. Design 1, in which trucks in design period (one direction) total 10.880.000.

- Load Safety Factors

  In the design procedure, the axle load calculated previously must be multiplied by a load-safety factor (LSF). These load-safety factors are the recommended:

  For interstate highways and other multilane projects where there will be uninterrupted traffic flow and high volumes of truck traffic, LSF = 1 .2.

  For highways and arterial streets where there will be moderate volumes of truck traffic, LSF = 1.1.

  For roads, residential streets, and other streets that will carry small volumes of truck traffic, LSF = 1.0.

  In exceptional cases, such as a very busy urban freeway with no alternative deviation routes for the traffic, the use of a load safety factor as high as 1 .3 might be justified for a premium facility to maintain a higher than normal level of pavement serviceability throughout the design period.

3.4.2.2. Design criteria

One aspect of the PCA (1984) [6] design procedure is the inclusion of an erosion analysis, in addition to the fatigue analysis. In the fatigue analysis, it is study the pavement failure due to the fatigue of concrete; in erosion analysis, pavements fail by pumping, erosion of foundation, and joint faulting.

a) Fatigue Analysis

Fatigue analysis is based on the edge stress midway between the transverse joints, with the most critical loading position being shown in Figure 3.13. The presence of the joints has practically no effect on the edge stress because the load is near the mid-slab far away from the joints. When a concrete shoulder is tied onto the mainline pavement, the magnitude of the critical stress is reduced considerably.

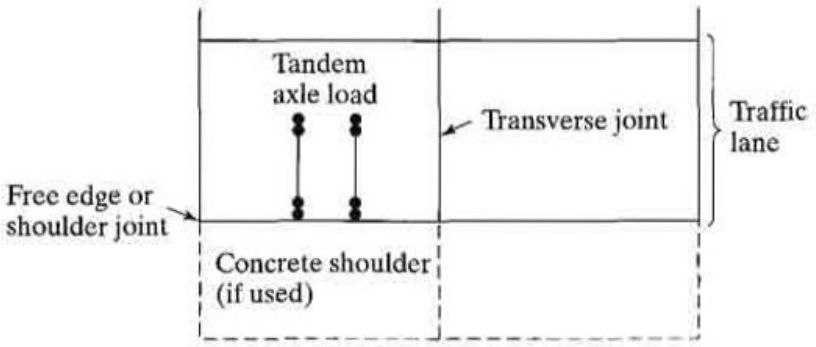

Figure 3.13 - Critical loading position for fatigue analysis [15]

The general cumulative damage concept (Mechanistic Design Procedure) is described by the equation 3.10, which combines loading and curling stresses for determining the stress ratio and thus the allowable number of load repetitions

$$D_r = \sum_{i=1}^{p} \sum_{k=1}^{3} \sum_{j=1}^{m} \frac{n_{i,k,j}}{N_{i,k,j}} \tag{3.10}$$

where D_r is the accumulated damage ratio over the design period at the critical location, i is the counter for periods or subgrade support values, p is the total number of periods, k is the counter for three curing conditions (day, night, and zero temperature gradient), j is the counter for load groups, m is the total number of load groups, $n_{i,k,j}$ is the predicted number of load repetitions for the jth load group, kth curling condition, and ith period, and $N_{i,k,j}$ is the allowable number of load repetitions for the jth load group, kth curling condition, and ith period.

For fatigue analysis, in PCA however, only an average modulus of subgrade reaction k is used for the entire design period, and the stresses due to warping and curling are not considered. Warping and curling are excluded because the moisture content and temperature are usually higher at the bottom of the slab than at the top. Thus, the combined effect of warping and curling stresses is subtractive from the loading stresses and the last equation is reduced to

$$D_t = \sum_{i=1}^{m} \frac{n_i}{N_i} \tag{3.11}$$

where D_r is the damage ratio accumulated over the design period due to all load groups m is the total number of load groups, n_i is the predicted number of repetitions for the ith load group, and N_i is the allowable number of repetitions for the ith load group, which can be determined from the equations 3.12-3.14. The accumulated damage ratio at the end of the design period should be smaller than 1.

For $\frac{\sigma}{S_c} \geq 0.55$:

$$\log N_f = 11.737 - 12.077\left(\frac{\sigma}{S_c}\right) \tag{3.12}$$

For $0.45 < \frac{\sigma}{S_c} < 0.55$:

$$N_f = \left(\frac{4.2577}{\frac{\sigma}{S_c} - 0.4325}\right)^{3.268} \tag{3.13}$$

For $\frac{\sigma}{S_c} \leq 0.45$:

$$N_f = unlimited \tag{3.14}$$

where σ is the flexural stress in the slab, S_c is the modulus of rupture of the concrete (M_R).

The position of the outside wheels has a significant role in the pavement thickness design. The placement of outside wheels at the pavement edge, as shown in the Figure 3.13, produces a critical stress higher than that at other locations. At increasing distances inward from the edge, the frequency of load applications increases, but the magnitude of edge stress decreases.

The theoretical procedure to compute the damage ratio at the pavement edge caused by each load placement and sum the total damage is too cumbersome for design purpose. In the simplified method developed by the PCA, fatigue at the pavement edge was computed by placing the load incrementally at different distances inward from the slab edge for typical distributions of truck placement. It was found

that the same fatigue damage can be obtained by considering the edge loading only and placing 6% of the total number of load repetitions at the pavement edge. If the total number of repetitions is used for design, the edge stress must be reduced to obtain the same fatigue consumption. For 6% truck encroachment, the edge stress must be multiplied by an adjusting factor of 0.894, as shown in Figure 3.14. This factor was used in preparing the design tables.

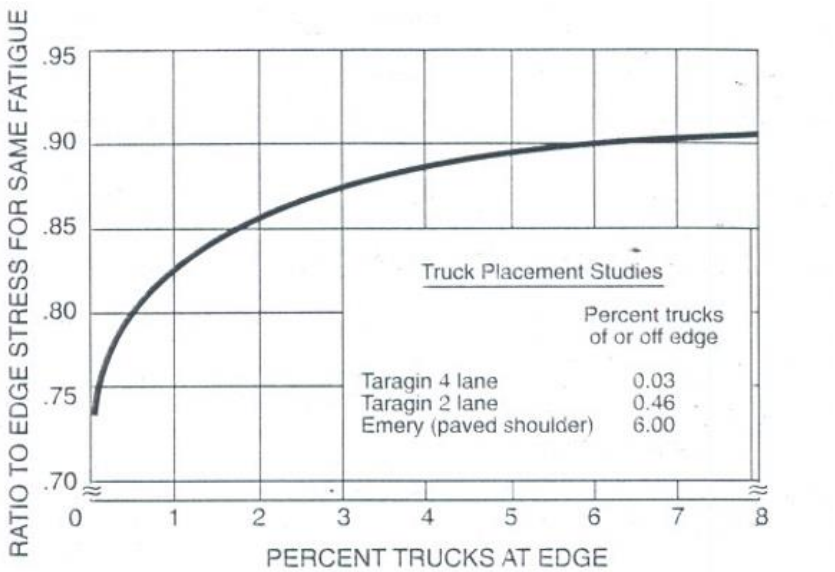

Figure 3.14 - Equivalent edge stress factor depends on the percent of trucks at edge [15]

Figure 3.15 shows the Fatigue analysis-allowable load repetitions based on stress ratio factor with and without concrete shoulder. The equivalent stresses are shown in tables 3.10 and 3.11 using shoulder, and 3.12 and 3.13 without shoulder.

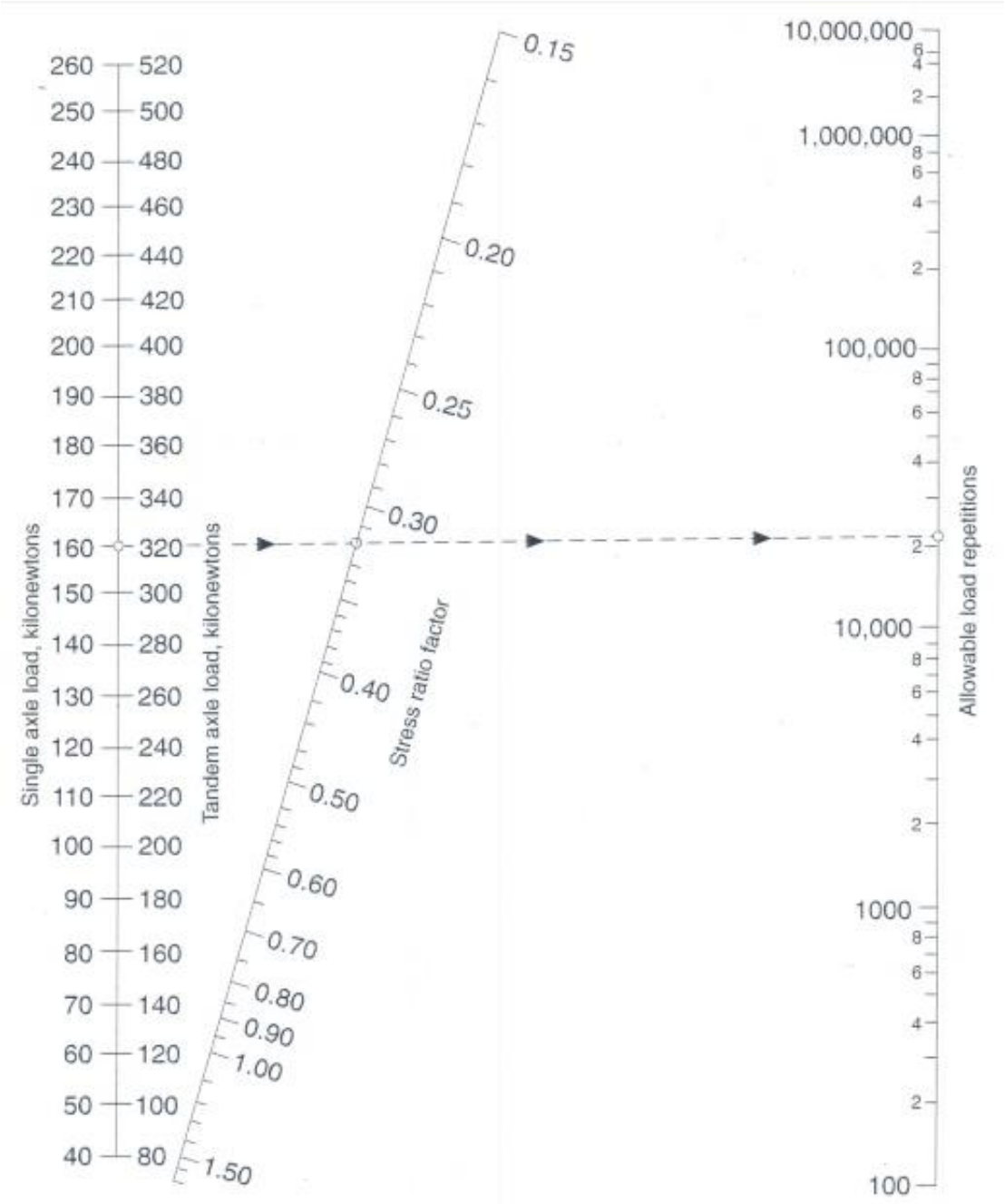

Figure 3.15 - Fatigue analysis-allowable load repetitions based on stress ratio factor (with and without concrete shoulder) [15]

Table 3.10 - Equivalent Stress-Concrete Shoulder (Single Axle/Tandem Axle/Tridem Axle) (adapted from [6])

Slab thickness (mm)	k of subgrade-subbase (MPa/m)								
	20			40			60		
	Single	Tandem	Tridem	Single	Tandem	Tridem	Single	Tandem	Tridem
150	2,44	2,08	1,62	2,15	1,80	1,44	2,00	1,67	1,37
160	2,24	1,93	1,49	1,97	1,66	1,32	1,84	1,53	1,24
170	2,06	1,79	1,38	1,82	1,54	1,21	1,70	1,42	1,14
180	1,91	1,67	1,28	1,69	1,43	1,12	1,57	1,32	1,05
190	1,77	1,57	1,19	1,57	1,34	1,04	1,46	1,23	0,98
200	1,65	1,48	1,12	1,46	1,26	0,98	1,37	1,16	0,91
210	1,55	1,40	1,05	1,37	1,19	0,92	1,28	1,09	0,85
220	1,45	1,32	0,99	1,29	1,12	0,86	1,20	1,03	0,80
230	1,37	1,26	0,93	1,21	1,70	0,81	1,13	0,98	0,76
240	1,29	1,20	0,88	1,15	1,01	0,77	1,07	0,93	0,71
250	1,22	1,14	0,84	1,08	0,97	0,73	1,01	0,88	0,68

Table 3.11 - Equivalent Stress-Concrete Shoulder (Single Axle/Tandem Axle/Tridem Axle) (adapted from [6])

Slab thickness (mm)	k of subgrade-subbase (MPa/m)								
	80			140			180		
	Single	Tandem	Tridem	Single	Tandem	Tridem	Single	Tandem	Tridem
150	1.90	1.59	1.33	1.73	1.48	1.24	1.66	1.44	1.60
160	1.75	1.46	1.20	1.59	1.35	1.15	1.53	1.31	1.13
170	1.62	1.35	1.10	1.48	1.24	1.04	1.42	1.20	1.03
180	1.50	1.25	1.01	1.37	1.15	0.96	1.32	1.11	0.94
190	1.40	1.17	0.94	1.28	1.07	0.88	1.23	1.03	0.86
200	1.30	1.10	0.87	1.19	1.00	0.82	1.15	0.96	0.80
210	1.22	1.03	0.81	1.12	0.93	0.76	1.08	0.90	0.74
220	1.15	0.97	0.76	1.05	0.88	0.71	1.01	0.85	0.69
230	1.08	0.92	0.72	0.99	0.83	0.67	0.96	0.80	0.65
240	1.02	0.87	0.68	0.94	0.79	0.63	0.90	0.76	0.61
250	0.97	0.83	0.64	0.89	0.75	0.59	0.86	0.72	0.57

Table 3.12 - Equivalent Stress-No Concrete Shoulder (Single Axle/Tandem Axle/Tridem Axle) (adapted from [6])

Slab thickness (mm)	k of subgrade-subbase (MPa/m)								
	20			40			60		
	Single	Tandem	Tridem	Single	Tandem	Tridem	Single	Tandem	Tridem
150	3.06	2.64	1.99	2.70	2.23	1.67	2.51	2.04	1.55
160	2.79	2.45	1.85	2.47	2.06	1.54	2.29	1.87	1.41
170	2.56	2.28	1.73	2.26	1.91	1.43	2.10	1.74	1.30
180	2.37	2.14	1.62	2.09	1.79	1.34	1.94	1.62	1.21
190	2.19	2.01	1.53	1.94	1.67	1.26	1.80	1.51	1.13
200	2.04	1.90	1.45	1.80	1.58	1.19	1.67	1.42	1.07
210	1.91	1.79	1.37	1.68	1.49	1.13	1.56	1.34	1.01
220	1.79	1.70	1.30	1.57	1.41	1.07	1.46	1.27	0.95
230	1.68	1.62	1.24	1.48	1.34	1.02	1.38	1.21	0.91
240	1.58	1.55	1.18	1.39	1.28	0.97	1.30	1.15	0.87
250	1.49	1.48	1.13	1.32	1.22	0.93	1.22	1.09	0.83

Table 3.13 - Equivalent Stress-No Concrete Shoulder (Single Axle/Tandem Axle/Tridem Axle) (adapted from [6])

Slab thickness (mm)	k of subgrade-subbase (MPa/m)								
	80			140			180		
	Single	Tandem	Tridem	Single	Tandem	Tridem	Single	Tandem	Tridem
150	2.37	1.92	1.48	2.13	1.72	1.40	2.03	1.65	1.37
160	2.17	1.76	1.34	1.95	1.57	1.25	1.86	1.50	1.23
170	1.99	1.63	1.23	1.80	1.45	1.14	1.71	1.38	1.11
180	1.84	1.51	1.14	1.66	1.34	1.04	1.58	1.27	1.01
190	1.71	1.41	1.06	1.54	1.25	0.96	1.47	1.18	0.92
200	1.59	1.33	0.99	1.43	1.17	0.89	1.37	1.11	0.85
210	1.48	1.25	0.93	1.34	1.10	0.83	1.28	1.04	0.79
220	1.39	1.18	0.88	1.26	1.03	0.78	1.20	0.98	0.74
230	1.31	1.12	0.84	1.18	0.98	0.73	1.13	0.92	0.70
240	1.23	1.06	0.80	1.11	0.93	0.69	1.06	0.87	0.66
250	1.16	1.01	0.76	1.05	0.88	0.66	1.00	0.83	0.62

b) Erosion Analysis

Pavement distresses such as pumping, erosion of foundation, and joint faulting are related more to pavement deflections than to flexural stresses. The most critical pavement deflection occurs at the slab corner when an axle load is placed at the joint near the corner, as shown in Figure 3.16.

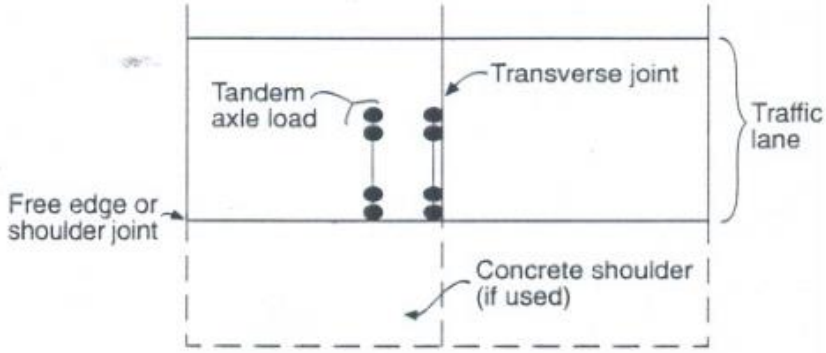

Figure 3.16 - Axle-load position for critical pavement deflection [15]

The principal mode of failure in the AASHO Road Test was pumping or erosion of the granular subbase from under the slabs. However, satisfactory correlations between corner deflections and the performance of these pavements could not be obtained. It was found that, to be able to predict their performance, different values of deflection criteria would have to be applied, depending on the slab thickness and, to a small extent, on the modulus of subgrade reaction. A better correlation was obtained by relating the performance to the rate of work, defined as the product of corner deflection w and pressure p at the slab-foundation interface, divided by the length of the deflection basin, which is a function of the radius of relative stiffness L. The concept is that a thin slab with a shorter deflection basin receives a faster load punch than a thicker slab. The following equation was developed to compute the allowable load repetitions:

$$\log N = 14.524 - 6.777(C_1 P - 9.0)^{0.103} \tag{3.15}$$

In this equation, N is the allowable number of load repetitions (based on a PSI of 3.0), C_1 is an adjustment factor (with a value of 1 for untreated subbases and 0 .9 for stabilized subbases), and P is the rate of work or power, defined by

$$P = 268.7 \frac{p^2}{hk^{0.73}} \tag{3.16}$$

In which p is the pressure on the foundation under the slab corner in psi (which is equal to kw for a liquid foundation), h is the thickness of slab in inches, and k is the modulus of subgrade reaction in pci. The equation for erosion damage is

$$Percentage\ erosion\ damage = 100 \sum_{i=1}^{m} \frac{C_2 n_i}{N_i} \tag{3.17}$$

where $C_2 = 0.06$ for pavements without concrete shoulders and 0 .94 for pavements with tied concrete shoulders. With a concrete shoulder, the corner deflection is not significantly affected by the truck load placement, so a large C_2 should be used. The percent erosion damage should be less than 100%.

Figure 3.17 shows the erosion analysis- allowable load repetitions based on erosion factor (without concrete shoulder). Figure 3.18 shows the erosion analysis- allowable load repetitions based on erosion factor (with concrete shoulder). Erosion factors for doweled Joints are shown in tables 3.14 and 3.15 using shoulder, and 3.16 and 3.17 without shoulder.

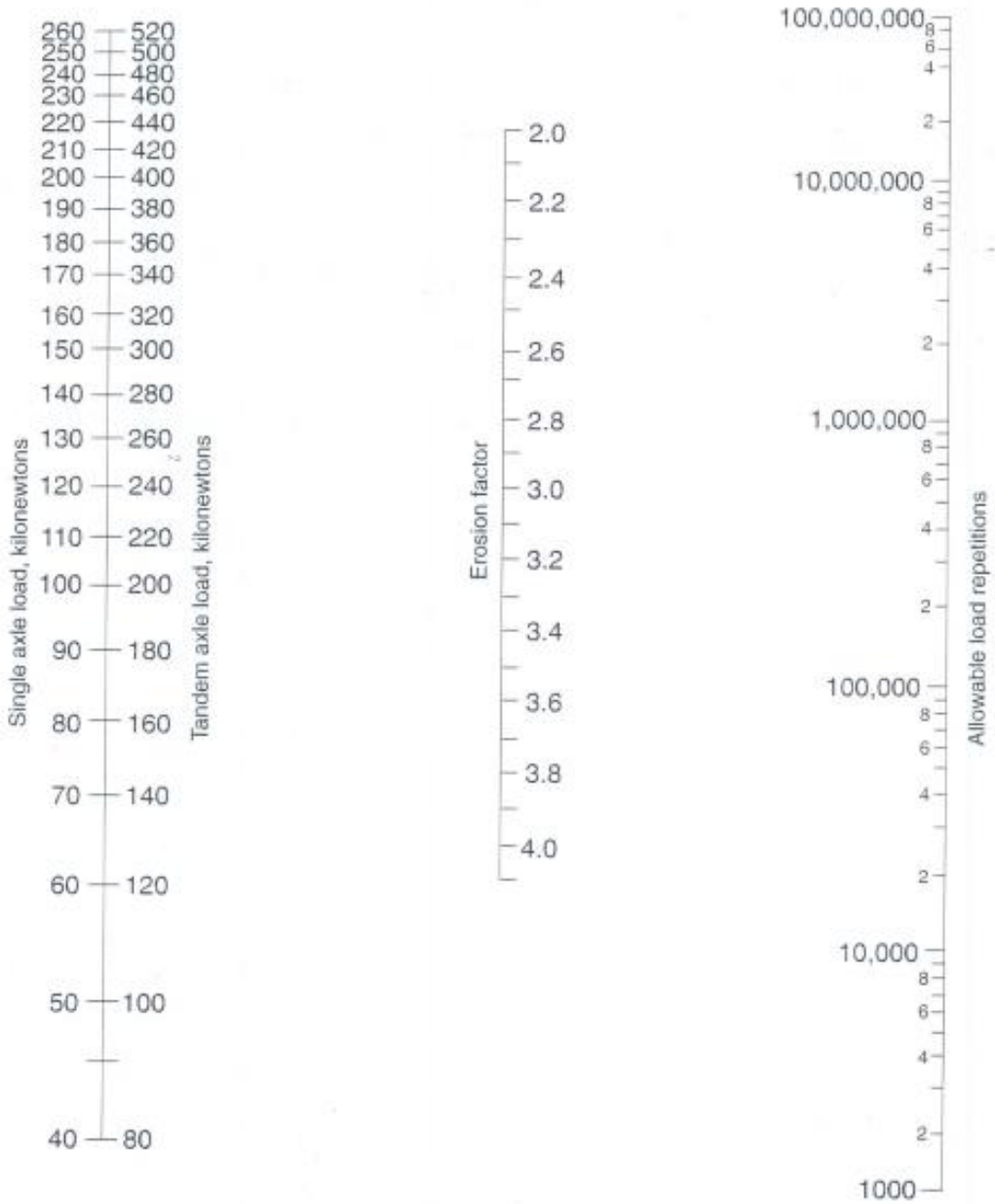

Figure 3.17 - Erosion analysis-allowable load repetitions based on erosion factor (without concrete shoulder) [15]

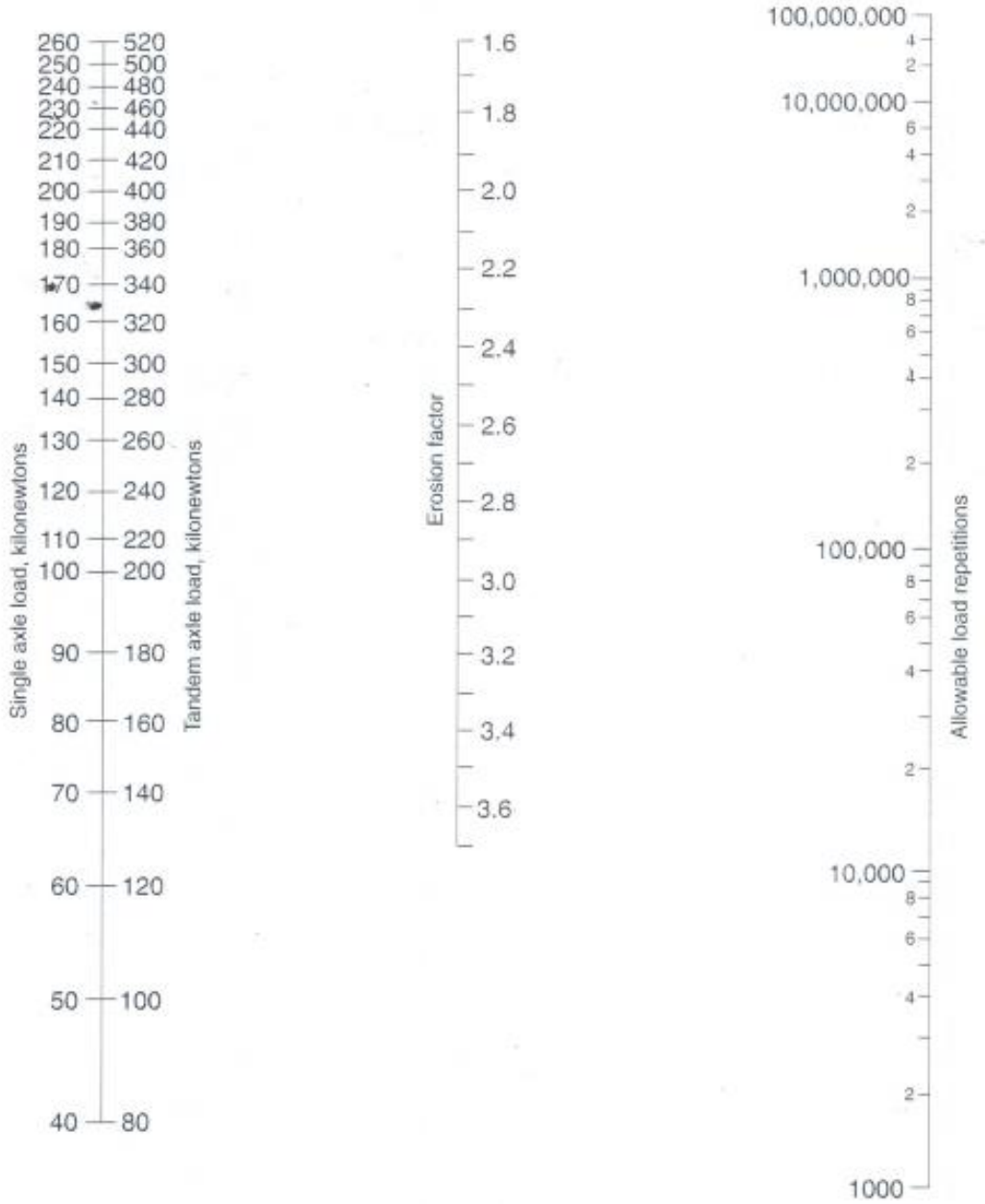

Figure 3.18 - Erosion analysis-allowable load repetitions based on erosion factor (with concrete shoulder) [15]

Table 3.14 - Erosion Factors-Doweled Joints, Concrete Shoulder (Single Axle/Tandem Axle/Tridem Axle) (adapted from [6])

Slab thickness (mm)	k of subgrade-subbase (MPa/m)								
	20			40			60		
	Single	Tandem	Tridem	Single	Tandem	Tridem	Single	Tandem	Tridem
150	2.79	2.88	2.95	2.74	2.77	2.80	2.72	2.71	2.73
160	2.71	2.82	2.91	2.66	2.71	2.76	2.64	2.65	2.67
170	2.64	2.77	2.86	2.59	2.65	2.71	2.57	2.59	2.62
180	2.57	2.72	2.82	2.52	2.60	2.67	2.50	2.54	2.58
190	2.51	2.67	2.79	2.46	2.56	2.63	2.43	2.49	2.54
200	2.45	2.63	2.75	2.40	2.51	2.59	2.37	2.44	2.50
210	2.39	2.58	2.72	2.34	2.47	2.56	2.31	2.40	2.47
220	2.34	2.54	2.68	2.29	2.43	2.53	2.26	2.36	2.43
230	2.29	2.50	2.65	2.23	2.39	2.49	2.21	2.32	2.40
240	2.24	2.46	2.62	2.18	2.35	2.46	2.16	2.28	2.37
250	2.19	2.43	2.59	2.14	2.31	2.44	2.11	2.24	2.34

Table 3.15 - Erosion Factors-Doweled Joints, Concrete Shoulder (Single Axle/Tandem Axle/Tridem Axle) (adapted from [6])

Slab thickness (mm)	k of subgrade-subbase (MPa/m)								
	80			140			180		
	Single	Tandem	Tridem	Single	Tandem	Tridem	Single	Tandem	Tridem
150	2.70	2.67	2.67	2.67	2.60	2.59	2.65	2.57	2.56
160	2.62	2.60	2.62	2.59	2.53	2.52	2.57	2.50	2.49
170	2.55	2.55	2.57	2.51	2.46	2.47	2.49	2.43	2.43
180	2.48	2.49	2.52	2.44	2.41	2.41	2.42	2.37	2.37
190	2.41	2.44	2.48	2.38	2.35	2.37	2.36	2.32	2.32
200	2.35	2.40	2.44	2.31	2.31	2.32	2.30	2.27	2.28
210	2.29	2.35	2.40	2.26	2.26	2.28	2.24	2.22	2.23
220	2.24	2.31	2.37	2.20	2.22	2.25	2.18	2.18	2.20
230	2.19	2.27	2.34	2.15	2.18	2.21	2.13	2.13	2.16
240	2.13	2.23	2.31	2.10	2.14	2.18	2.08	2.10	2.13
250	2.09	2.20	2.28	2.05	2.10	2.15	2.03	2.06	2.10

Table 3.16 - Erosion Factors-Doweled Joints, No Concrete Shoulder (Single Axle/Tandem Axle/Tridem Axle) (adapted from [6])

Slab thickness (mm)	k of subgrade-subbase (MPa/m)								
	20			40			60		
	Single	Tandem	Tridem	Single	Tandem	Tridem	Single	Tandem	Tridem
150	3.22	3.36	3.47	3.21	3.30	3.36	3.20	3.27	3.31
160	3.14	3.28	3.41	3.12	3.22	3.30	3.11	3.19	3.25
170	3.06	3.22	3.35	3.04	3.15	3.24	3.03	3.12	3.19
180	2.99	3.16	3.30	2.97	3.09	3.19	2.96	3.06	3.13
190	2.92	310	3.25	2.90	3.03	3.14	2.88	2.99	3.08
200	2.85	3.05	3.21	2.83	2.97	3.09	2.82	2.94	3.03
210	2.79	2.99	3.16	2.77	2.92	3.05	2.75	2.88	2.99
220	2.73	2.95	3.12	2.71	2.87	3.01	2.69	2.83	2.94
230	2.67	2.90	3.08	2.65	2.82	2.97	2.64	2.78	2.90
240	2.62	2.86	3.05	2.60	2.78	2.93	2.58	2.73	2.86
250	2.57	2.82	3.01	2.54	2.73	2.89	2.53	2.69	2.83

Table 3.17 - Erosion Factors-Doweled Joints, No Concrete Shoulder (Single Axle/Tandem Axle/Tridem Axle) (adapted from [6])

Slab thickness (mm)	k of subgrade-subbase (MPa/m)								
	80			140			180		
	Single	Tandem	Tridem	Single	Tandem	Tridem	Single	Tandem	Tridem
150	3.19	3.25	3.28	3.17	3.21	3.22	3.16	3.19	3.19
160	3.10	3.17	3.21	3.09	3.13	3.15	3.08	3.12	3.12
170	3.02	3.10	3.15	3.01	3.06	3.08	3.00	3.04	3.05
180	2.95	3.03	3.09	2.93	2.99	3.02	2.92	2.97	2.99
190	2.88	2.7	3.04	2.86	2.93	2.96	2.85	2.91	2.93
200	2.81	2.91	2.99	2.79	2.87	2.91	2.78	2.85	2.88
210	2.75	2.86	2.94	2.73	2.81	2.86	2.72	2.79	2.83
220	2.69	2.80	2.90	2.67	2.76	2.82	2.66	2.73	2.78
230	2.63	2.75	2.86	2.61	2.70	2.77	2.60	2.68	2.74
240	2.57	2.71	2.82	2.55	2.66	2.73	2.54	2.63	2.69
250	2.52	2.66	2.78	2.50	2.61	2.69	2.49	2.59	2.65

3.4.2.3. Other features

The previous sections presented the PCA design method if axle load data are available. If it is not the case, the PCA design manual also includes a simplified design procedure to be used when axle load data are not available, as well as an analysis of concrete pavements with a lean concrete subbase, and an analysis of tridem-axle loads. These features are described in this section.

a) Simplified Design Procedure

- Traffic Category

  Traffic is divided into four axle load categories. The ADT and ADTT values should not be used as the primary criteria for selecting the axle load category. Instead, it should be placed on word descriptions of the expected maximum axle loads. The axle load distributions used to prepare the simplified design tables for each traffic category are shown in Table 3.18. Each of these is the average of several W-4 tables representing pavement facilities in the appropriate category.

Table 3.18 - Axle-Load Categories [15]

Axle-Load category	Description	Traffic			Maximum axle loads, kN	
			ADTT**			
		ADT	%	Per day	Single axles	Tandem axles
1	Residential streets Rural and secondary roads (low to medium*)	200—800	1-3	Up to 25	98	160
2	Collector streets Rural and secondary roads (high*) Arterial streets and primary roads (low*)	700-5000	5 - 18	40-1000	115	195
3	Arterial streets and primary roads (medium) Expressways and urban and rural interstate highways (low to medium*)	3000-12000 2 lanes 3000-50000+ 4 lanes or more	8-30	500-5000+	133	230
4	Arterial streets, primary roads, expressways (high*) Urban and rural interstate highways (medium to high)	3000-20000 2 lanes 3000-150000+ 4 lanes or more	8-30	1500-8000+	151	267

* The descriptors high, medium, or low refer to the relative weights of axle loads for the type of the street or road; that is, “low" for a rural provincial would represent heavier loads than "low" for a secondary road.

** Trucks, two-axle, four-tire trucks excluded.

- Subgrade–Subbase Strength
  Subgrade–subbase strength is characterized by the descriptive terms low, medium, high, and very high. These terms are related to the modulus of subgrade reaction k, as shown in the next table.

Table 3.19 - Subgrade Soil Types and Approximate k Values [15]

Type of soil	Subgrade strength	k values range, MPa/m
Fine-grained soils in which silt and clay-size particles predominate	Low	20-34
Sands and sand-gravel mixtures with moderate amounts of silt and clay	Medium	35-49
Sands and sand-gravel mixtures relatively free of plastic fines	High	50-60
Cement-treated subbases	Very high	70-110

When a subbase is used, the increase in k value can be determined from Table 3.5 or 3.6, depending on whether the subbase is untreated or stabilized.

- Design Tables
  The PCA design manual contains a series of tables showing the allowable ADTT for pavements with either doweled or aggregate interlock joints. Individual tables were developed for each axle load category. As an example of the method, Figure 3.19 and 3.20 for axle load category 2 with doweled joints and aggregates interlock are presented below

	No Concrete Shoulder or Curb						With Concrete Shoulder or Curb				
	Slab thickness, mm	Subgrade-subbase support (MPa/m) Low (20-34)	Medium (35-49)	High (50-60)	Very High (70 +)		Slab thickness, mm	Subgrade-subbase support (MPa/m) Low (20-34)	Medium (35-49)	High (50-60)	Very High (70+)
MR = 4.4 MPa	140				3	MR = 4.4 MPa	120				6
	150			5	26		130		4	12	53
	160	2	12	35	150		140	6	30	86	330
	170	15	68	190	740		150	44	180	470	1700
	180	77	320	820	3100		160	240	890	2200	
	190	330	1300	3200			170	1000	3700		
	200	1200	4500				180	4100			
	210	4100									
MR = 4.1 MPa	150				5	MR = 4.1 MPa	130				12
	160		2	8	38		140		7	20	87
	170	3	16	47	200		150	10	46	130	470
	180	18	82	220	870		160	60	240	620	2100
	190	85	350	900	3300		170	290	1100	2600	
	200	330	1300	3300			180	1200	4100		
	210	1200	4400				190	4200			
	220	3700									
MR = 3.8 MPa	160				8	MR = 3.8 MPa	140			4	18
	170		3	9	46		150		9	28	110
	180	3	17	51	220		160	12	56	150	550
	190	18	82	220	870		170	67	270	670	2300
	200	78	320	840	3100		180	290	1100	2600	
	210	290	1100	2900			190	1100	3900		
	220	940	3600				200	3700			
	230	2900									

Note: Fatigue analysis controls the design.
* ADTT is two way for 20-year design life and excludes two-axle, four-tire trucks, so total number of trucks allowed will be greater—see text.

Figure 3.19 - Allowable ADTT, Axle-Load Category 2* - Pavements with Doweled Joints [15]

The allowable ADTT is based on a 20-year design period and does not include any two-axle, four-tire trucks. If the design period is not 20 years, the predicted ADTT must be changed proportionately. The load safety factors are incorporated already in the tables. The tables were developed by first assuming an ADTT and then determining the percentages of fatigue and erosion damage from the given slab thickness, concrete modulus of rupture, and subgrade-subbase k value.

The allowable ADTT was then computed as

$$Allowable\ ADTT = \frac{100 \times (assumed\ ADTT)}{\%\ fatigue\ or\ erosion\ damage} \tag{3.18}$$

	No Concrete Shoulder or Curb						With Concrete Shoulder or Curb				
	Slab thickness, mm	Subgrade-subbase support (MPa/m) Low (20-34)	Medium (35-49)	High (50-60)	Very High (70 +)		Slab thickness, mm	Subgrade-subbase support (MPa/m) Low (20-34)	Medium (35-49)	High (50-60)	Very High (70+)
MR = 4.4 MPa	140				3	MR = 4.4 MPa	120				6
	150			5	26		130		4	12	53
	160	2	12	35	150		140	6	30	86	330
	170	15	68	190	740		150	44	180	470	840**
	180	77	320	820	1300**		160	240	800**	1100**	1500**
	190	330	1200**	1500**	2000**		170	800**	1300**	1800**	2800**
	200	1200	1700**	2100**	3000**		180	1200**	2100**	3100**	
	210	1600**	2300**	3100**			190	1900**	3500**		
	220	2100**	3200**				200	2900**			
	230	2900**									
MR = 4.1 MPa	150				5	MR = 4.1 MPa	130			2	12
	160		2	8	38		140		7	20	87
	170	3	16	47	200		150	10	46	130	470
	180	18	82	220	870		160	60	240	620	1500**
	190	85	350	900	2000**		170	290	1100	1800**	2800**
	200	330	1300	2100**	3000**		180	1200**	2100**	3100**	
	210	1200	2300**	3100**			190	1900**	3500**		
	220	2100**	3200**				200	2900**			
	230	2900**									
MR = 3.8 MPa	160				8	MR = 3.8 MPa	140			4	18
	170		3	9	46		150		9	28	110
	180	3	17	51	220		160	12	56	150	550
	190	18	82	220	870		170	67	270	670	2300
	200	78	320	840	3000**		180	290	1100	2600	
	210	290	1100	2900			190	1100	3500**		
	220	940	3200**				200	2900**			
	230	2900**									

*ADTT is two way for 20-year design life and excludes two-axle, four-tire trucks, so total number of trucks allowed will be greater—see text.
** Erosion analysis controls the design; otherwise fatigue analysis controls.

Figure 3.20 - Allowable ADTT, Axle-Load Category 2* - Pavements with Aggregate-Interlock Joints [15]

b) Lean-Concrete Subbase

Design charts were developed by PCA for both bonded and unbounded cases. In the finite-element analysis, the two layers of slab were assumed to have the same width. This assumption provides additional margin of safety to the design because the lean-concrete subbase is usually built at least 0.60m wider than the pavement on each side to support the tracks of the slip form paver.

Figure 3.21 is the design chart for concrete pavements with lean-concrete sub bases. To use the design chart, the slab thickness required for a conventional pavement without a lean-concrete subbase must be determined by the procedure described previously. For a given thickness of lean-concrete subbase, the thickness of concrete slab can be reduced, depending on the moduli of rupture of the two concrete materials. The use of the design chart will ensure that the fatigue and erosion damage in the two layers of concrete does not exceed that in the conventional pavement. The use of a very low modulus of rupture, e.g., 1.4 MPa, is recommended to minimize reflection cracking from the unjointed subbase through the concrete surface.

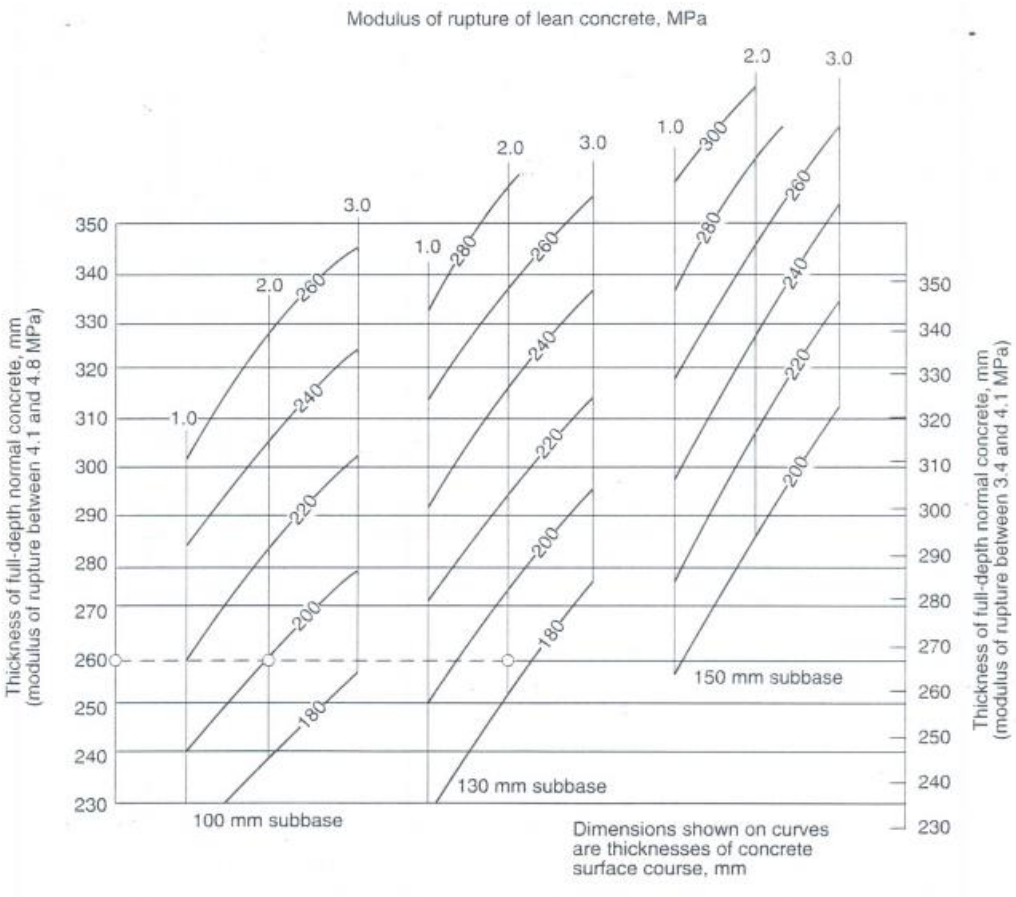

Figure 3.21 - Design chart for composite concrete pavement (lean concrete subbase) [15]

3.4.3. AASHTO DESIGN METHOD

The American Association of State Highway and Transportation Officials method (AASHTO method) is the most used design method for rigid pavement in the Unite State of America. About 85% of the state highway agencies use the AASTHO pavement design procedure for rigid pavements [15]. In several countries of Central and South America is the AASHTO method used, as well.

The design is based on the empirical equations obtained from the AASHO Road Test, with further modifications based on the theory and experience. In the following subsections, taken from [15], the details of the design equations and design parameters are presented:

3.4.3.1. Design equations

As it was mentioned, the equations were based on the AASHO Road Test findings. Then the original equations were modified to consider a range of the subgrade and climate conditions.

a) Original Equations

$$G_t = \beta(\log W_t - \log \rho) \tag{3.19}$$

$$\beta = 100 + \frac{3.63(L_1 + L_2)^{5.20}}{(D+1)^{8.46} {L_2}^{3.52}} \tag{3.20}$$

$$\log \rho = 5.85 + 7.35 \log(D+1) - 4.62 \log(L_1 + L_2) + 3.28 \log L_2 \tag{3.21}$$

where $G_t =$ log [(4.5 - p_t) / (4.5-1.5)], where 4.5 is the initial serviceability for rigid pavements at the AASHO Road Test; p_t = serviceability at end of time t; L_1 is the load on one single axle or a set of tandem axles, in kip; L_2 =is the axle code (1 for single axle, 2 for tandem axle); D is the slab thickness in inches.

Using an equivalent 80-kN single axle load, i.e., $L_1 = 18$ and $L_2 = 1$, and combining equations, 3.19, 3.20, and 3.21, the final expression is expressed as follows

$$\log W_{t18} = 7.35 \log(D+1) - 0.06 + \frac{\log\left[(4.5 - p_t)/(4.5 - 1.5)\right]}{1 + 1.624 \times 10^7/(D+1)^{8.46}} \tag{3.22}$$

where: W_{t18} is the number of 18-kip (80-kN) single-axle load applications to time t and p_t is the terminal serviceability index.

Equation 3.22 is applicable only to the pavements in the AASHO Road Test with the following conditions:

Modulus of elasticity of concrete $E_c = 4.2 \times 10^7 psi$ (29 GPa),

Modulus of rupture of concrete $S_c = 690\ psi$ (4.8 MPa),

Modulus of subgrade reaction $k = 60\ pci$ (16 MN/m^3),

Load transfer coefficient $J = 3.2$, and

Drainage coefficient $C_d = 1.0$.

b) Modified Equations

To use the equation 3.22 with subgrade coefficient and climate conditions different from those presented in the AASHO Road Test, the equation must be modified considering experimental and theoretical knowledge.

After comparing stresses calculated from strain measurements on the Road Test pavements with theoretical solutions, the Spangler equation for corner loading was selected for its simplicity by AASHTO (1972) to extend equation 3.22 to other conditions. The Spangler equation is given as:

$$\sigma = \frac{JP}{D^2}\left(1 - \frac{a_1}{l}\right) \tag{3.23}$$

where σ is the maximum tensile stress in concrete in psi, J is the load transfer coefficient, P is the wheel load in lb, a_1 is the distance from corner of slab to center of load, and l is the radius of relative stiffness rewritten as:

$$l = \left[\frac{ZD^3}{12(1-\vartheta^2)}\right]^{0.25} \tag{3.24}$$

In which $Z = E_c/k$ and ϑ is the Poisson ratio of concrete. If a_1 = 10 in. (254 mm) and $\vartheta = 0.2$ and substituting equation 3.24 into 3.23 gives

$$\sigma = \frac{JP}{D^2}\left(1 - \frac{18.42}{Z^{0.25}D^{0.75}}\right) \tag{3.25}$$

$$\log W_t = a - (4.22 - 0.32p_t)\log\frac{\sigma}{S_c} \tag{3.26}$$

Stresses were calculated for different combinations of Road Test variables by using equation 3.25. The ratio between the calculated stresses and the modulus of rupture, σ/S_c, was subsequently compared with axle-load applications. These comparisons indicated the following relationship:

Assuming the same form of equation for other pavements with W_t', σ, and S_C' yields

$$\log W_t' = a - (4.22 - 0.32p_t)\log\frac{\sigma'}{S_C'} \tag{3.27}$$

Combining equations 3.26 and 3.27 and using the equivalent 18-kip (80-kN) single-axle load gives

$$\log W_{t18}' = \log W_{t18} + (4.22 - 0.32p_t)\log\left(\frac{S_C'\sigma}{S_c\sigma'}\right) \tag{3.28}$$

From equation 3.25,

$$\frac{\sigma}{\sigma'} = \frac{J}{J'}\frac{[1 - 18.42/(Z^{0.25}D^{0.75})]}{[1 - 18.42/(Z'^{0.25}D^{0.75})]} \tag{3.29}$$

Combining equations. 3.22, 3.28, and 3.29 results in

$$\log W'_{t18} = 7.35\log(D+1) - 0.06 + \frac{\log\left[(4.5 - p_t)/(4.5-1.5)\right]}{1 + 1.624\times10^7/(D+1)^{8.46}} + (4.22 - 0.32p_t)\log\left[\left(\frac{S'_C J}{S_c J'}\right)\left(\frac{D^{0.75} - 18.42/Z^{0.25}}{D^{0.75} - 18.42/Z'^{0.25}}\right)\right] \quad (3.30)$$

Letting

$Z = \frac{E_c}{k} = \frac{4.2\times10^6}{60} = 70.000$, $S_c = 690$, and $J = 3.2$; adding a drainage coefficient C_d and a reliability term $Z_R S_o$; replacing the term $(4.5 - p_t)$ by ΔPSI; and removing the primes for simplicity, the final design equation for rigid pavements becomes

$$\log W_{18} = Z_R S_o + 7.35\log(D+1) - 0.06 + \frac{\log\left[\frac{\Delta\text{PSI}}{4.5-1.5}\right]}{1 + \frac{1.624\times10^{7^{8.46}}}{D+1}} + (4.22 - 0.32p_t)\log\left\{\frac{S_c C_d (D^{0.75} - 1.132)}{215.63J[D^{0.75} - 18.42/(E_c/k)^{0.25}]}\right\} \quad (3.31)$$

There are several ways to design the rigid pavement thickness:

Using AASHTO software, such as the AASHTOWare, available in the AASHTO homepage, the software package is not free, but they offer technical support and the team has a lot of expertise.

Using a monograph available if some textbooks, such as the book pavement analysis and design by Huang [15]. Note that p_t does not appear in the monograph because it was assumed that $p_t = 4.5 - \Delta PSI$,

Programming the equations in a spreadsheet,

Using a free online calculator or application. Since the goal of this document is not the thickness design, the solving method selected is the usage of the app, available in Pavement Interactive homepage [13], for solving the 1993 AASHTO Rigid Pavement Structural Design equations.

3.4.3.2. Design Variables

The variables considered in the 1993 AASHTO Rigid Pavement Structural Design method are [13, 15]:

a) Time Constraints

The use of a longer analysis period for high-volume facilities, including at least one rehabilitation period, is encouraged by the AASHTO design guide. Thus, the analysis period should be equal to or greater than the performance period, as bellow.

- Performance Period
  It refers to the time that an initial pavement structure will last before it needs rehabilitation or the performance time between rehabilitation operations. It is equivalent to the time elapsed as a new, reconstructed, or rehabilitated structure deteriorates from its initial serviceability to its terminal serviceability.

- Analysis Period
  It is the period that any design strategy must cover. It may be identical to the selected performance period. However, realistic performance limitations may necessitate the consideration of staged construction or planned rehabilitation for the desired analysis period. Guidelines for the length of analysis period according with the road conditions are presented in Table 3.20.

Table 3.20 - Length of Analysis Period [15]

Road conditions	Analysis period (years)
High-volume urban	30–50
High-volume rural	20–50
Low-volume pave	15–25
Low-volume aggregate surface	10–20

b) Traffic

The design procedures are based on cumulative expected 80-kN (18-kip) equivalent single-axle load (ESAL). The determination of equivalent axle load factors (EALF) for rigid pavements is discussed below.

- Equivalent axle load factor (EALF)
  The EALF defines the damage per pass to a pavement by the axle in question relative to the damage per pass of a standard axle load, usually the 18-kip (80-kN) single-axle load. The design is based on the total number of passes of the standard axle load during the design period, defined as the equivalent single-axle load (ESAL) and computed by

$$ESAL = \sum_{i=1}^{m} \mathrm{F}_i \mathrm{n}_i \tag{3.32}$$

where: m is the number of axle load groups, F_i is the EALF for the ith-axle load group, and n_i is the number of passes of the ith-axle load group during the design period. The EALF depends on the type of pavements, thickness or structural capacity, and the terminal conditions at which the pavement is considered failed. Most of the EALFs in use today are based on experience. One of the most widely used methods is based on the empirical equations developed from the AASHO Road Test (AASHTO, 1972). The EALF can also be determined theoretically based on the critical stresses and strains in the pavement and the failure criteria.

AASHTO Equivalent Factors the AASHTO equations for determining the EALF of rigid pavements are as follows:

$$\log\left(\frac{W_{tx}}{W_{t18}}\right) = 4.62\log(18+1) - 4.62\log(L_x + L_2) + 3.28\log L_2 + \frac{G_t}{\beta_x} - \frac{G_t}{\beta_{18}} \tag{3.33}$$

$$G_t = \log\left(\frac{4.5 - p_t}{4.5 - 1.5}\right) \tag{3.34}$$

$$\beta_x = 1.00 + \frac{3.63(L_x + L_2)^{5.20}}{(D+1)^{8.46} L_2^{3.52}} \tag{3.35}$$

where W_{tx} is the number of x-axle load applications at the end of time t, W_{t18} is the number of 18-kip (80-kN) single-axle load applications to time t, L_x is the load in kip on one single axle, one set of tandem axles, or one set of tridem axles, L_2 is the axle code (1 for single axle, 2 for tandem axles, and 3 for tridem axles), p_t is the terminal serviceability, which indicates the pavement conditions to be considered as failures, β_{18} is the value of β_x when L_x is equal to 18 and L_2 is equal to one, and D is the slab thickness in inches.
The use of Table 3.21 for lane distribution factors and Table 3.22 for total growth factors and is recommended.

Table 3.21 - Lane Distribution Factor [15]

No. of lanes on each direction	Percentage of 18-kip ESAL in design lane
1	100
2	80–100
3	60–80
4	50–75

If a pavement is designed for the analysis period without any rehabilitation or resurfacing, all that is required is the total ESAL over the analysis period. However, if stage construction is considered and rehabilitation or resurfacing is anticipated, a graph or equation of cumulative ESAL versus time is needed so that the ESAL traffic during any given stages can be obtained.

Table 3.22 - Total Growth Factor [15]

Design period (year)	Annual growth rate (%)							
	No growth	2	4	5	6	7	8	10
1	1.0	1.00	1.00	1.00	1.00	1.00	1.00	1.00
2	2.0	2.02	2.04	2.05	2.06	2.07	2.08	2.10
3	3.0	3.06	3.12	3.15	3.18	3.21	3.25	3.31
4	4.0	4.12	4.25	4.31	4.37	4.44	4.51	4.64
5	5.0	5.20	5.42	5.53	5.64	5.75	5.87	6.11
6	6.0	6.31	6.63	6.80	6.98	7.15	7.34	7.72
7	7.0	7.43	7.90	8.14	8.39	8.65	8.92	9.49
8	8.0	8.58	9.21	9.55	9.90	10.26	10.64	11.44
9	9.0	9.75	10.58	11.03	11.49	11.98	12.49	13.58
10	10.0	10.95	12.01	12.58	13.18	13.82	14.49	15.94
11	11.0	12.17	13.49	14.21	14.97	15.78	16.65	18.53
12	12.0	13.41	15.03	15.92	16.87	17.89	18.98	21.38
13	13.0	14.68	16.63	17.71	18.88	20.14	21.50	24.52
14	14.0	15.97	18.29	19.16	21.01	22.55	24.21	27.97
15	15.0	17.29	20.02	21.58	23.28	25.13	27.15	31.77
16	16.0	18.64	21.82	23.66	25.67	27.89	30.32	35.95
17	17.0	20.01	23.70	25.84	28.21	30.84	33.75	40.55
18	18.0	21.41	25.65	28.13	30.91	34.00	37.45	45.60
19	19.0	22.84	27.67	30.54	33.76	37.38	41.45	51.16
20	20.0	24.30	29.78	33.06	36.79	41.00	45.76	57.28
25	25.0	32.03	41.65	47.73	54.86	63.25	73.11	98.35
30	30.0	40.57	56.08	66.44	79.06	94.46	113.28	164.49
35	35.0	49.99	73.65	90.32	111.43	138.24	172.32	271.02

c) Reliability ($Z_R S_o$)

Reliability is basically a means of incorporating some degree of certainty into the design process to ensure that the various design alternatives will last the analysis period. The higher the volume of traffic, difficulty of diverting traffic, and public expectation of availability increase, the higher should be the level of reliability to be used for design. Table 3.23 presents recommended levels of reliability for various functional classifications.

Table 3.23 - Suggested Levels of Reliability for Various Functional Classifications [15]

Functional classification	Recommended level of reliability	
	Urban	Rural
Interstate and other freeways	85-99.9	80-99.9
Principal arterials	80—99	75—95
Collectors	80-95	75-95
Local	50-80	50-80

The local conditions can be considered by application a standard deviation for the reliability concept. It is suggested that standard deviations of 0.39 for rigid pavements. These correspond to variances of 0.1521. When stage construction is considered, the reliability of each stage must be compounded to achieve the overall reliability as follows

$$R_{stage} = (R_{overall})^{\frac{1}{n}} \tag{3.36}$$

In which n is the number of stages being considered. For example, if two stages are contemplated and the desired level of overall reliability is 90%, the reliability of each stage must be $(0.90)^{\frac{1}{2}}$, or 94.8%.

d) Environmental Effects

Since the AASHO design equations were based on the results of traffic tests over a two-year period, the long-term effects of temperature and moisture on the reduction of serviceability were not included. If problems of swell clay and frost heave are significant in each region and have not been properly corrected, the loss of serviceability over the analysis period should be estimated and added to that due to cumulative traffic loads.

Figure 3.22 shows the serviceability loss versus time curves for a specific location. These curves indicate that the serviceability loss due to environment increases at a decreasing rate. This may favor the use of stage construction because most of the loss will occur during the first stage and can be corrected with little additional loss in later stages. The environmental loss is a summation of losses from both swelling and frost heave. The chart may be used to estimate the serviceability loss at any intermediate period, for example, a loss of 0 .73 at the end of 13 years. If only swelling or frost heave is considered, there will be only one curve on the graph [15].

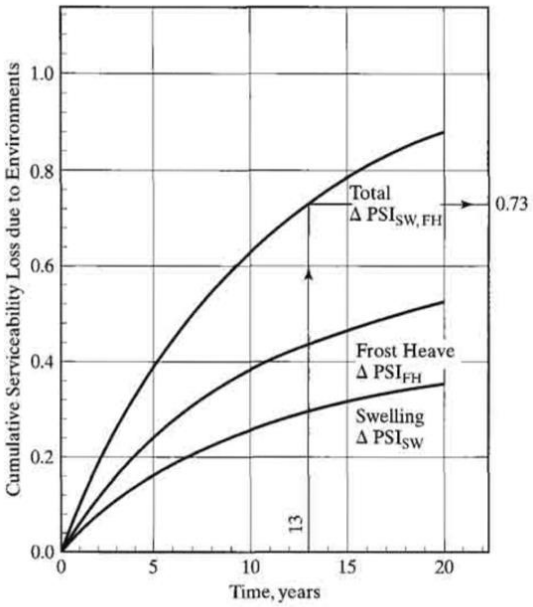

Figure 3.22 - Environmental serviceability loss versus time for a specific location [15]

The serviceability loss due to roadbed swelling depends on the swell rate constant, the potential vertical rise, and the swell probability; that due to frost heave depends on the frost heave rate, the maximum potential serviceability loss, and the frost heave probability.

e) Serviceability

The change in serviceability, ΔPSI, to be used in the design equations is computed from the initial and terminal serviceability indexes. The initial serviceability index is a function of pavement type and construction quality. Typical values from the AASHO Road Test were 4.2 for flexible pavements and 4.5 for rigid pavements.

A terminal serviceability index of 2.5 or higher is suggested for design of major highways and 2.0 for highways with lower traffic. For relatively minor highways where economics dictates a minimum initial capital outlay, it is suggested that this be accomplished by reducing the design period or total traffic volume, rather than by designing a terminal serviceability index less than 2.0. This index is the lowest index that will be tolerated before rehabilitation, resurfacing, and reconstruction become necessary.

f) Modulus of Subgrade Reaction (k value)

As mentioned previously, there are several correlations between the modulus of subgrade reaction for liquid foundation and the resilient modulus for solid foundation. Any relationship between k and M_R is arbitrary and depends on whether stresses or deflections are to be compared and on whether the loads are applied at the interior, edge, or corner of the slab.

- Without Subbase
  AASHTO suggested the use of the following theoretical relationship if the slab is placed directly on the subgrade without a subbase

$$k = \frac{M_R}{19.4} \tag{3.37}$$

with k in pci and M_R in psi. This equation is based on an analysis of a plate (30in diameter) bearing test and it gives a k value that is too large.

The modulus of subgrade reaction, which is defined as the ratio between an applied pressure q and the deflection w_0, can be expressed as

$$k = \frac{q}{w_0} = \frac{2M_R}{\pi(1-\vartheta^2)a} \tag{3.38}$$

where ϑ is the Poisson ratio of the foundation and a is the radius of the plate. If ϑ = 0.45 and a = 15 in. (381 mm), then equation 3.37 becomes

$$k = \frac{M_R}{18.8} \tag{3.39}$$

The equation 3.39 is more appropriate than equation 3.37. However, both equations give values too large because the value of k is inversely proportional to a. To correlate k with M_R, a very large plate should be used. Too small stresses and deflections, as compared with those based on M_R, are obtained if the equations 3.37 and 3.39 are used. Since 2011 the 3.37 and 3.39 are no longer used [13].

- With subbase
  If a subbase is used, the composite modulus of subgrade reaction can be estimated using the Figure 3.23. The modulus is based on a subgrade of infinite depth and is denoted by k_∞. The chart was developed by using the same method as for a homogeneous half-space. Therefore, the k values obtained from the chart are too large and do not represent what occurs in the field.

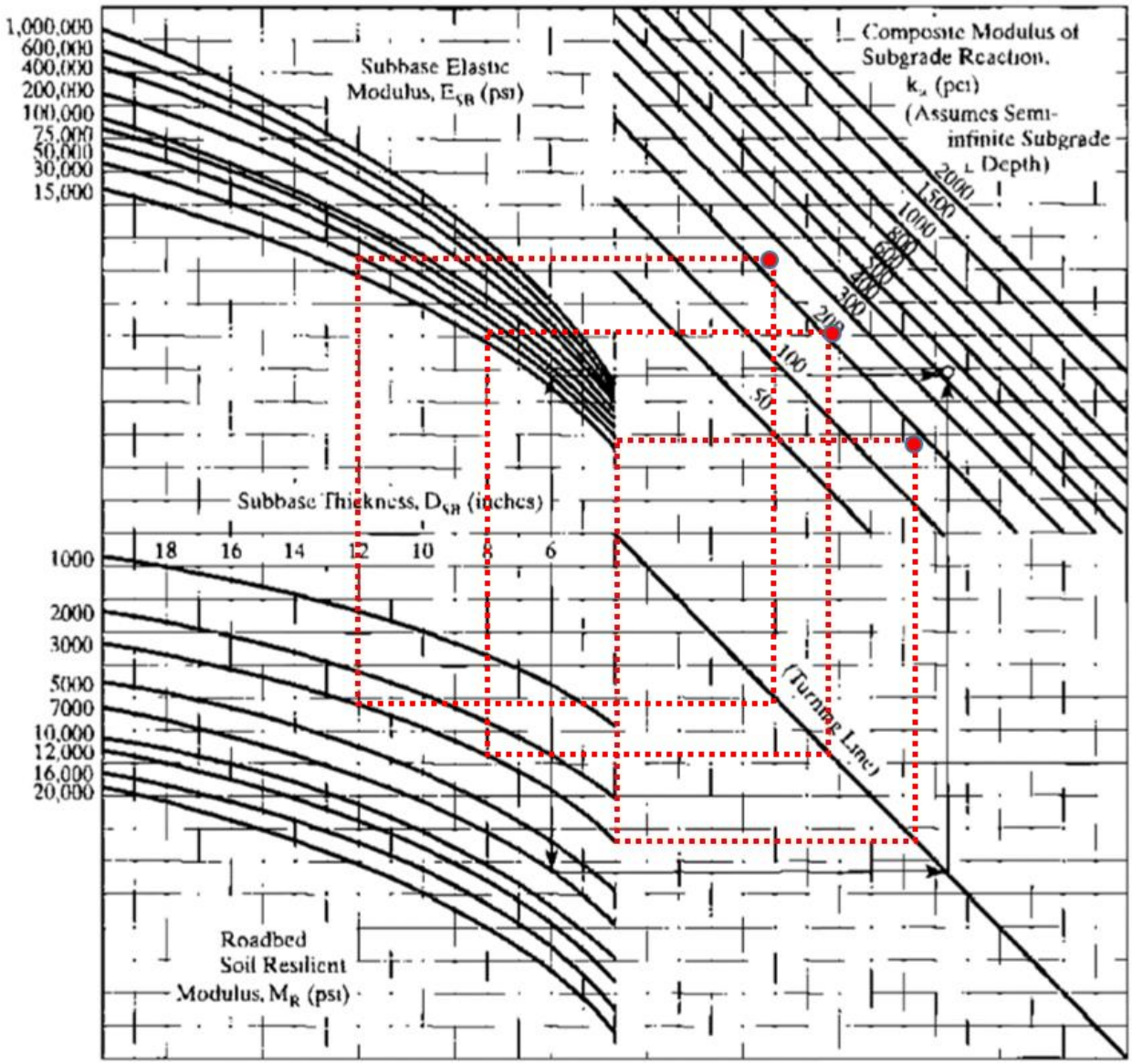

Figure 3.23 - Chart for estimating the modulus of subgrade reaction (1in=25.4mm, 1 psi=6.9kPa, 1 pci=271.3kN/m^3) [15]

- Rigid Foundation at Shallow Depth
  The modulus of subgrade reaction must be modified if a rigid foundation lies below the subgrade and the subgrade depth to rigid foundation D_{SG} is smaller than 3 m. For the correction chart shown in Figure 3.24 can be used. The chart can be applied to slabs either with or without a subbase.

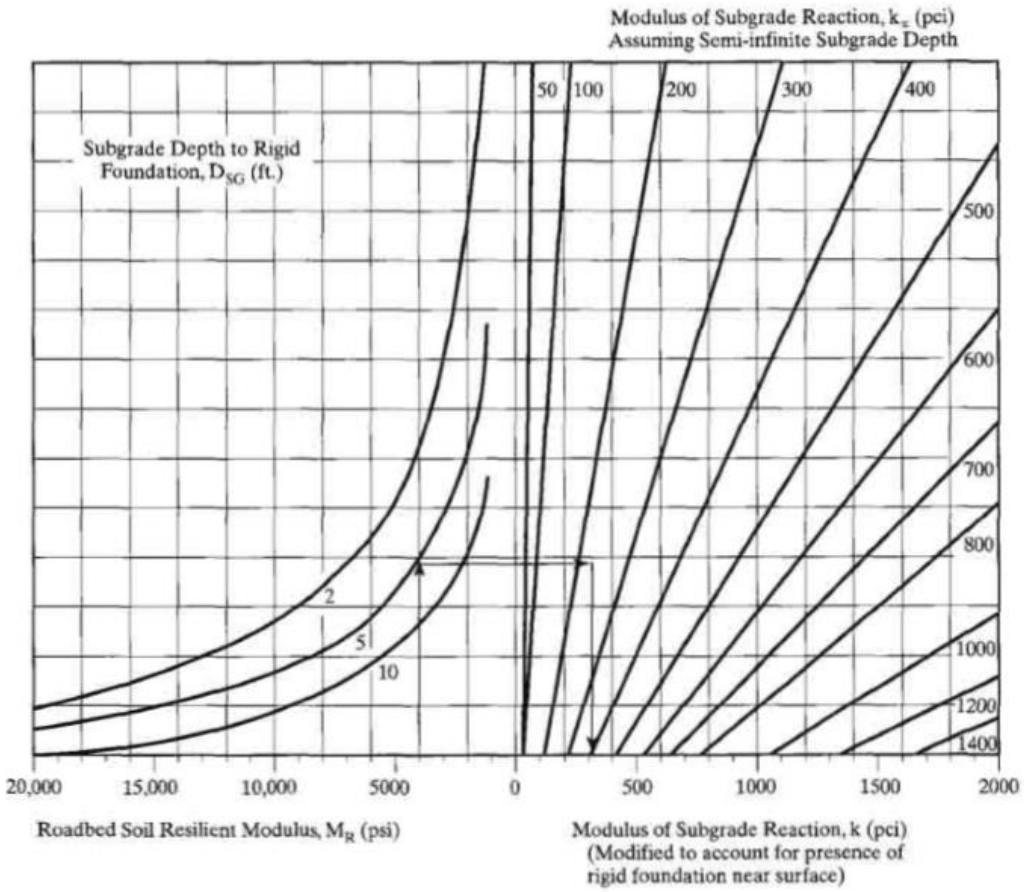

Figure 3.24 - Chart for modifying modulus of subgrade reaction due to rigid foundation near surface (1 ft = 0 .305 m, 1 psi = 6.9 kPa, 1 pci = 271 .3 kN/m3) [15]

- Effective Modulus of Subgrade Reaction
  The effective modulus of subgrade reaction is an equivalent modulus that would result in the same damage if seasonal modulus values were used throughout the year.

- Loss of Subgrade Support (LS)
  The effective modulus of subgrade reaction must be reduced by a factor to consider the potential loss of support by foundation erosion or differential vertical soil movements. Figure 3.25 shows a chart for correcting the effective modulus of subgrade reaction due to the loss of foundation support.
  The result of the AASHO Road Test indicates that the stresses produced in a concrete pavement are proportional to the number of load applications it can carry, so the equivalent *k* value for partial contact can be obtained by varying the k values until the maximum principal stress for full contact is equal to that for partial contact. The maximum principal stress under a single-axle load for four different contact conditions with LS = 0, 1, 2, and 3. The best case is LS = 0, when the slab and foundation are assumed to be in full contact. worst case is LS = 3, when an area of slab 2.7 m long and 2.2 m wide along the pavement edge, is assumed not to be in contact with the subgrade. The area assumed not to be in contact for LS = 2 is smaller than that for LS = 3 but greater than that for LS = 1. The results of that study are presented in the next figure.

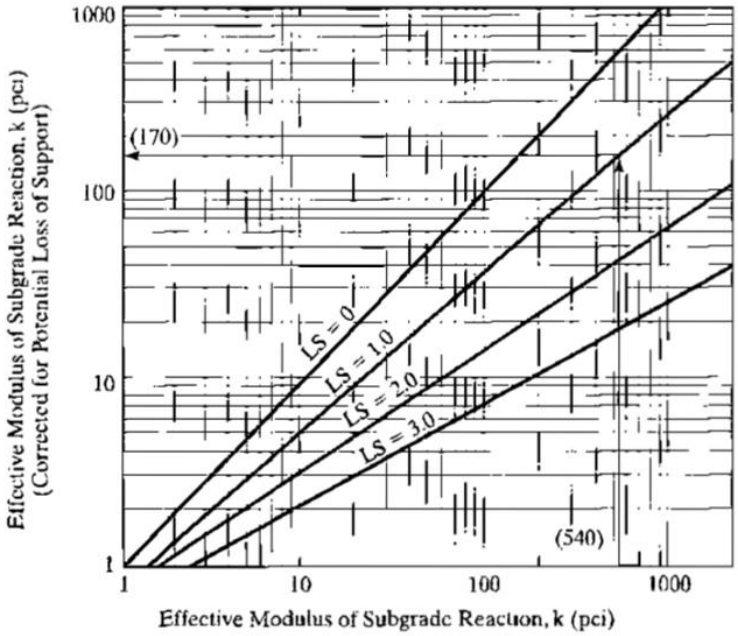

Figure 3.25 - Correction of effective modulus of subgrade reaction due to loss of foundation support [15]

Typical ranges of LS factors for several types of materials are given in Table 3.24. In the selection of LS factor, consideration should be given to differential vertical soil movements that may result in voids beneath the pavement. Even though a non-erosive subbase is used, LS values of 2 .0 to 3.0 may still be used for active swelling clays or excessive frost heave.

Table 3.24 -Typical Ranges of LS Factors for Several Types of Materials [15]

Type of material	Loss of support (LS)
Cement-treated granular base (E = 1 x 10^6 to 2 x 10^6 psi)	0.0 to 1.0
Cement aggregate mixtures (E = 500,000 to 1 x 10^6 psi)	0.0 to 1.0
Asphalt-treated bases (E = 350,000 to 1 x 10^6 psi)	0.0 to 1.0
Fine-grained or natural subgrade materials (E = 3000 to 40,000 psi)	0.0 to 1.0
Bituminous-stabilized mixture (E = 40,000 to 300,000 psi)	0.1 to 3.0
Lime-stabilized materials (E = 20,000 to 70,000 psi)	0.1 to 3.0
Unbound granular materials (E = 15,000 to 45,000 psi)	0.2 to 3.0

In this table, E refers to the general symbol of the resilient modulus.

g) Elastic Modulus of Concrete (E_c)

It can be determined according to the procedure described in ASTM C469 or correlated with the compressive strength. The American Concrete Institute recommends the following correlation:

$$E_c = 57000\sqrt{f'_c} \tag{3.40}$$

where: E_c is the concrete elastic modulus in psi and f'_c is the concrete compressive strength in psi as determined by AASHTO T22, T140, or ASTM C39.

h) Concrete Modulus of Rupture (S_c)

As described in the PCA method, the modulus of rupture required by the design procedure is the mean value determined after 28 days by using third-point loading, as specified in AASHTO T97 or ASTM C78.

i) Load Transfer Coefficient (J)

The J coefficient is a factor used to account for the ability of a concrete pavement structure to transfer a load across joints and cracks. The use of load transfer devices and tied concrete shoulders increases the amount of load transfer and decreases the load transfer coefficient. The AASHO Road Test conditions represent a J value of 3.2, because all joints were doweled and there were no tied concrete shoulders. Recommended load transfer coefficients for various pavement types and design conditions are shown below.

Table 3.25 - Recommended Load Transfer Coefficient for Various Pavement Types and Design Conditions [15]

Type of shoulder	Asphalt		Tied PCC	
Load transfer devices	Yes	No	Yes	No
JPCP and JRCP	3.2	3.8—4.4	2.5—3.1	3.6—4.2
CRCP	2.9—3.2	N/A	2.3—2.9	N/A

j) Drainage Coefficient (C_d)

The drainage coefficient C_d has the same effect as the load transfer coefficient J. C_d and J cause an increase in W_{18}, as shown in the equation 3.31. Recommended C_d values based on the quality of drainage and the percentage of time during which the pavement structure would normally be exposed to moisture levels approaching saturation are presented in Table 3.26. The percentage of time is dependent on the average yearly rainfall and the prevailing drainage conditions.

Table 3.26 - Recommended Values of Drainage Coefficients C_d for Rigid Pavements [15]

Quality of drainage		Percentage of time pavement structure is exposed to moisture levels approaching saturation			
Rating	Water removed within	Less than 1%	1—5%	5—25%	Greater than 25%
Excellent	2 hours	1.25—1.20	1.20—1.15	1.15—1.10	1.1
Good	1 day	1.20—1.15	1.15—1.10	1.10—1.00	1.0
Fair	1 week	1.15—1.10	1.10—1.00	1.00—0.90	0.9
Poor	1 month	1.10—1.00	1.00—0.90	0.90—0.80	0.8
Very poor	Never drain	1.00—0.90	0.90—0.80	0.80—0.70	0.7

4

INFLUENCE OF THE FOUNDATION ON THE SLAB THICKNESS DESIGN-NUMERICAL SIMULATION

4.1. PARAMETRIC STUDY WITH THE PCA AND AASHTO METHOD

4.1.1. GENERAL ASPECTS

The modelling of rigid pavement requires over 30 input parameters. Since the objective of this research is evaluate the influence of the geotechnical characteristics of the foundation on the performance of rigid pavements, a parametric study of the foundation is carried out. In this study, the load data will be constant. The slab thickness will be determined according to the k-values. The material parameters are presented as follows:

- Concrete slab data:
  These parameters are considered constant for the thickness design and for the numerical simulation.

Table 4.1 - Concrete slab data

Parameters	Assumed Value
Rupture modulus MR (MPa)	4.5
Elasticity modulus (MPa)	28.000
Poisson's ratio	0,15
Density (kg/m^3)	2400
Coefficient of thermal expansion (ºC-1)	1,1x10-5

- Foundation data:
  The influence of the base and stabilized subgrade k-value is the main variable considered. The thickness design methods presented in this study only consider the mechanical characteristics of the foundation by meaning of the k-value. Therefore, it was determined the minimum thickness of the concrete slab for several types of soil presented in table 4.2. The k-values in table 4.2 were computed using correlation from the typical resilient modulus, E (psi). The conversion from resilient modulus of the subgrade to k-value was updated in the fall of 2011 to

better reflect published test results; the constant conversion factor of 19.4 as suggested in the AASHTO Guide for Design of Pavement Structures 1993 is no longer used [13] Instead, a constant conversion factor of 40,5 is used.

Table 4.2 – Typical geotechnical values for common types of Soil (NCHRP 1-37A, 2004, adapted from [14])

Unified Soil	Soil Description	Density (kg/m3)	Typical Poisson's ratio	Typical E (psi)	k-value (psi/in)	k-value (MPa/m)
CH	Highly Plastic Clays	1400	0,4	3000	74	20
		1400		8000	185	50
CL	Silty Clays	1700	0,3	17000	295	80
ML	Silts and Clayey Silts	1700	0,3	20000	334	90
SC	Clayey Sands	1800	0,25	24000	405	110
SM	Silty Sands	1800	0,32	32000	572	155
SP	Poorly-graded Sands	1750	0,4	28000	480	130
SW	Well-graded Sands	1850	0,3	32000	572	155
GC	Clayey Gravel w/sands	1900	0,25	31000	553	150
GP	Poorly-graded gravels	1900	0,2	38000	665	180
GW	Well-graded Gravels	2100	0,15	41000	737	200

In the following three subsections (sections from 4.1.2 to 4.1.4), the slab thickness is determined considering that the slab is supported directly on the subgrade, as shown in Figure 4.1.

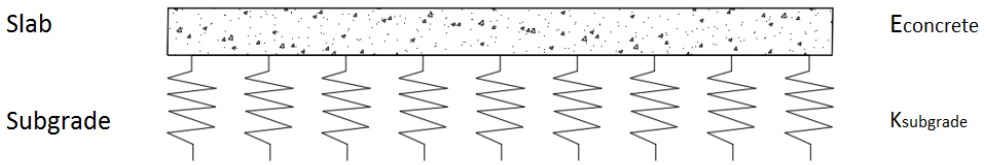

Figure 4.1 – Slab supported directly on the subgrade

4.1.2. PCA METHOD

In this study, the concrete properties are as shown in table 4.2, the axel load data (column 1 in the worksheet, page 78) are taking from example data in table 3.9. a load safety factor of 1.2 was considered and the design period is 20 years. It was computed the minimum thickness with- and without shoulders. K-values were taken from the table 4.2. The worksheets were filled using the next procedures:

a) Fatigue Analysis Procedure Steps:

1. Enter as items 8, 11 and 14 on the worksheet from the appropriate table (tables 3.10 and 3.11 with concrete shoulders and tables 3.12 and 3.13 without shoulders) the equivalent stress factors depending on trial thickness and k value.

2. Divide these by the concrete modulus of rupture and, enter as items 9, 12 and 15.

3. Fill in Column 4, "Allowable Repetitions," determined from figure 3.15.

4. Compute Column 5 by dividing Column 3 by Column 4, multiplying by 100; then total the fatigue at the bottom.

b) Erosion Analysis Procedure Steps:

1. Enter the erosion factors from the appropriate table (tables 3.14 and 3.15 with concrete shoulders and tables 3.16 and 3.17 without shoulders) as items 10, 13 and 16 in the worksheet.

2. Fill in Column 6, "Allowable Repetitions," from figure 3.17 (without concrete shoulder) or figure 3.18 (with concrete shoulder).

3. Compute Column 7 by dividing Column 3 by Column 6, multiplying by 100; then total the erosion damage at the bottom.

As mentioned previously, in the section 3.4.2, neither the fatigue analyses nor the erosion analyses can overpass 100%. It means, the total sum in column 5 and column 7 should be less than 100%.

As example, two 4-lane rural section designs for a k-value equals to 20MPa/m are presented. In the first example the design does not consider shoulders. In the second example, it is considered the use of concrete shoulders.

The design for the remaining k-values are presented in Annex A.1.

Calculation of Pavement Thickness (adapted from [15])

Project 4-LANE RURAL SECTION

Trial thickness	260	mm	Doweled Joints:	yes
Subbase-subgrade k	20	MPa/m	Concrete Shoulder:	no
Modulus of rupture, MR	4.5	MPa	Design period (years):	20
Load safety factor, LSF	1.2			

Axel load, (kN)	Multiplied by LSF	Expected repetitions	Fatigue Analysis		Erosion Analysis	
			Allowable repetitions	Fatigue percent	Allowable repetitions	Fatigue percent
1	2	3	4	5	6	7
			8. Equivalent stress	1.41	10. Erosion factor	2.52
			9. Stress ratio factor	0.31		
Single Axles						
133	160	6310	36000	17.5	2500000	0.3
125	150	14690	85000	17.3	3500000	0.4
115	138	30140	300000	10.0	6500000	0.5
107	129	64410	1100000	5.9	9000000	0.7
98	118	106900	Unlimited	0.0	19000000	0.6
89	107	235800	Unlimited	0.0	50000000	0.5
80	96	307200	Unlimited	0.0	Unlimited	0.0
			11. Equivalent stress	1.41	13. Erosion factor	2.78
			12. Stress ratio factor	0.31		
Tandem Axles						
231	278	21320	300000	7.1	1100000	1.9
213	256	42870	2000000	2.1	1800000	2.4
195	234	124900	Unlimited	0.0	3000000	4.2
178	214	372900	Unlimited	0.0	5000000	7.5
160	192	885800	Unlimited	0.0	10000000	8.9
142	171	930700	Unlimited	0.0	30000000	3.1
125	150	1656000	Unlimited	0.0	Unlimited	0.0
			14. Equivalent stress	1.07	16. Erosion factor	2.89
			15. Stress ratio factor	0.24		
Tridem Axles						
240	96	250000	Unlimited	0.0	4000000	6.3
			Total	60.0	Total	37.0

Calculation of Pavement Thickness adapted from [15])

Project 4-LANE RURAL SECTION

Trial thickness	230	mm	Doweled Joints:	yes
Subbase-subgrade k	20	MPa/m	Concrete Shoulder:	yes
Modulus of rupture, MR	4.5	MPa	Design period (years)	20
Load safety factor, LSF	1.2			

Axel load, (kN)	Multiplied by LSF	Expected repetitions	Fatigue Analysis		Erosion Analysis	
			Allowable repetitions	Fatigue percent	Allowable repetitions	Fatigue percent
1	2	3	4	5	6	7
			8. Equivalent stress	1.45	10. Erosion factor	2.34
			9. Stress ratio factor	0.32		
Single Axles						
133	160	6310	21000	30.0	450000	1.4
125	150	14690	55000	26.7	950000	1.5
115	138	30140	180000	16.7	1600000	1.9
107	129	64410	700000	9.2	3000000	2.1
98	118	106900	9000000	1.2	10000000	1.1
89	107	235800	Unlimited	0.0	40000000	0.6
80	96	307200	Unlimited	0.0	Unlimited	0.0
			11. Equivalent stress	1.32	13. Erosion factor	2.54
			12. Stress ratio factor	0.29		
Tandem Axles						
231	278	21320	2000000	1.1	350000	6.1
213	256	42870	Unlimited	0.0	580000	7.4
195	234	124900	Unlimited	0.0	1200000	10.4
178	214	372900	Unlimited	0.0	2300000	16.2
160	192	885800	Unlimited	0.0	6000000	14.8
142	171	930700	Unlimited	0.0	Unlimited	0.0
125	150	1656000	Unlimited	0.0	Unlimited	0.0
			14. Equivalent stress	0.99	16. Erosion factor	2.68
			15. Stress ratio factor	0.22		
Tridem Axles						
240	96	250000	Unlimited	0,0	1300000	19,2
			Total	85,0	Total	82,7

4.1.3. AASHTO Method

As mentioned previously, a numerical online solver for the AASHTO method (AASHTO 93) was used [13]. The parameters used are:

Table 4.3 – Design data for the AASHTO

Parameters	Assumed value
W_{18}	8000000
R (%)	85
S_0	0.35
p_i	4.5
p_t	2.0
E_c (psi)	4350000
MR (psi)	650
C_d	1.0
J	2.5 (shoulder), 3.6 (no-shoulder)
$K - value$	Variable

Annex A.2. shows the procedure for determining the values of the parameters in Table 4.3. The k-values are taken from tables 4.2.

As example, Figure 4.2 shows the user interface of the AASHTO 93 equation solver. There are two panels. In the first panel, “INPUT”, the variables presented in Table 4.3 are inserted. The “OUTPUT” panel shows the standard normal deviate,ΔPSI and the thickness in inches.

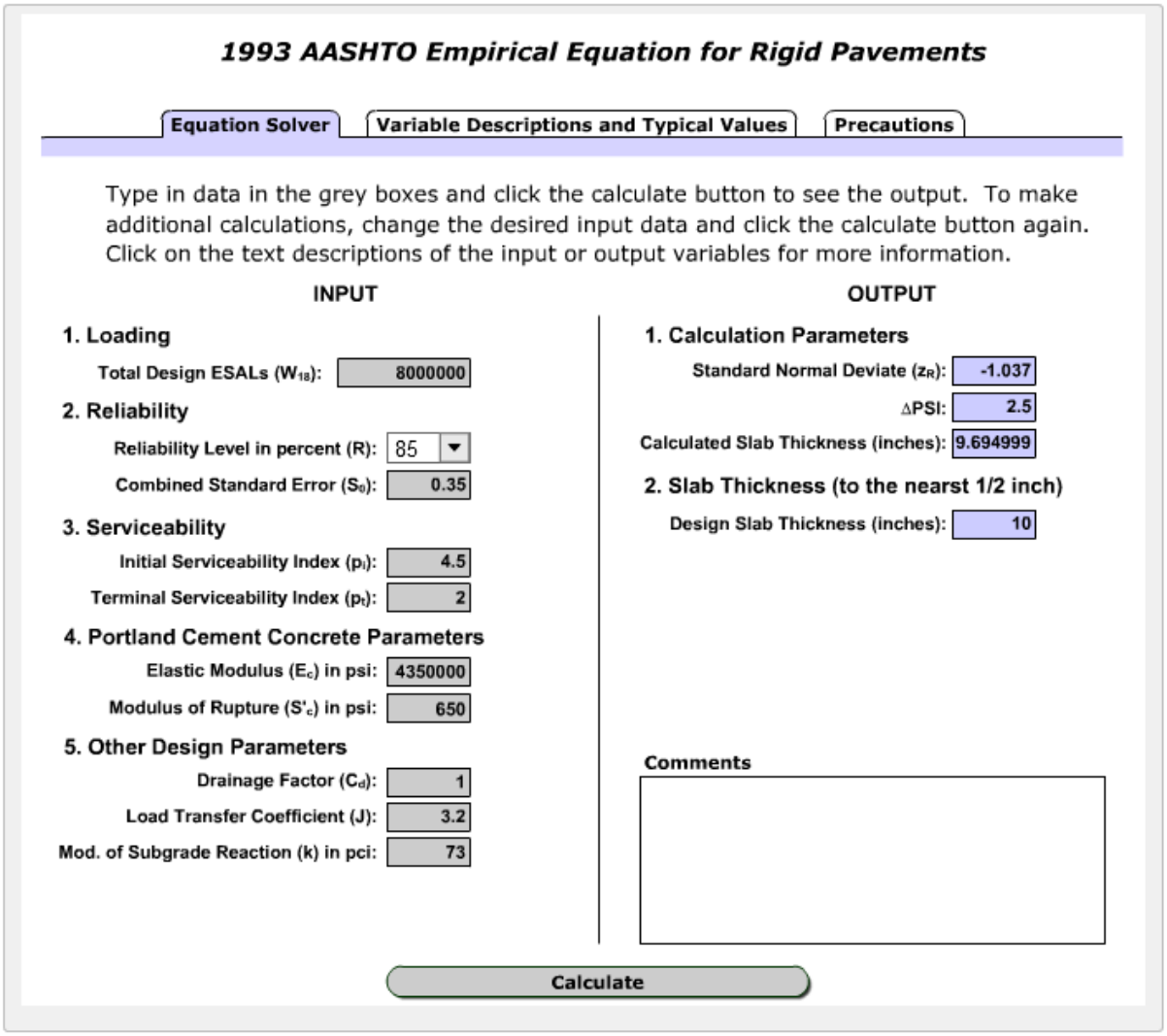

Figure 4.2 - User interface of the AASHTO 93 equation solver [13].

4.1.4. Comparison of Results obtained with PCA- and AASHTO Method

The mechanical performance of the rigid pavements is conditioned, among other factors, by the slab thickness. Therefore, a comparative study between the PCA method and the AASHTO method was conducted. Figure 4.3 shows the influence of the subgrade support on the thickness design for both methods.

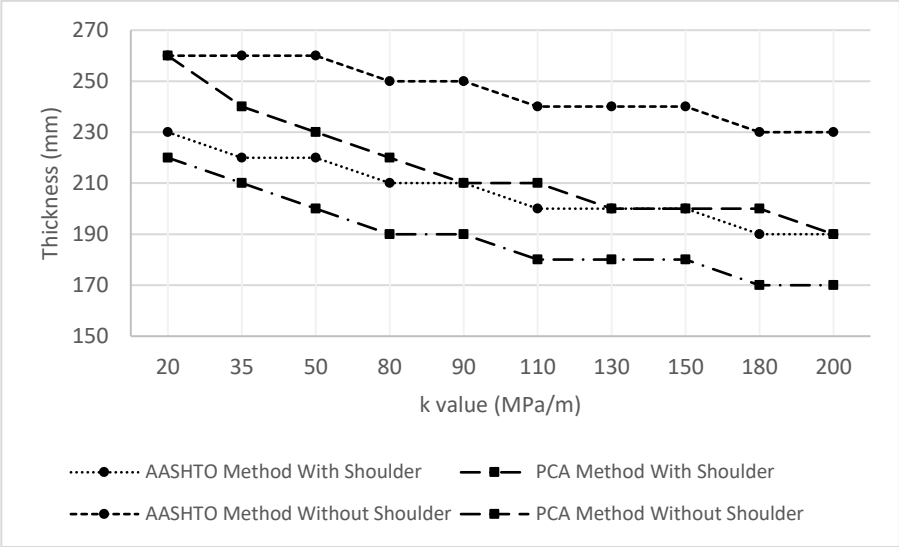

Figure 4.3 - Influence of the subgrade k-value on the thickness design

The results suggest that the PCA method is more sensitive to the changes of the k-value, it results in a decrement of 5 cm when considering shoulders and 7 cm without shoulders, by changing the k-value from 20 MPa/m to 200 MPa/m. In the case of the AASHTO method, the decrements were 4 cm when considering shoulders and 3 cm without shoulders. Finally, it is observed that the AASHTO method, under the conditions assumed in this study, is more conservative. The slab thickness using the AASHTO method is 4 cm higher than the thickness computed using the PCA method with shoulder. Without shoulder the difference is 3 cm.

4.1.5. Influence of the base or stabilized subgrade on the AASHTO method thickness design

Good pavement practices suggest the use of base or stabilized subgrade. In this case the objective is not improve the k-value, but prevent erosion problems. Nevertheless, the design methods allow to reduce the slab thickness by considering an improved k-value (named here compound k-value).

Figure 4.4 shows the original configuration of the pavement structure studied in this section.

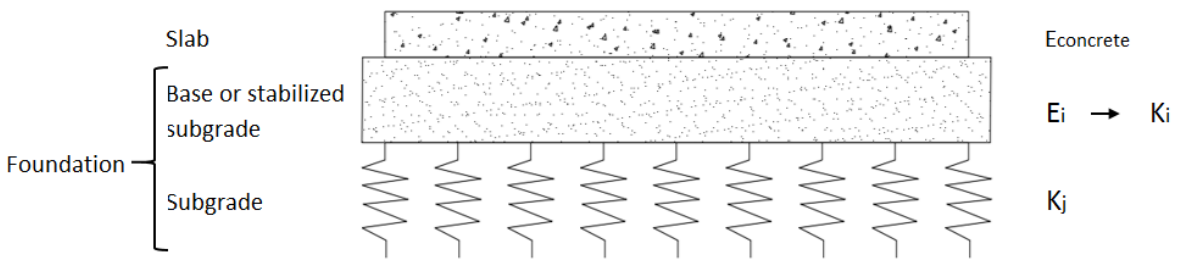

Figure 4.4 - Scheme of the original layer configuration

The design method considers only one k-value. To overcome this limitation, the original layer configuration is simplified (using the compound k-value), as shown in Figure 4.5.

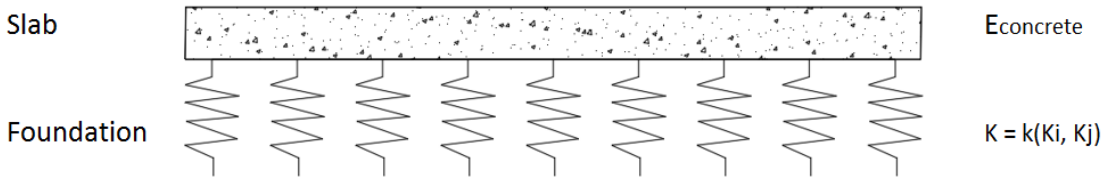

Figure 4.5 - Scheme of the simplified layer configuration

The compound k-value was calculated when a base or a stabilized-subgrade was used. As example, as shown in Figure 3.23, for a highly plastic clays subgrade (E = 3000 psi, table 4.2) and a non-stabilized base (E = 30000 psi, table 4.4), the compound k-value for 4 inches, 8 inches and 12 inches are 170 pci, 205 pci and 250 pci, respectively.

Table 4.4 – Base and stabilized subgrade data (after AASHTO 93, adapted from [15])

Support Description	E Range (psi)	E (psi)	E (MPa)	Density (kg/m3)	Poisson's ratio
Non-Stabilized Base	15,000 - 45,000	30000	210	1800	0,30
Cement Stabilized Subgrade	50,000 - 1,000,000	500000	3550	1900	0,30
Lime Stabilized Subgrade	20,000 - 70,000	45000	310	1900	0,35
Cement Treated Base	500,000 - 1,000,000	750000	5170	2000	0,25
Lean Concrete Base	1,000,000 - 2,000,000	1500000	10350	2100	0,20

The calculation of the compound k-value using the Figure 3.23 is tedious. Alternatively, an online calculator provided by the APCA is used. Figure 4.3 shows the calculation of the compound k-value for 4 inches base as in the last example.

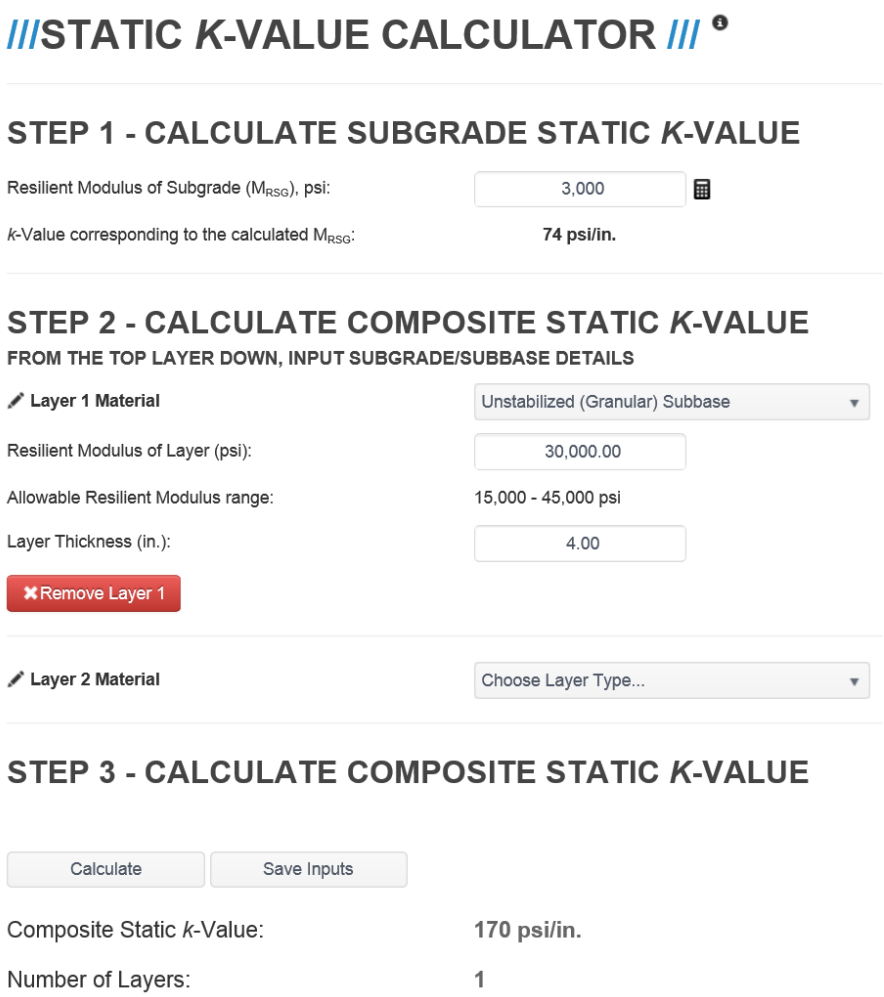

Figure 4.6 - Calculation of the compound k-value (app available on [23])

In the following figures, the solid (continued) lines represent the thickness design considering only the natural subgrade. The remaining three lines present the decrement of the thickness considering 4 inches, 8 inches and 12 inches base or stabilized subgrade (For simplification, thicknesses were rounded to 100 mm, 200 mm and 300 mm, respectively). In this case, the slab thickness was calculated as in section 4.1.3 using Table 4.3 (the k-value is not the subgrade k-value, but the compound k-value). The k-values vary from 20 MPa/m to 80 MPa/m. When the compound k-value (k-value subgrade plus k-value base or stabilized subgrade) was very high, the thickness was not taking it into account.

- Non-Stabilized Base

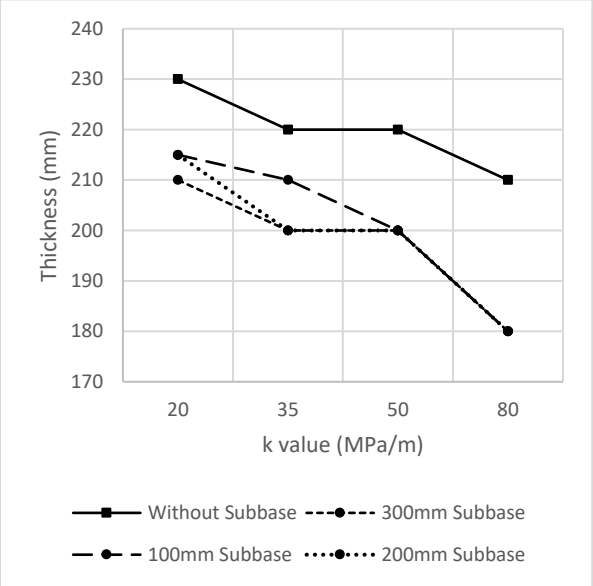

Figure 4.7 - Non-stabilized base with shoulder

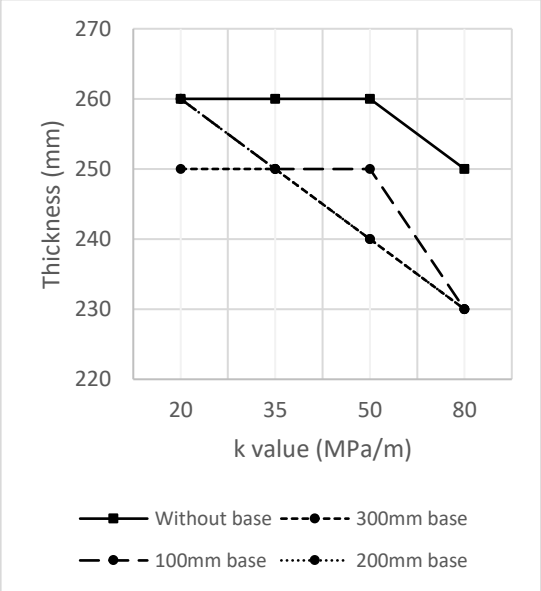

Figure 4.8 - Non-stabilized base without shoulder

- Cement Stabilized Subgrade

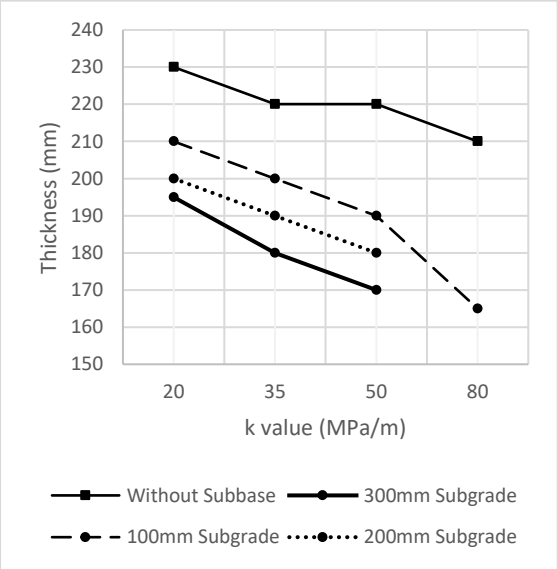

Figure 4.9 - Cement stabilized subgrade with shoulder

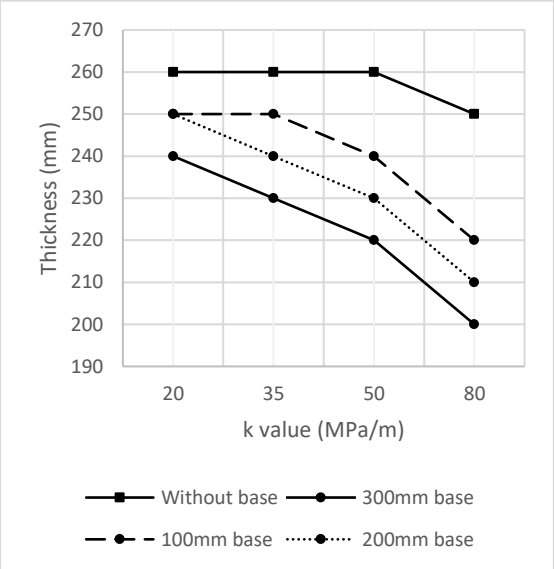

Figure.4.10 - Cement stabilized subgrade without shoulder

- Lime Stabilized Subgrade

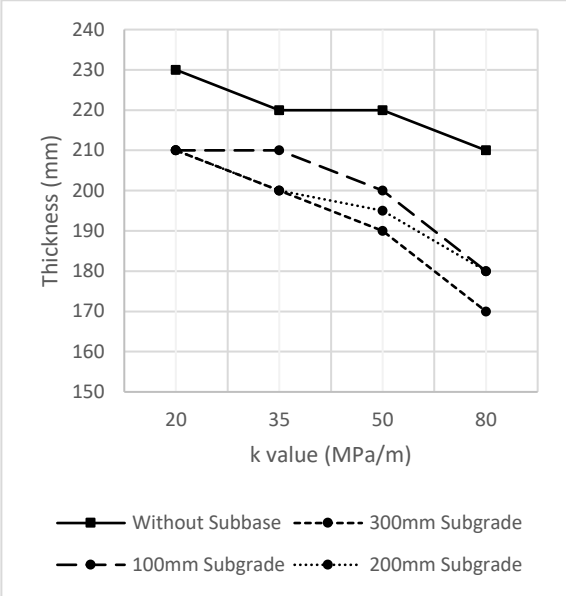

Figure 4.11 - Lime stabilized subgrade with shoulder

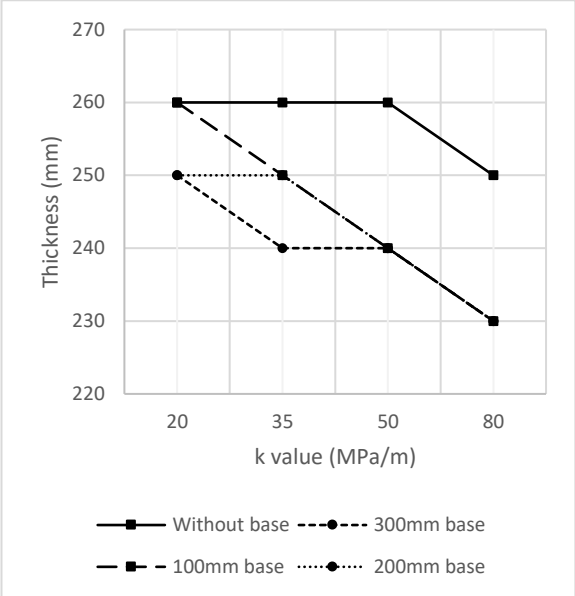

Figure 4.12 - Lime stabilized subgrade without shoulder

- Cement Treated Base

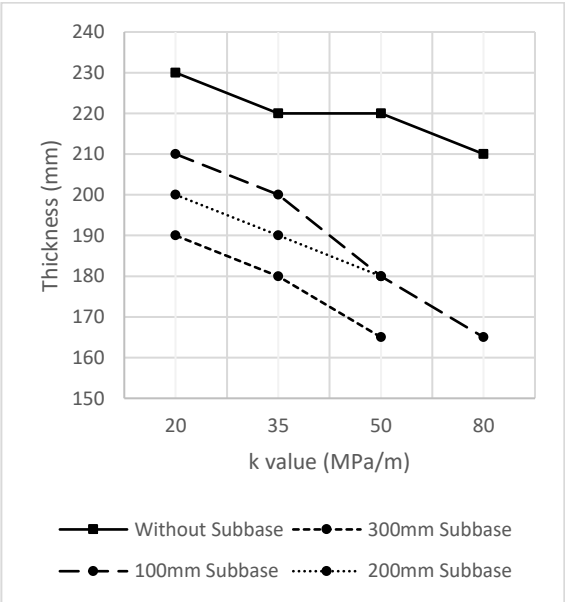

Figure 4.13 - Cement treated base with shoulder

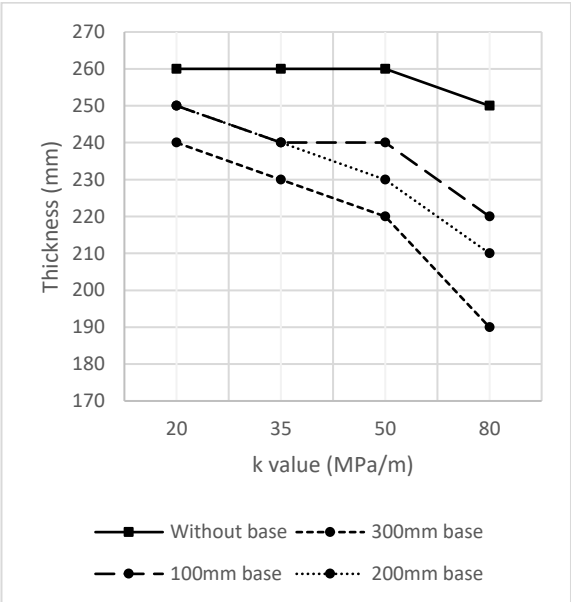

Figure 4.14 - Cement treated base without shoulder

- Lean Concrete Base

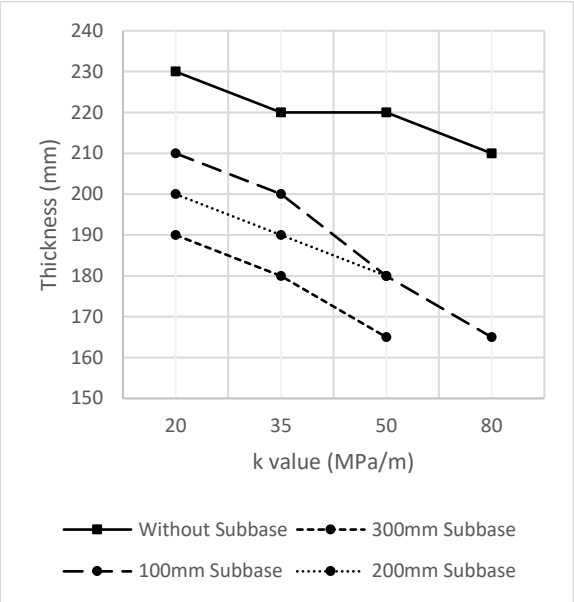

Figure 4.15 - Lean concrete base with shoulder

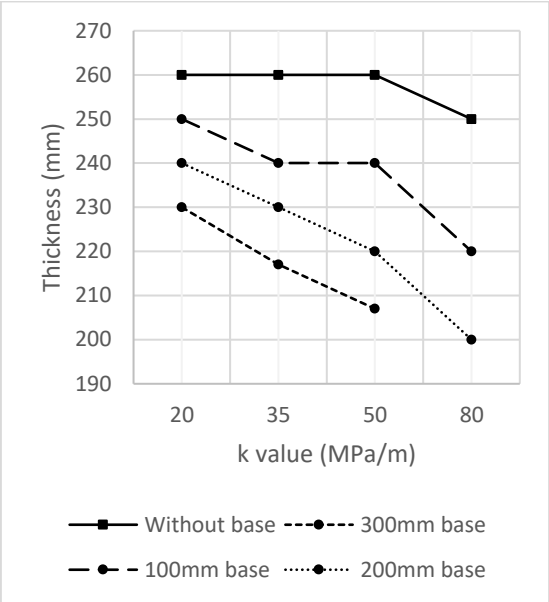

Figure 4.16 - Lean concrete base without shoulder

For all the bases and stabilized subgrade considered, the results show almost the same tendency. For low k-values, such as 20 MPa/m and 40 MPa/m, the slab thickness decreased maximum 1 cm by using additional 100 mm of base or stabilized subgrade. When the k-values are 80 MPa/m, the results are more heterogeneous:

In the case of the non-stabilized base the maximum decrement, for the three-base thickness variation, was 2.5 cm with shoulder and 2 cm without shoulder.

Using 100 mm cement stabilized subgrade can reduce the slab thickness 4 cm with shoulder. There were not conclusive results when using 200 mm and 300 mm because the k-values were extremely high (the slab thickness was too low). Without shoulder, the maximum decrements were 3 cm for 100 mm, 4 cm for 200 mm and 5 cm for 300 mm-stabilized subgrades.

The lime stabilized subgrade allows to reduce maximum 3.5 cm the slab thickness with shoulder and 2 cm without shoulder.

The use of the cement treated base has the same variation as the cement stabilized subgrade with shoulder. Without shoulder, the maximum decrement was 6 cm for 300 mm- cement treated base.

Finally, in the lean concrete base the maximum decrement was 4.5 cm for 100 mm- base with shoulder. Without shoulder, the maximum decrements were 3 cm for 100 mm, 5 cm for 200 mm- lean concrete base.

4.2. EVERFE SOFTWARE

EverFE is a 3D finite element analysis (FEA) tool for simulating the response of JPCP systems to both axle loads and environmental effects. The FE code was written in object-oriented C++. In this section, the FE implementation of EverFE is presented. The topics are organized as follows: i) FE discretization; ii) slab-base interface, iii) dowels and ties modeling; iv) aggregate interlock modeling; v) Axle and thermal loads. The information in this section is taken from [25].

4.2.1. BASIC FINITE-ELEMENT DISCRETIZATION

EverFE´s FE-library concludes five elements: i) quadratic brick (20-noded) elements used to discretize the slab and elastic base and sub-base layers, ii) planar quadratic (8-noded) elements incorporate the dense liquid foundation below the bottom-most elastic layer, iii) quadratic interface (16-noded) elements implement both aggregate interlock joint shear transfer and shear transfer at the slab-base-interface, iv) embedded flexural (3-noded)- and v) shear beam (2-noded) elements coupled to model dowels at transverse joints and ties at longitudinal joints. The first three types of elements are shown in the next figure, the last two are type of elements are discussed in subsequent subsections.

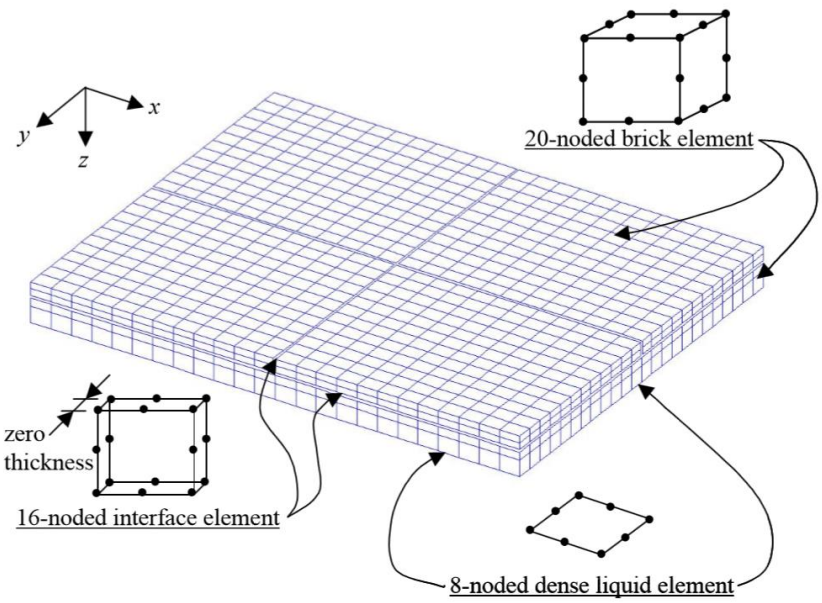

Figure 4.17 - Basic Finite-Element Discretization [25]

4.2.1.1. Model boundary conditions

The boundary conditions are the minimum required to prevent rigid-body motion. There are two scenarios, the first one when a base layer is modeled, the second one when the slab is directly support by the dense liquid foundation, i.e., slabs founded on the subgrade, see in Section 4.2.2.

When the base layer is missing, each slab is restrained against x- and y-direction displacements at one node on its –x face, and against x-direction displacement at a second node on its –x face to prevent rigid-body motion of each slab. If the base layer is modeled, the slabs are restrained in the horizontal x-y plane by the shear stiffness of the slab-base-interface and receive vertical support from contact with the base. Rigid body motion of the base and sub-base layers is prevented by restricting the x- and y- displacements of one node on the –x face, and restricting the x-displacement of a second node on the –x face.

In both cases, vertical support of the system is provided by the dense liquid foundation placed below the bottommost layer of the model.

4.2.1.2. Modeling of the slab, base and sub-base layers

Base and sub-base layers are treated as 3D, linearly elastic, isotropic continua. Each layer is discretized with standard 20-noded coincidence brick elements. The FE meshes are rectilinear, and the same number of element divisions is used for each slab and the base/sub-base layers below the slab in the x-y plane to ensure compatibility at the slab-base-interface. The isoparametric element formulation is used and all required element integration is performed numerically using 8-point (2x2x2) Gauss quadrature.

4.2.1.3. Modeling of the dense liquid foundation

The dense liquid foundation, discretized by the 8-noded element illustrated in Figure 4.17, can either support tension, or be tensionless. The element incorporates standard quadratic shape functions for interpolation of vertical displacements within the element ensuring that it displaces compatibly with the 20-noded brick element with which it shares nodes. An isoparametric element formulation is used, and all necessary element integrations are performed numerically using 9-point (3x3) Gauss quadrature to ensure accurate results when the tensionless option is selected.

The distributed stiffness of the dense liquid foundation (force/volume) is the constitutive parameter needed. For the tensionless foundation, if tension occurs at an element integration point during the solution process, the stress and stiffness at that point are set to zero during integration of the element stiffness matrix and equivalent force vector. For the conventional, tension-supporting dense liquid, the stiffness remains constant at all points

4.2.2. Slab-Base Interface

Either perfect bond between the slab and base, or separation of the slab and base under tension is allowed by EverFE. As shown in Figure 4.18, the slab and base do not share nodes, and nodal constraints are used to satisfy the required contact conditions in both cases. The solution algorithm relies on a perturbed Lagrangian formulation and a nodal constraint updating scheme based on the current normal stress between the slab and base.

Zero-thickness quadratic interface elements (16-noded), that are meshed between the slab and base, are employed by EverFE to capture slab-base. The element incorporates standard quadratic shape functions for interpolation of displacements, ensuring that it displaces compatibly with the 20-node brick elements with which it shares nodes. The element tracks relative displacements between the slab and base in the vertical (z) and both horizontal (x and y) directions. An isoparametric element formulation is used, and all necessary element integrations are performed numerically using 9-point Gauss quadrature.

Figure 4.18 illustrates the constitutive relationship, which is characterized by an initial distributed stiffness k_{SB} (force/volume) and slip displacement δ_0.While k_{SB} has the same units dense liquid foundation modulus, k_{SB}. This constitutive relationship is assumed to apply independently in both the x- and y-directions if the slab and base remain in contact (i.e., a compressive normal stress exists at the slab-base-interface). The fact that there will be little or no shear transfer when slab-base separation occurs is accommodated by setting the interface stiffness and shear stress to zero whenever the relative

vertical displacement $\delta_0 > 0$. Modeling this loss of shear transfer with loss of slab-base contact can be important, especially when thermal gradients are simulated.

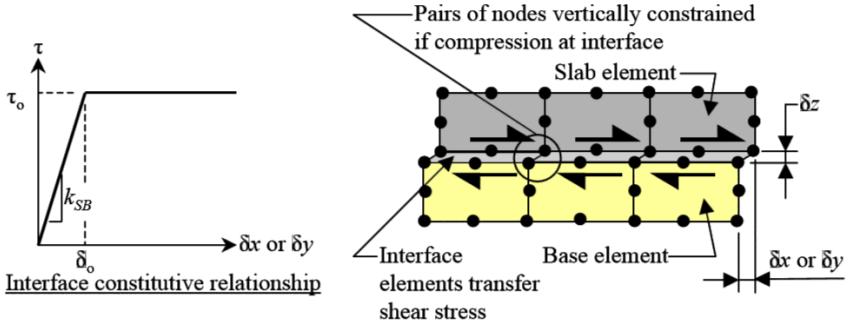

Figure 4.18 - Modeling Separation and Shear Transfer at the Slab-Base Interface [25]

Shear transfer between the slab and base can be important when analyzing pavements subjected to thermal and/or shrinkage strains. Studies shown that the type of supporting base significantly affects slab stresses [25].

4.2.3. DOWELS AND TIES MODELLING

3-noded, quadratic embedded flexural elements are used to model dowels and transverse tie bars explicitly. This approach has the advantage of allowing the dowels and tie bars to be precisely located irrespective of the slab mesh lines as shown in Figure 4.19. This embedded element formulation also permits significant savings in computation time by allowing a range of load transfer efficiencies to be simulated without requiring a highly refined mesh at the joint.

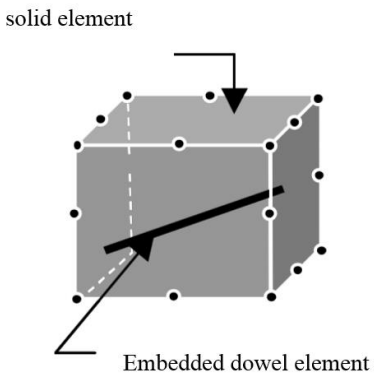

Figure 4.19 - Dowel Element [25]

Dowel looseness (gaps between the dowel and the slabs) is rigorous treated with the embedded dowel formulation. Another option is modeling the dowels as beams on an elastic foundation, where Winkler foundation springs are sandwiched between the dowels and the slabs. Both options are conceptually shown in figure 4.20 (a).

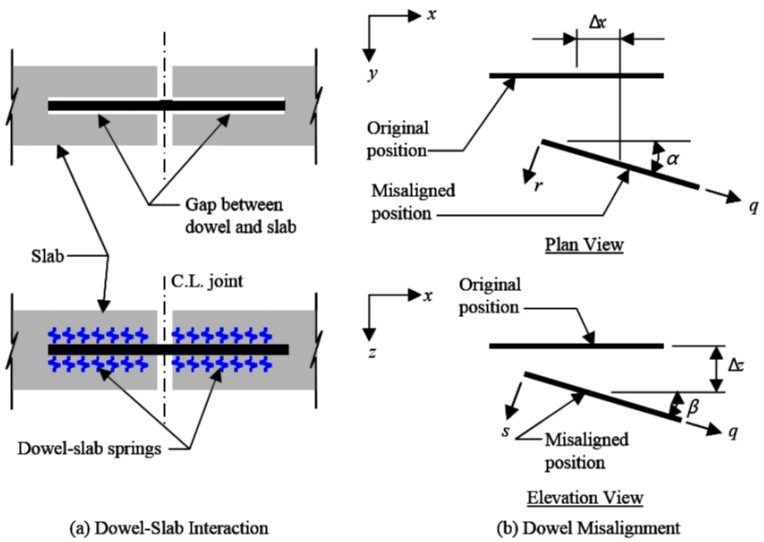

Figure 4.20 - Dowel Modeling [25]

Dowel misalignment and/or mislocation can be simulated through the specification of four parameters ($\Delta x, \Delta z, \alpha, \beta$) that shift an individual dowel along the x- and z-axes and define its angular misalignment in the horizontal and vertical planes, see Figure 4.20 (b). The dowel support and restraint moduli coincide with the local dowel coordinate axes (q,r,s), which are rotated from the global (x,y,z) axes by the angles, α and β. The meshing algorithm precisely locates individual flexural elements within the solid elements by first solving for the intersection of each dowel with solid element faces, and then subdividing each dowel into at least 12 individual quadratic embedded flexural elements on each side of the joint face as discussed previously.

4.2.4. Aggregate interlock Modelling

EverFE employs a 16-noded, zero-thickness quadratic interface element that is meshed between the joint faces, as shown in Figure 4.17, for the simulation of aggregate interlock shear transfer. Either linear or nonlinear, the shear transfer is assumed to occur across the entire width of each transverse joint in the FE-model. With the linear option, the shear stress developed between the joint faces is proportional to the relative vertical movement at the joint, and the shear stress is independent of the joint opening. The nonlinear option includes both the nonlinearity in the shear stress-relative vertical displacement relation as well as the nonlinear variation in shear stress transfer with changes in joint opening.

The linear option is the simplest approach for modeling aggregate interlock load transfer at longitudinal joints. A joint stiffness parameter (analogous to a dense liquid k-value in that it can be interpreted as a spring stiffness per unit area, but expressed in force/volume) is specified to control the degree of aggregate interlock load transfer.

The specified joint stiffness is constant over the entire area of the joint, and does not vary with relative vertical displacement or joint opening. If the joint stiffness is set to zero (the default value), there will be no aggregate interlock load transfer, and a very large value will result in high load transfer efficiency. The joint stiffness applies only in the vertical (z) direction, and y-direction relative joint movement is unrestrained.

Details on the nonlinear aggregate interlock load transfer can be found in the EverFE user manual [25].

4.2.5. Axle Loads and Thermal Effects

EverFE allows the consideration of simultaneous axle loads and pre-strains due to thermal or shrinkage effects. This section documents the methods by which these loads are included in each EverFE finite-element model.

4.2.5.1. Axle Loads

A wheel load is defined by the (x,y) location of its geometric center, the length L and width W of the tire contact area, and the magnitude of the wheel load P. The load is assumed to produce a constant pressure over the wheel contact area.

The critical issue regarding the application of the wheel loads in the FE- model is determining the set of nodal forces that are equivalent to the uniformly distributed pressure generated by the wheel. Since the wheel load contact area is not restricted to coincide with an element face, and in fact can partially load several elements faces the application of the wheel loads is challenging. EverFE handles this by dividing each wheel contact area into smaller rectangular sub-areas by using a grid having $n_x \times n_y$ divisions along each edge. The ith sub-area of the wheel defined by the grid thus has an area of $LW/(n_x n_y)$ and sees a total force of $p_i = P/(n_x n_y)$.

The equivalent nodal force vector due to each p_i is then computed by first determining the solid element that it contacts using the same fast geometric search procedures needed for the finite-element solver. The work-equivalent set of nodal forces is then computed as the product of p_i and the vector of element shape functions evaluated at the point of application of p_i. The sum of all work-equivalent nodal force vectors is the total nodal force vector applied by the entire wheel. This procedure is consistent with the virtual work and energy principles that form the basis of the FEM, using a rectangular rule to numerically integrate the tire contact pressure over its area of application.

4.2.5.2. Thermal and Shrinkage Effects

EverFE allows the specification of linear, bi-linear, or tri-linear temperature changes throughout the slab thickness, and the pre-strain is computed as the product of the specified temperature change and the user-specified coefficient of thermal expansion. Specification of shrinkage strains can be accomplished by converting the desired shrinkage strain into an equivalent temperature change using the coefficient of thermal expansion. The element pre-strains are converted to an equivalent nodal force vector by the usual element integration, and are subtracted from the total strain during the calculation of internal stresses.

Details on the FE nonlinear solution strategy and the multigrid solver can be found on the publication by Davids [25].

4.2.6. Simulation of the mechanical response of rigid pavements using EverFE

Influence of the foundation on the mechanical response of rigid pavements is studied using the finite element program EverFE version 2.24. Since the PCA method results are more critical only the thickness obtained using PCA method are considered. For simplification, only the designs for five k-values are simulated, see Table 4.5.

Table 4.5 –Slab thickness design for simulation

k-value Subgrade (MPa/m)	Slab thickness - PCA	
	With Shoulder (mm)	Without shoulder (mm)
20	220	260
80	190	220
110	180	210
150	180	200
200	170	190

One hundred simulations (50 for the designs considering shoulders and 50 for the designs without shoulders) are carry out. The slab thickness is a variable depending on the k-value, as shown in Table 4.5. Only the original slab thicknesses are considered, i.e., slab thickness reduction due the use of base or stabilized subgrade was neglected in this analysis, but depending on the results the slab thickness can be decreased in a second phase.

4.2.6.1. Model

a) Geometry

EverFE allows to simulate up to three base layers. In this case, it is possible to consider the original layer configuration as shown in Figure 4.4. Four geometries were simulated:

- With shoulder, 100 mm base,
- With shoulder, 200 mm base,
- Without shoulder, 100 mm base,
- Without shoulder, 200 mm base.

In all cases, the lane width is 3.6 m and the joints are spaced every 4.2 m. In the geometry with shoulder, a 2.1 m wide shoulder was considered.

Figures 4.21 to 4.24 show the geometry of the scenarios with 20 MPa/m with 100 mm- and 200 mm base as an example of the software interface.

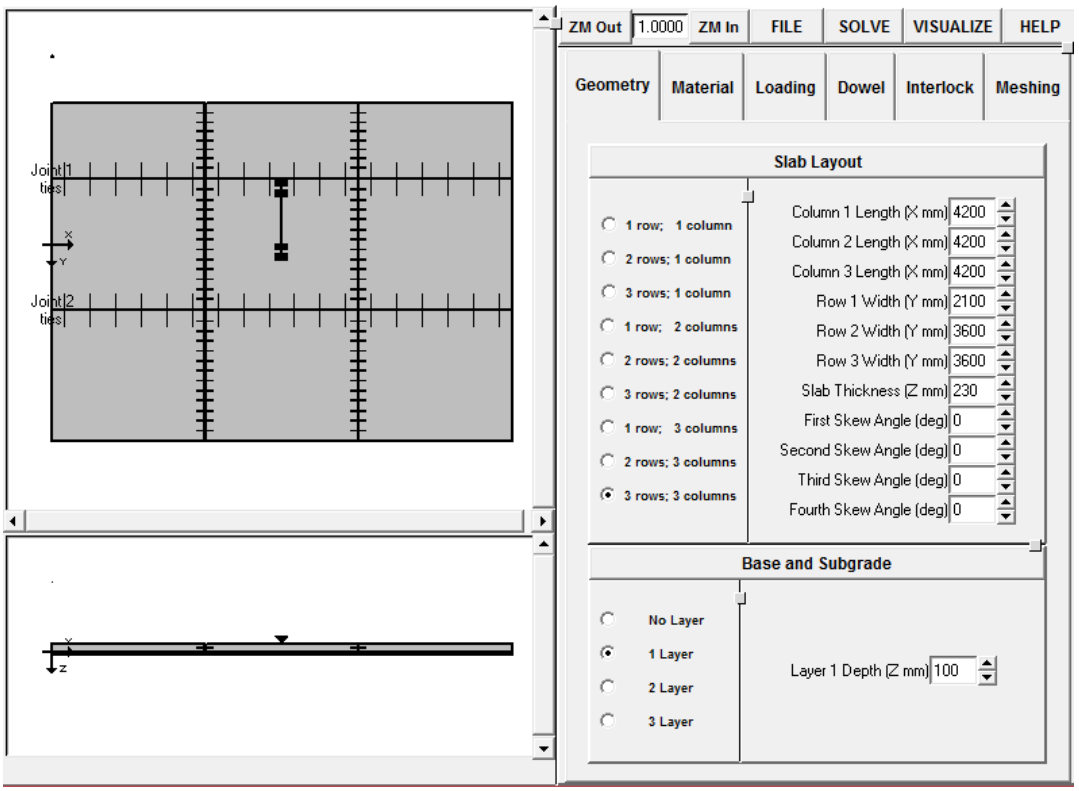

Figure 4.21 - Geometry panel: k-value = 20MPa/m, with shoulder, 100mm base.

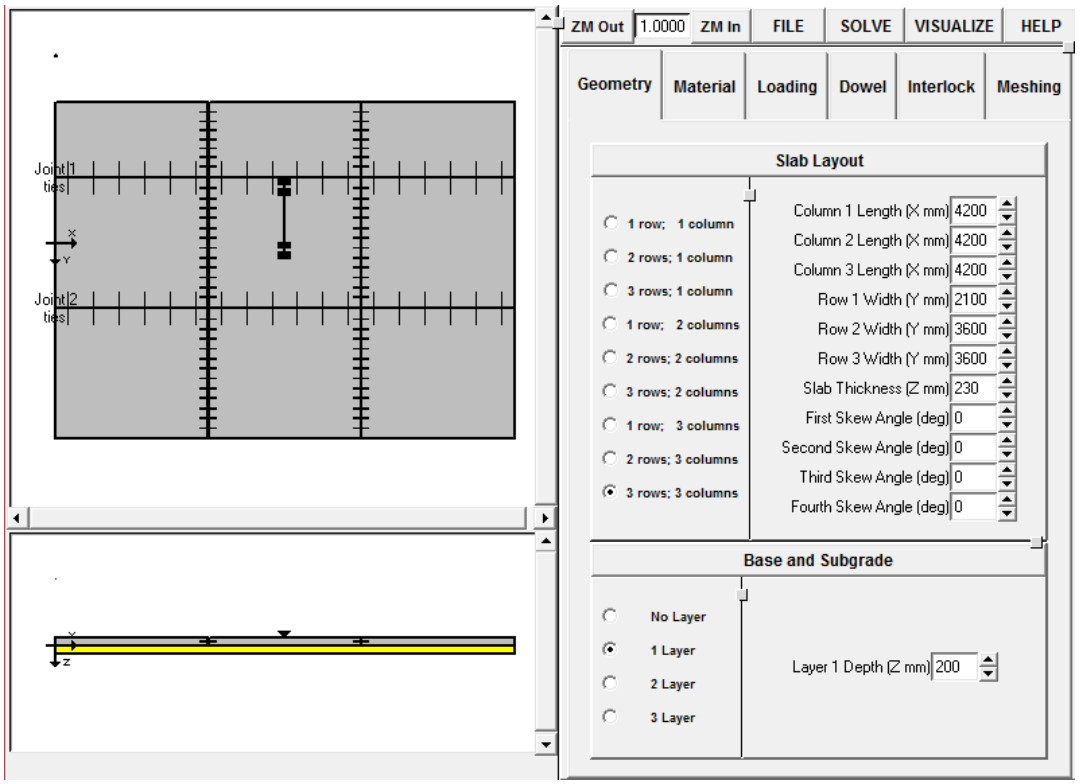

Figure 4.22 - Geometry panel: k-value = 20MPa/m, with shoulder, 200mm base.

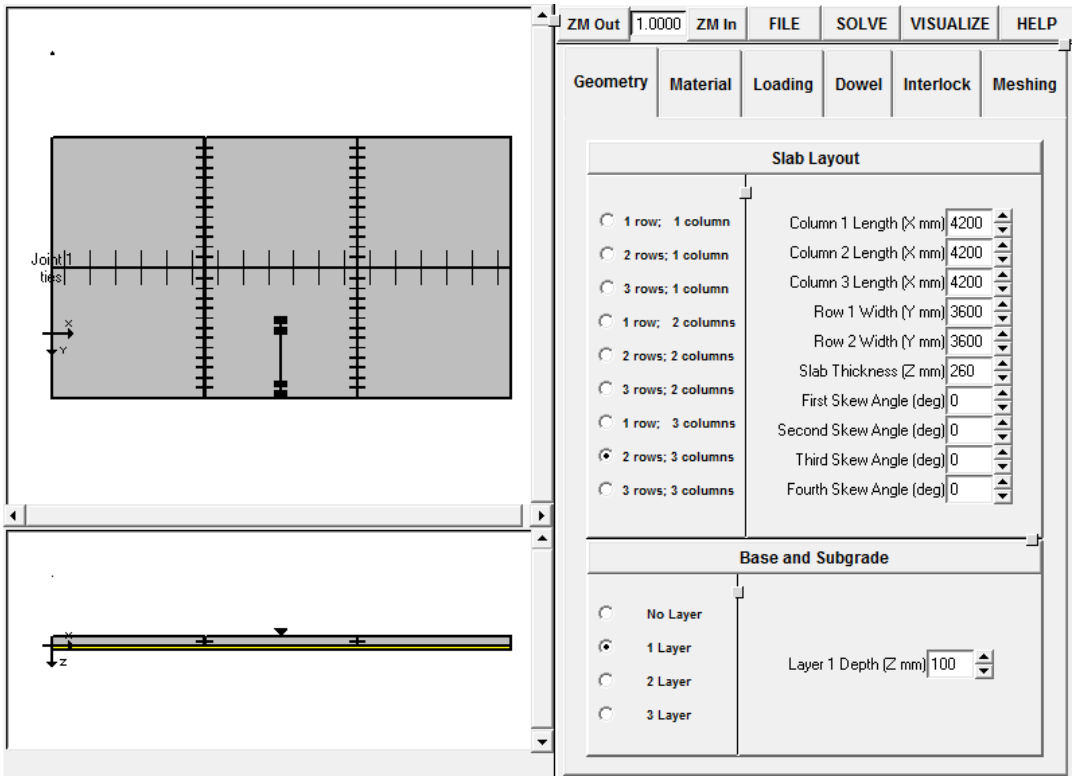

Figure4.23 - Geometry panel: k-value = 20MPa/m, without shoulder, 100mm base.

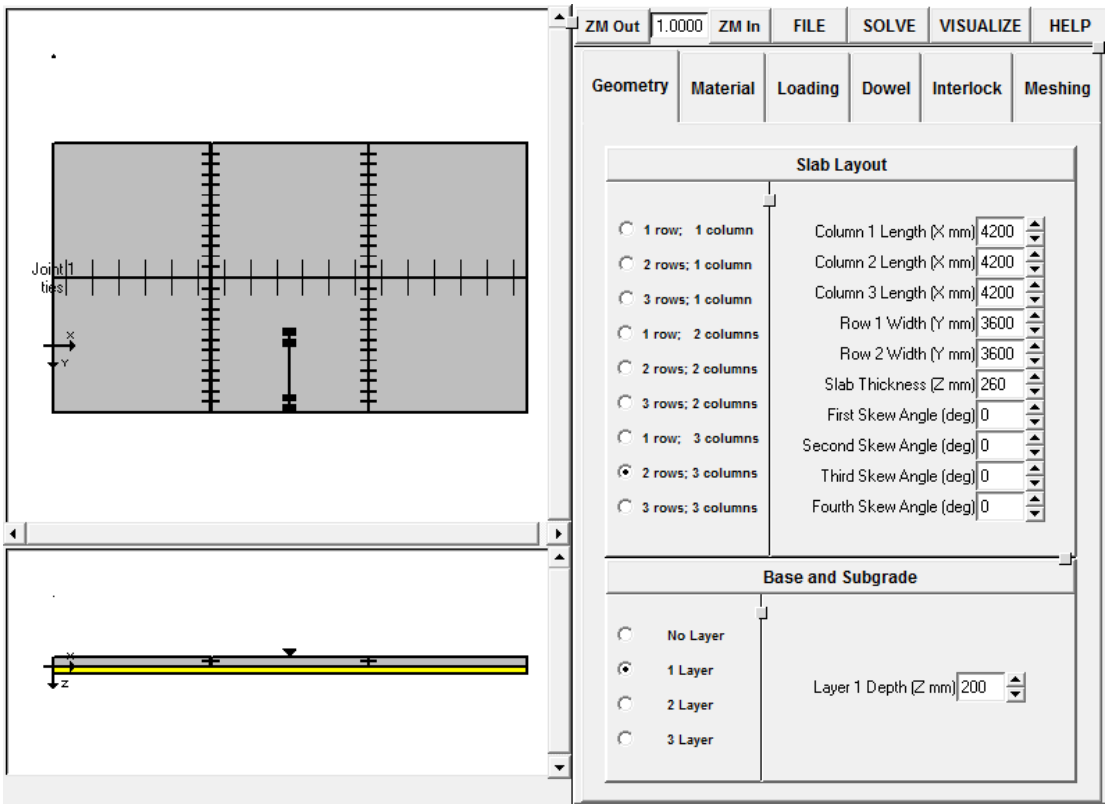

Figure 4.24 - Geometry panel: k-value = 20MPa/m, without shoulder, 200mm base.

b) Slab Material Properties

As mentioned before, the slab concrete properties were constant for all the models. Table 4.2 shows the property values. The slab material subpanel is presented in figure 4.25.

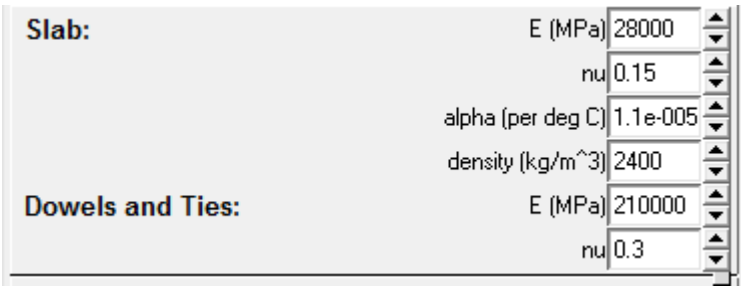

Figure 4.25 - Slab, Dowels and Ties material EverFE-subpanel.

c) Foundation Material Properties

Five types of bases were considered: non-stabilized base, cement stabilized subgrade, lime stabilized subgrade, cement treated base, and lean concrete base (table 4.4). For each base and stabilized subgrade two thickness were modelled as shown in the geometry item. These variables were used for several subgrade k-value (as shown in Table 4.5) and its corresponding slab thickness. Figures 4.26 shows the foundation parameters subpanel for the non-stabilized base and k-value of 20 MPa/m.

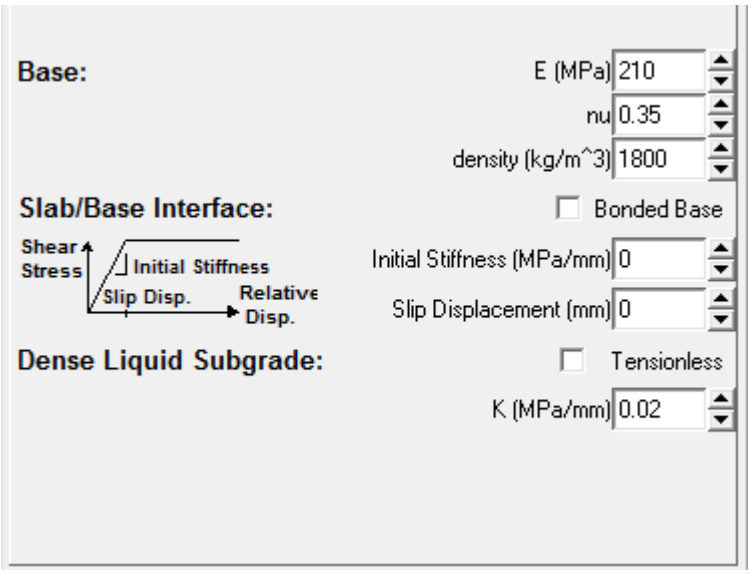

Figure 4.26 - Foundation material parameters EverFE-subpanel.

d) Loads

A 195 kN wheel dual axle (four wheels) and a temperature gradient of 10 °C were assumed as a traffic- and environmental load respectively. It was considered a tire pressure of 760kPa, which results in a contact area of

$$A = \frac{133kN/4}{760kPa} = 0.0438\,m^2$$

With this area, the dimensions W and L can be computed using equations 3.1 and 3.2.

$$L = \sqrt{\frac{0.0438}{0.523}} = 0.290\,m$$

$$W = 0.6 \times 0.290m = 0.174\,m$$

The traffic load is located at the fatigue analysis critical position as discussed in section 3.4.2.2, Figure 3.13. Figures 4.27 shows the loading panel with more details.

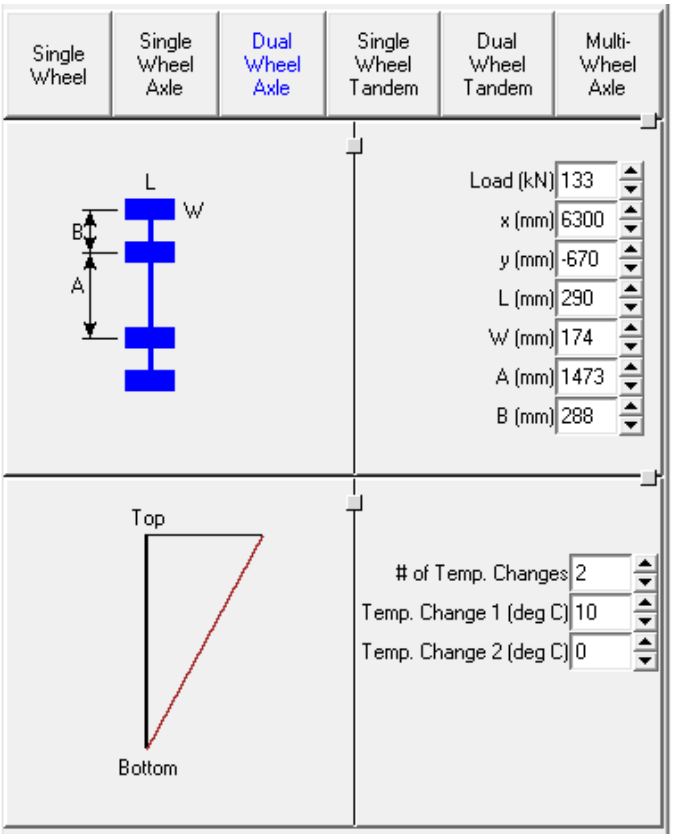

Figure 4.27 - Loading EverFE-panel

e) Dowel and Interlock

For the dowel and interlock solver, a linear model was considered, see Figure 4.28. The dowels and ties parameter values are summarized in table 4.6.

Table 4.6 - Dowels and ties parameters

Parameters	Dowels	Ties
Elasticity modulus, (MPa)	210 000	210 000
Poisson's ratio	0,30	0,30
Diameter (mm)	32,0	12,5
Length (m)	0,50	1,00
Embedment (m)	0,23	0,47
Spacing (m)	0,30	0,75

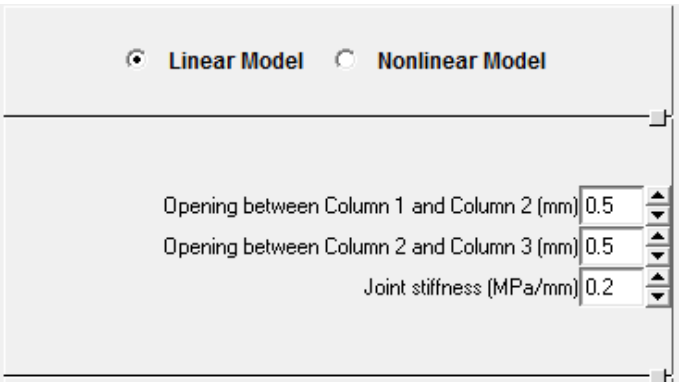

Figure 4.28 - Linear model for dowel and aggregate interlock

f) Meshing

As suggested by EverFE user manual, an element aspect ratio less than five was guaranteed. This value should be kept to less than five to minimize mesh distortion errors and computational time. Table 4.7 summarizes the number of each element type discussed in section 4.1.1.

Table 4.7 - Model discretization

Type of element	Number of element:	
	With shoulder	Without shoulder
20-noded quadratic brick elements	3072	2304
8-noded planar quadratic elements	1024	768
16-noded quadratic interface elements	128	80
3-noded embedded flexural elements	98	66
2-noded shear beam elements	98	66
Total	4420	3284

Figure 4.29 shows the 2 plane geometries considered, as well as the meshing subpanel for both cases, with- and without shoulder.

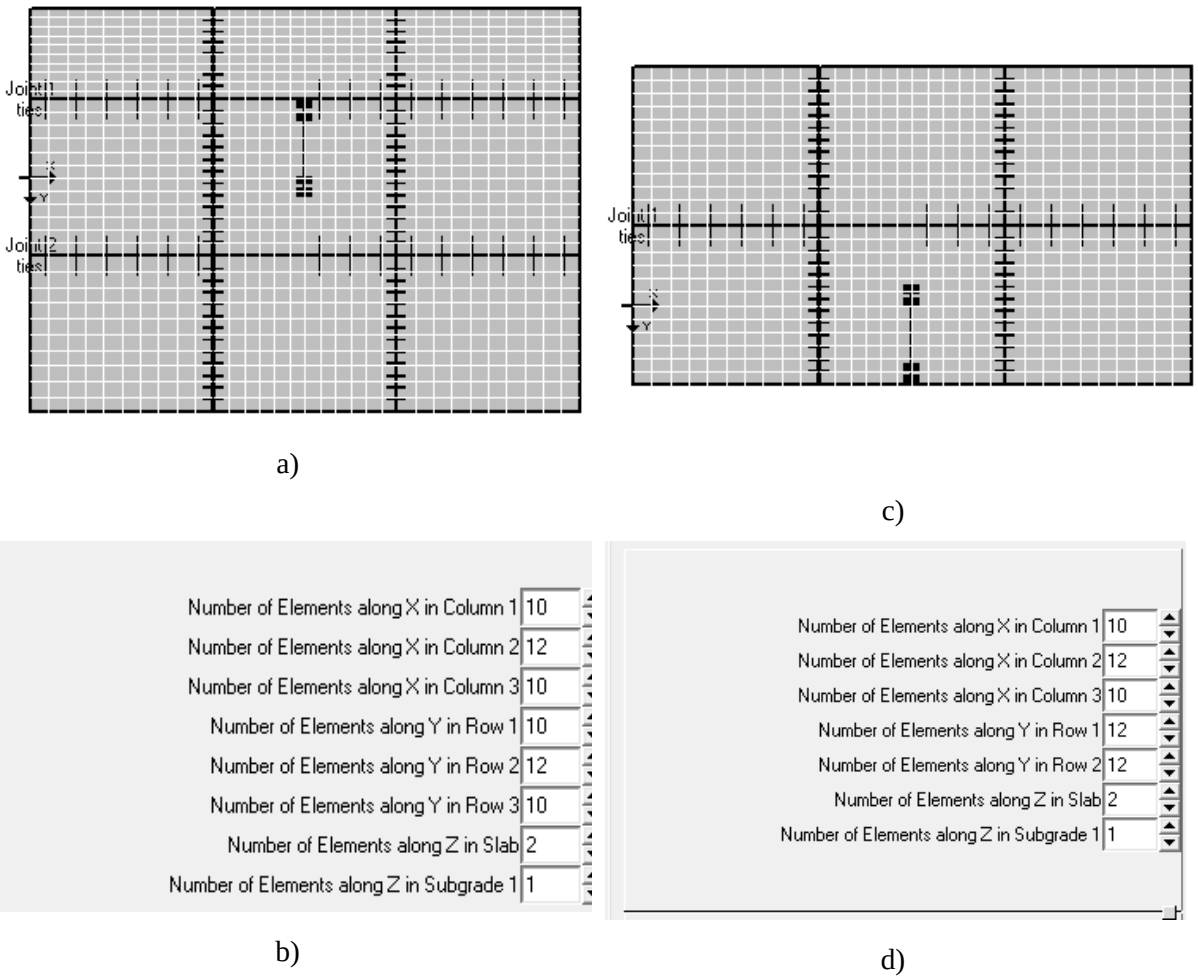

Figure 4.29 - Meshing: a) geometry discretization with shoulder, b) meshing panel geometry with shoulder, c) geometry discretization without shoulder, d) meshing panel geometry without shoulder.

4.2.6.2. Visualization of the results

As example, the next two figures show the non-stabilized base results for: a) k-value 20 MPa/m and base of 100 mm thickness, and b) k-value 20 MPa/m and base of 200 mm thickness, both considering shoulders.

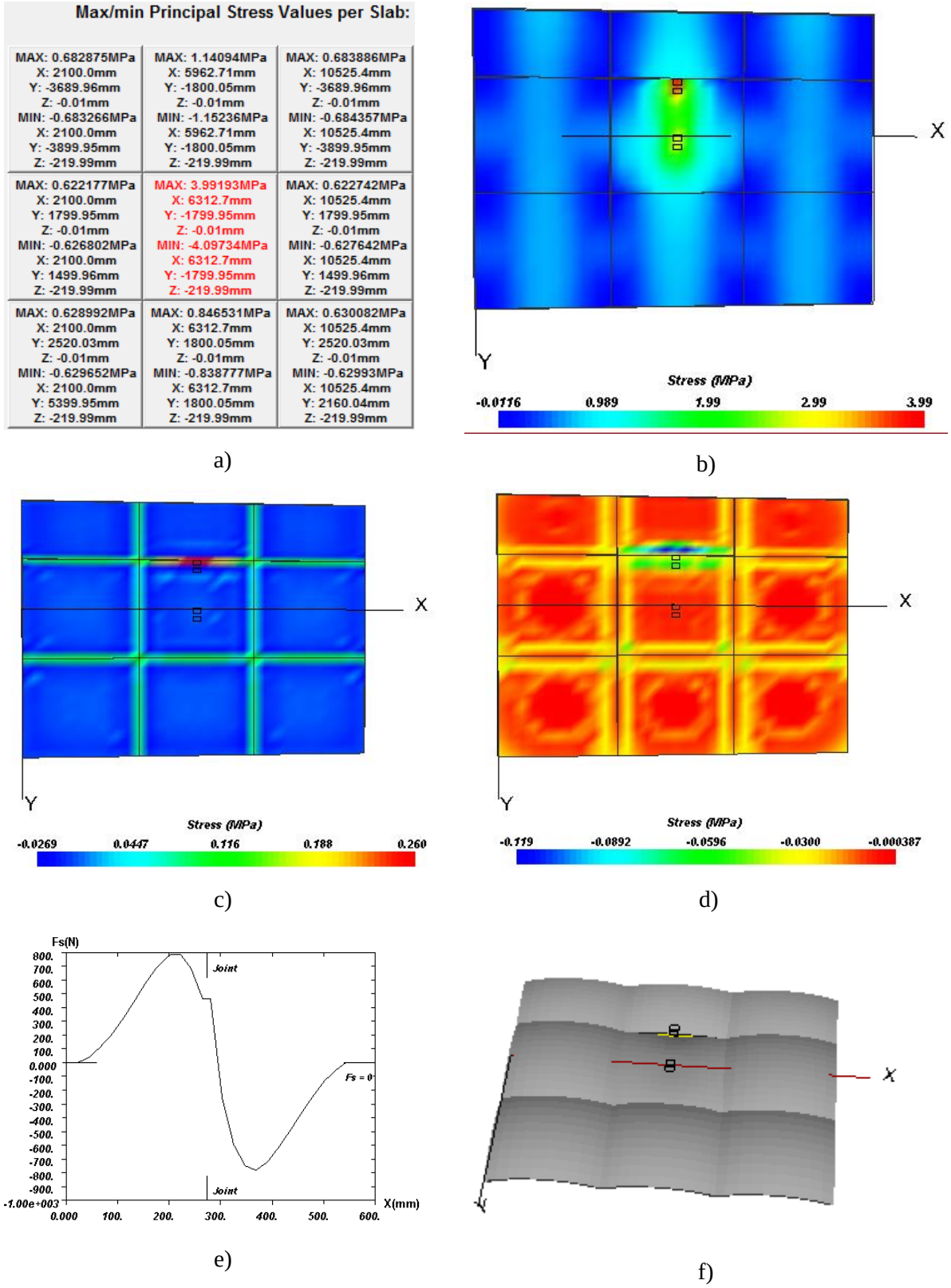

Figure 4.30 - Non-stabilized (100mm, with shoulder) base results data: a) principal stress values per slabs, b) maximum stress value at the slab bottom, c) maximum stress value at the bottom of the base, d) minimum stress value at the bottom of the base, e) dowel maximum shear force, f) deformed slabs.

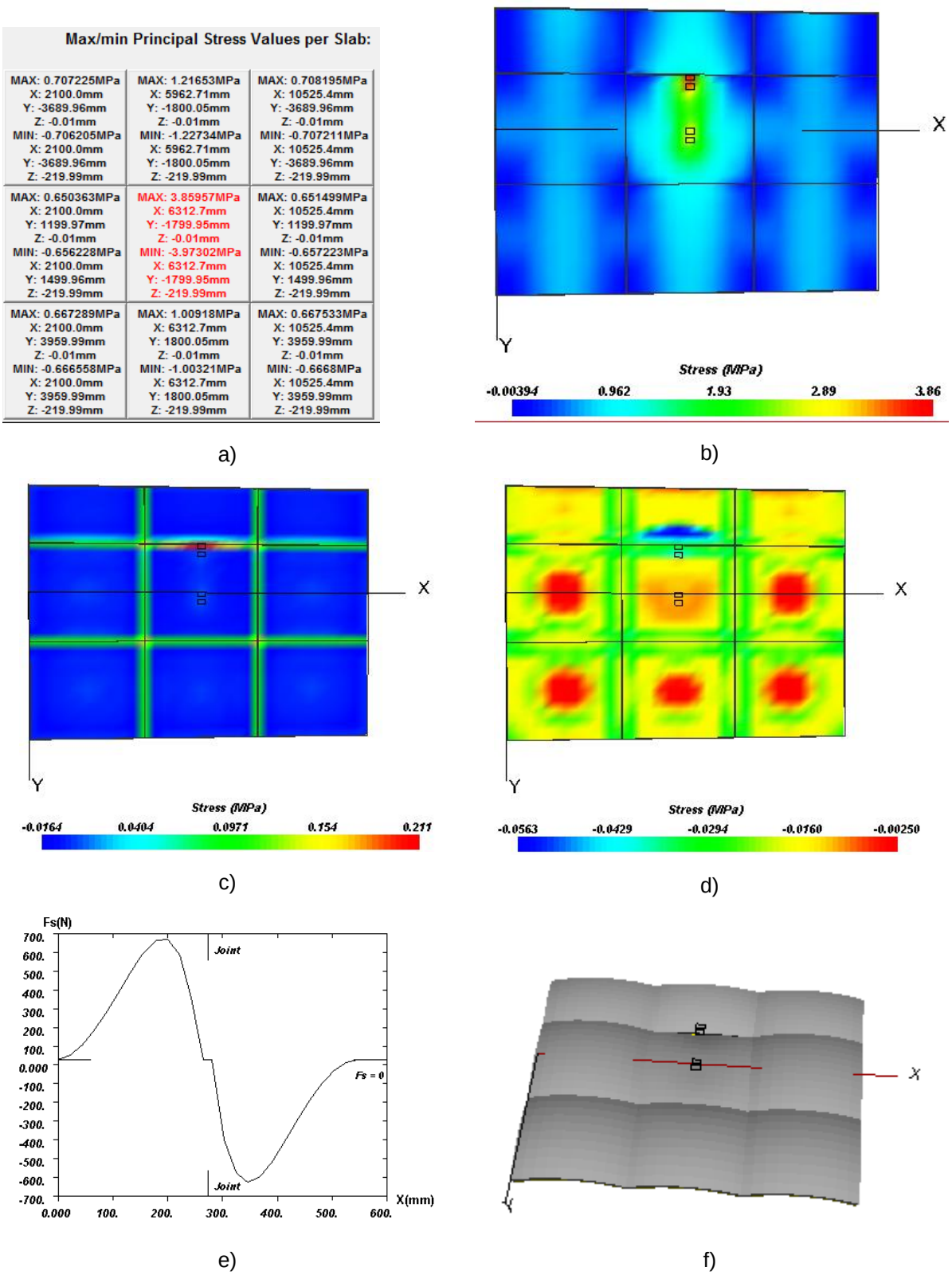

Figure 4.31 - Non-stabilized (200mm, with shoulder) base results data: a) principal stress values per slabs, b) maximum stress value at the slab bottom, c) maximum stress value at the bottom of the base, d) minimum stress value at the bottom of the base, e) dowel maximum shear force, f) deformed slabs.

The next two figures show the non-stabilized base results for: a) k-value 20 MPa/m and base of 100 mm thickness, and b) k-value 20 MPa/m and base of 200 mm thickness, both without shoulders.

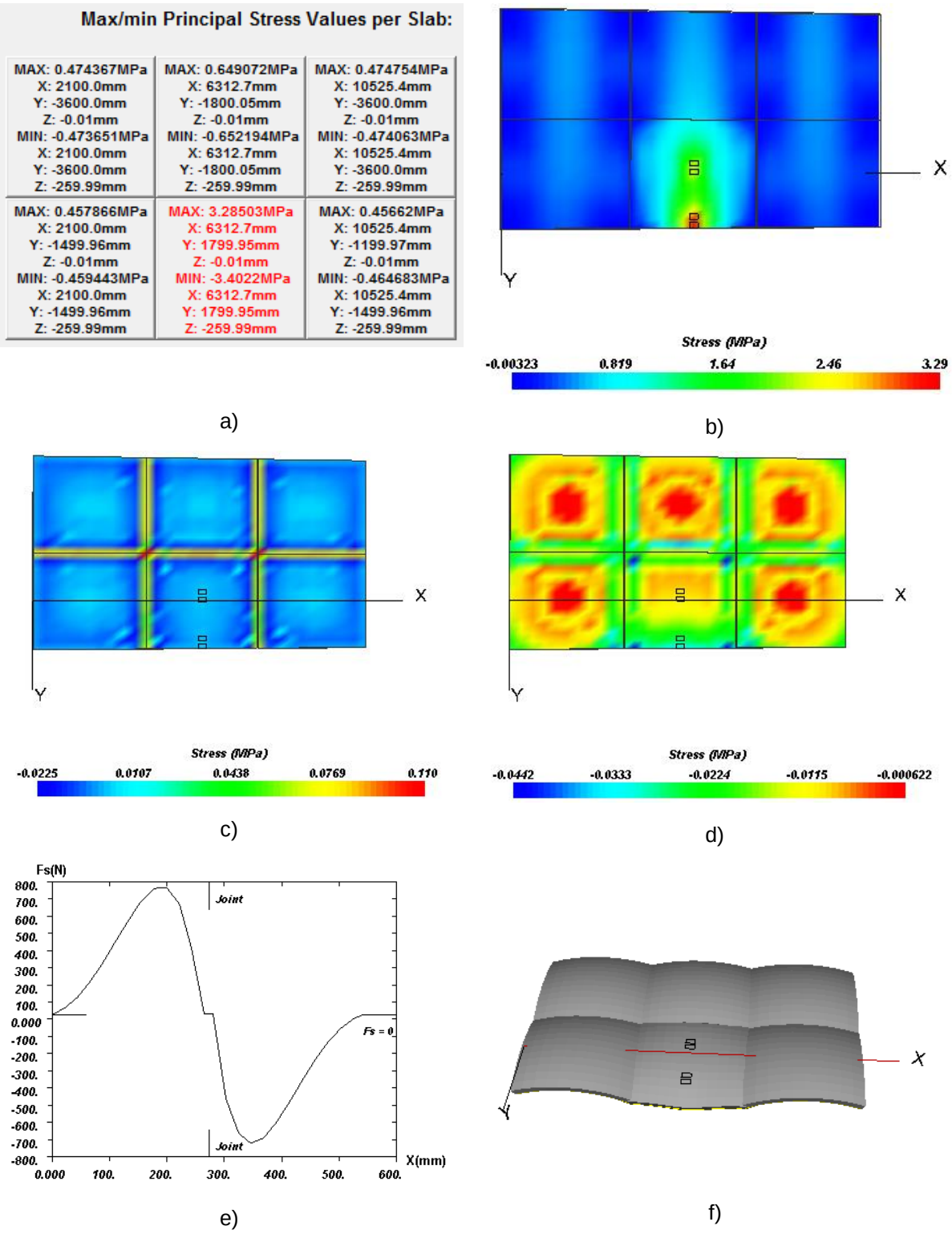

Figure 4.32 - Non-stabilized (100mm, without shoulder) base results data: a) principal stress values per slabs, b) maximum stress value at the slab bottom, c) maximum stress value at the bottom of the base, d) minimum stress value at the bottom of the base, e) dowel maximum shear force, f) deformed slabs.

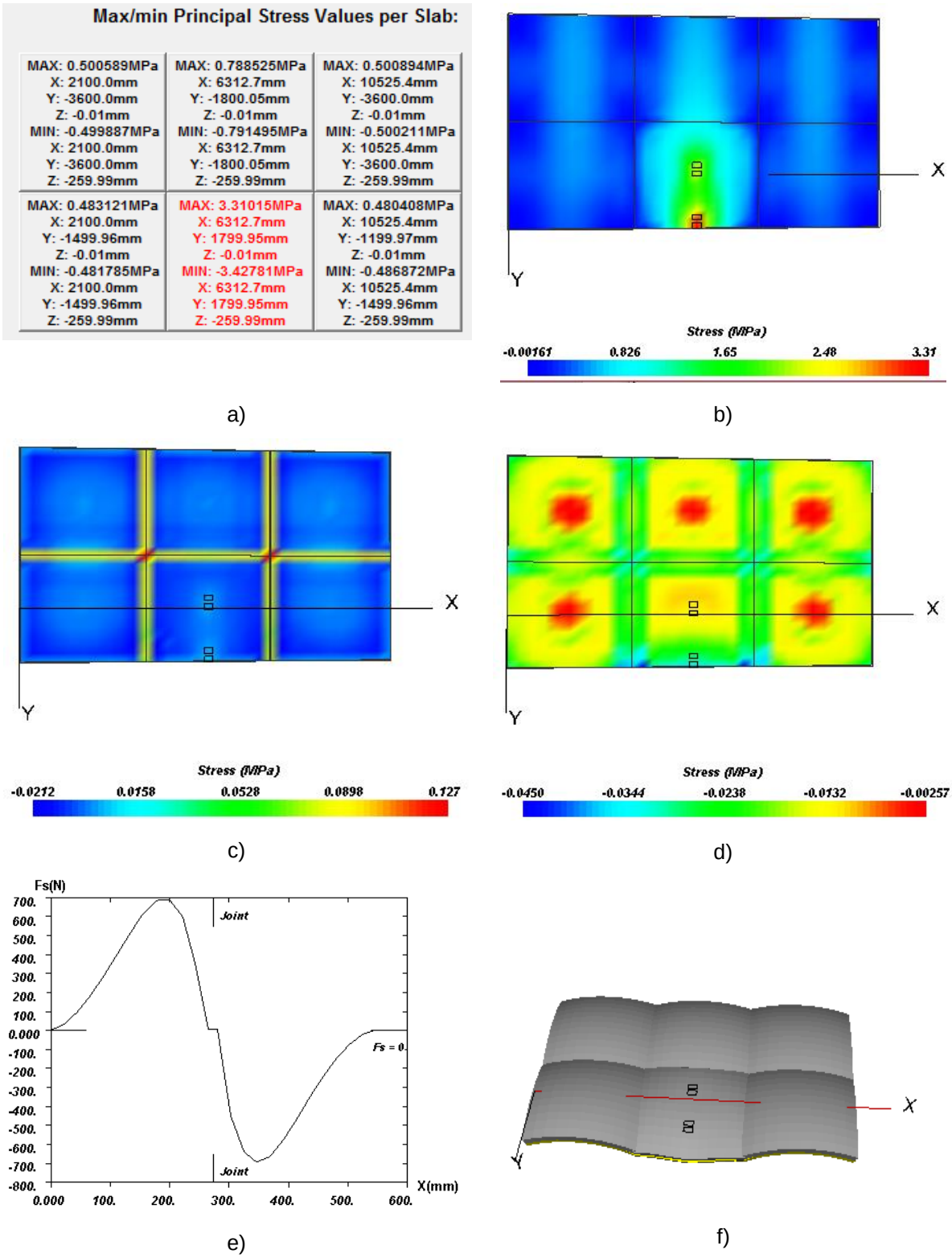

Figure 4.33 - Non-stabilized (200mm, without shoulder) base results data: a) principal stress values per slabs, b) maximum stress value at the slab bottom, c) maximum stress value at the bottom of the base, d) minimum stress value at the bottom of the base, e) dowel maximum shear force, f) deformed slabs.

4.2.6.3. Analysis of the results

As mentioned before, the simulations were carried out considering the thickness design for five representative k-values, (20 MPa/m, 80 MPa/m, 110 MPa/m, 150 MPa/m, and 200 MPa/m), as well as five different type of support (non-stabilized base, cement stabilized subgrade, lime stabilized subgrade, cement treated base, and lean concrete base). Each type of base or stabilized subgrade was modelled using two thickness, 100 mm and 200 mm. The most import parameter from the model results is the maximum stress at the slab bottom because it can be contrasted with the modulus of rupture. Maximum stresses at the bottom of the slab are summarized as follows:

a) With shoulder

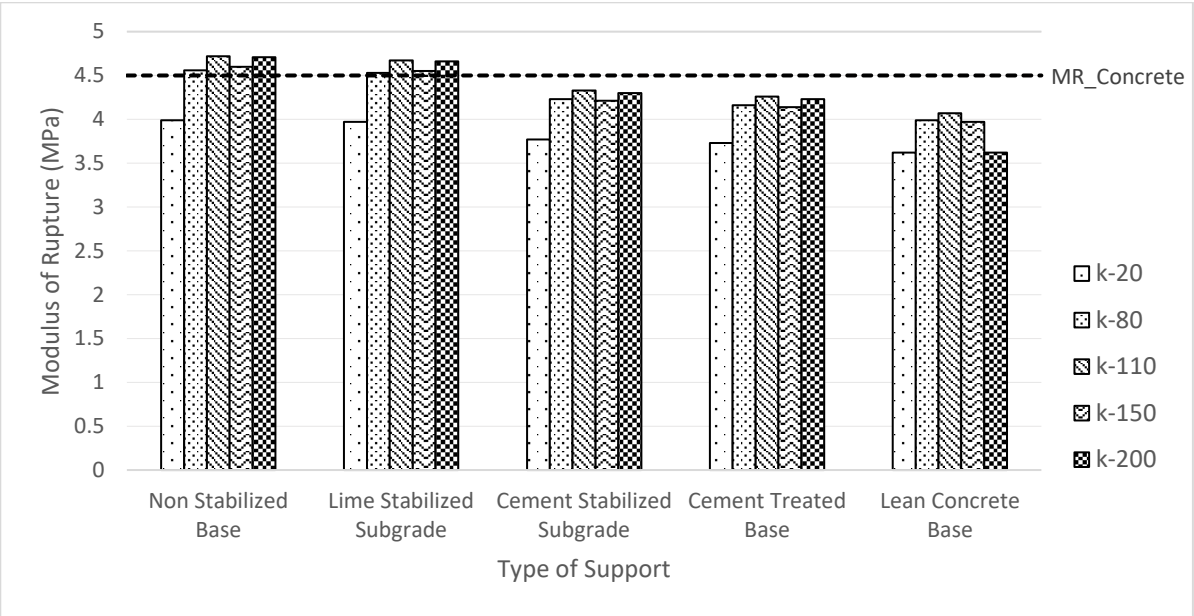

Figure 4.34 - Maximum stress value for 100mm base or stabilized subgrade (with shoulder)

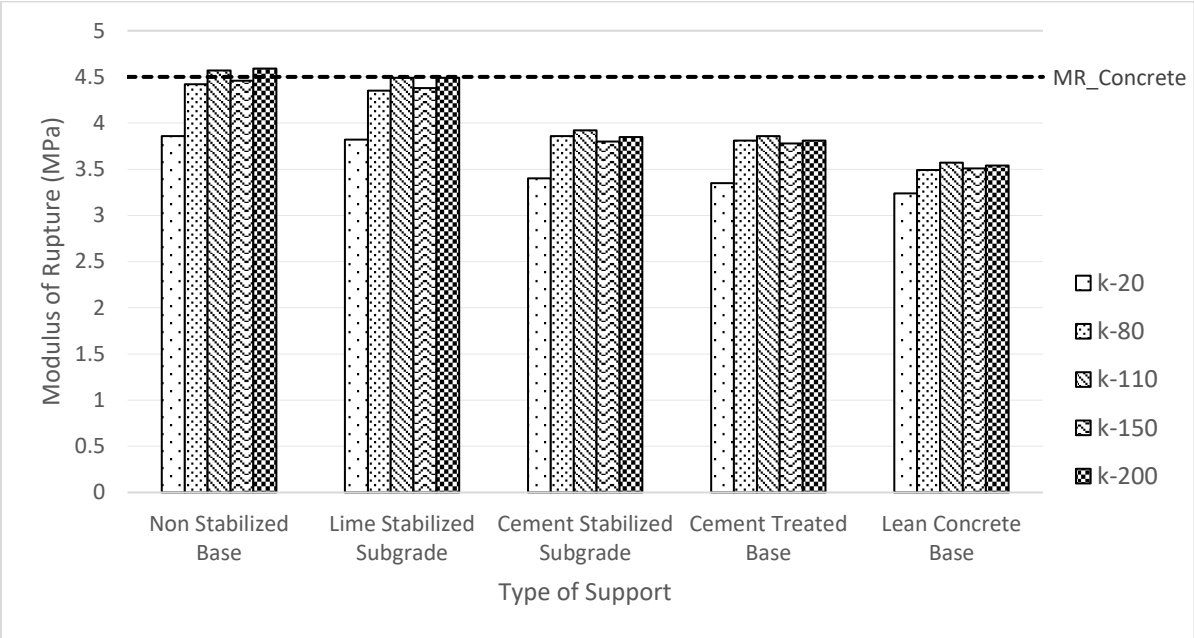

Figure 4.35 - Maximum stress value for 200mm base or stabilized subgrade (with shoulder)

The results confirm that the k-value influence the mechanical response of the rigid pavements. Changing from 80 MPa/m to 200 MPa/m, without considering the type of the base or stabilized subgrade, results in an almost steady tendency of the maximum stress. For the 20 MPa/m the maximum stress is lower, because the slab thickness is considerably higher.

For the 100 mm-base or stabilized subgrade simulations, the non-stabilized base and the lime stabilized subgrade, for k-values between 80 MPa/m and 200 MPa/m, present similar maximum stress value, which is in average 4.6 MPa. On the other hand, cement stabilized subgrade, cement treated base, and lean concrete base have similar maximum stress values between them. In the last three cases, the average maximum stress is 4 MPa.

For the 200 mm-base or stabilized-subgrade simulations, the non-stabilized base and the lime stabilized subgrade have similar values as those obtained in the 100 mm-base or stabilized-subgrade. For the remaining three types of bases and stabilized-subgrades, the maximum stresses decreased considerably. The average maximum stress is 3,7 MPa, which mean they did not reach the modulus of the rupture of the concrete.

b) Without shoulder

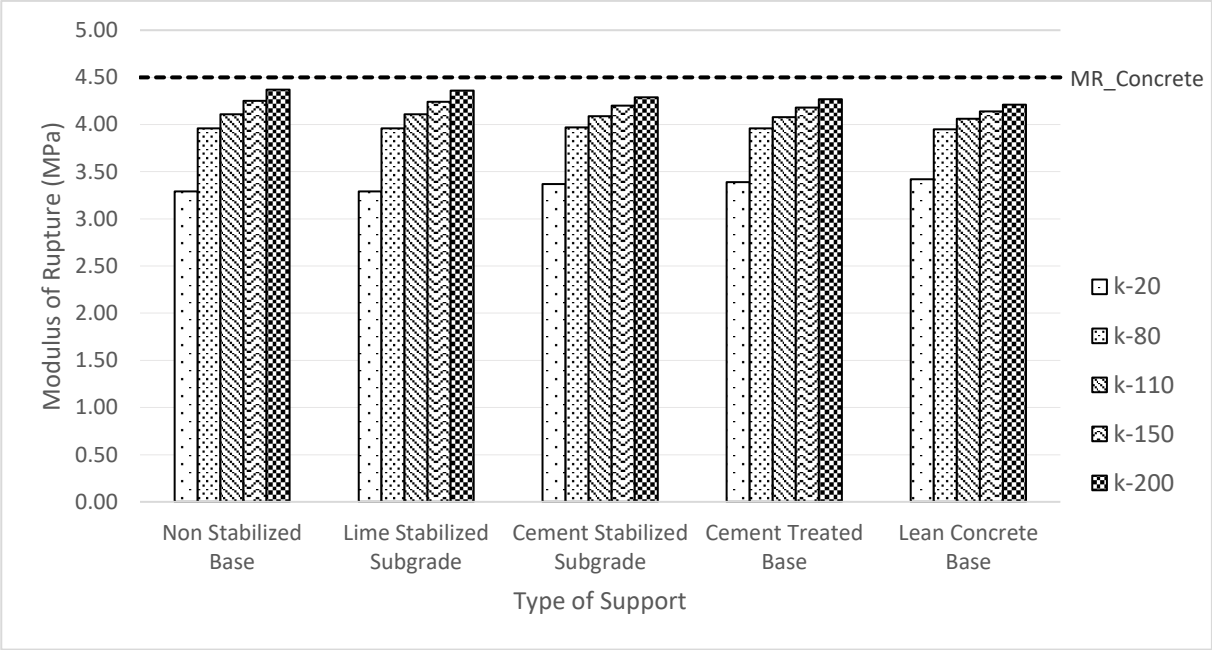

Figure 4.36 - Maximum stress value for 100mm base or stabilized subgrade (without shoulder)

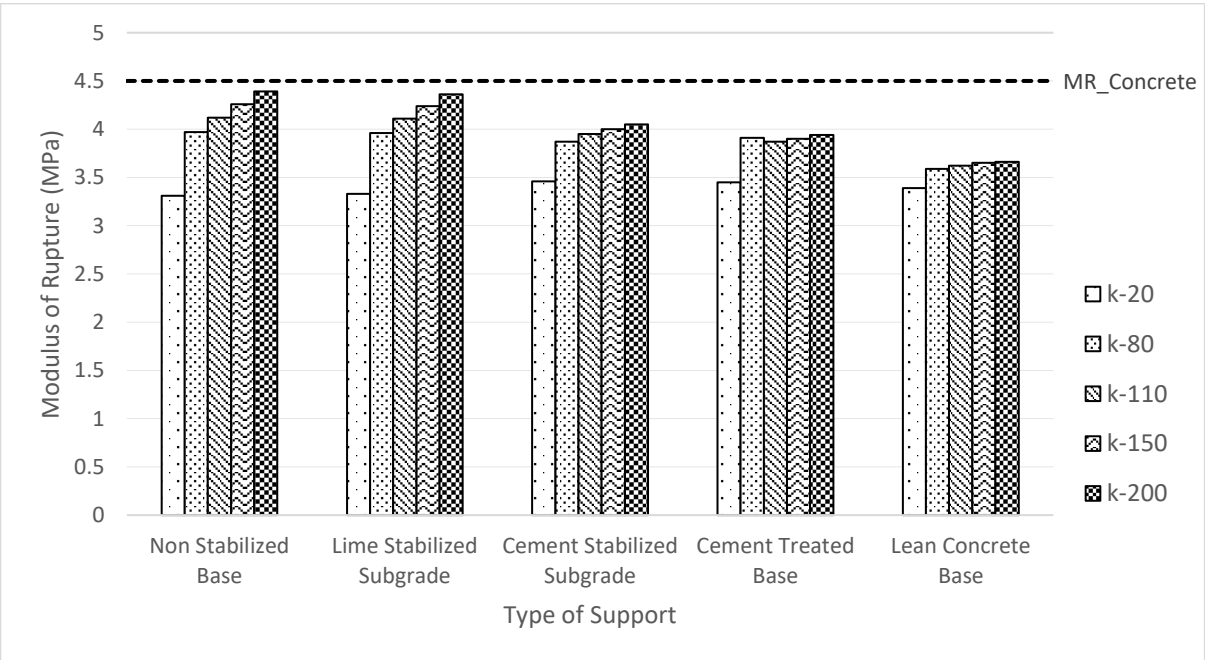

Figure 4.37 - Maximum stress value for 200mm base or stabilized subgrade (without shoulder)

As in the previous case, changing from 20 MPa/m to 200 MPa/m affected the maximum stress. The lower k-values presented a lower maximum stress values in all the scenarios, because the slab thickness design resulted in a higher slab thickness values when the k-values are lower.

For the 100 mm-base or stabilized-subgrade simulations, the five scenarios presented a similar performance. The minimum maximum stress of 3.29 MPa was obtained for the 20 MPa/m k-value and the maximum stress was 4.37 MPa for the 200 MPa/m k-value.

For the 200 mm-base or stabilized-subgrade simulations, the non-stabilized base and the lime stabilized subgrade have the same values as those obtained in the 100 mm-base or stabilized-subgrade. For the remaining three types of base and stabilized-subgrade, the maximum stress was 3.8 MPa, in the remaining three cases the maximum stress is very similar between the different k-values.

5

CONCLUSION AND FURTHER WORK

5.1. CONCLUSION

It was presented a briefly introduction of the history of rigid pavements. The key issues of the conception of rigid pavement, such the material, type of rigid pavements, the use of bases and the thickness design, were presented.

The influence of the foundation geotechnical characteristics on the performance of rigid pavement was studied. Since the mechanical performance of rigid pavements depends (among other factors) on the k-value, a sensitive analysis of the k-value on the thickness design was conducted. Finally, the numerical simulation to study the influence of the geotechnical parameters on the mechanical performance of rigid pavements was carried out. The main findings are presented as follows:

- The k-value has a key role in the thickness design of rigid pavement. Furthermore, determining the slab thickness according to the k-value results in a homogenous performance of the pavement system. In other words, the better foundation the lower the slab thickness. This fact validates the effectiveness of the design methods.
- Considering the benefits of the shoulders for decreasing the slab thickness could result in very high values of maximum stress, when they are loaded at a critical position. Under the conditions studied, it does not matter the improvement of the foundation, the result will be the same if 100 mm base or stabilized-subgrade is used.
- Strong base or stabilized-subgrade, e.g. elasticity modulus greater than 5000 MPa and an adequate thickness could prevent mechanical failure of the concrete slab.
- The slab thickness design using the PCA is less conservative than the AASHTO method, but it is still safe without shoulders. When using shoulder and the non-stabilized base or the lime stabilized subgrade, the slab thickness should be slightly increased.

5.2. FURTHER WORK

For a better understanding of the mechanical response of rigid pavement, based on the geotechnical characteristics, further research is recommended. Additional studies could include, for example:

- The influence of the foundation erosion on the pavement performance using another more powerful finite element software, such as Abaqus or ANSYS that is no limited to a uniform foundation like EverFE. The analysis of erosion can be simulated using, for example, cavities of several sizes in the foundation.
- The analysis of the foundation using other constitutive models, in comparison to the elastic model used in this study, for a better understanding of the mechanical response of the bounded and unbounded granular materials used in rigid pavement foundation.
- The rigid pavement performance, based on geotechnical characteristics, should also be studied also in a dynamics framework. For example, the influence of the dynamic loads application (such as takeoff and landing of airplanes airport pavements) on the resilient modulus (and back calculation of the k-value) of the pavement foundation.
- Considering that the resilient modulus varies depending on factors such as the water content, density and stress level, as reported by Fortunato et. al. [26], instead of considering a constant average value of resilient modulus determined at the optimum water content and a unique load application as used in this study, it will be interesting to study the impact of the resilient modulus variation (determined by statics and dynamics aggregate characterization) on the design and performance of rigid pavement.

BIBLIOGRAPHY

[1]. Hein, D.K., S. Rao, and H. Lee, *Bases and Subbases for Concrete Pavements*. 2016. FHWA USDoT Washinton DC.

[2]. Ceylan, H., et al., *Sensitivity analysis frameworks for mechanistic-empirical pavement design of continuously reinforced concrete pavements.* Construction and Building Materials, 2014. **73**: p. 498-508.

[3]. Belshe, M., et al., *Temperature Gradient and Curling Stresses in Concrete Pavement with and without Open-Graded Friction Course.* Journal of Transportation Engineering, 2010. **137**(10): p. 723-729.

[4]. Zokaei-Ashtiani, A., et al., *Impact of different approaches to modelling rigid pavement base layers on slab curling stresses.* International Journal of Pavement Engineering, 2016. **17**(10): p. 861-869.

[5]. Zokaei-Ashtiani, A., C. Carrasco, and S. Nazarian, *Finite element modeling of slab–foundation interaction on rigid pavement applications.* Computers and Geotechnics, 2014. **62**: p. 118-127.

[6]. Packard, R.G., *Thickness design for concrete highway and street pavements.* 1984, PCA.

[7]. Davids, W., et al., *Three-dimensional finite element analysis of jointed plain concrete pavement with EverFE2. 2.* Transportation Research Record: Journal of the Transportation Research Board, 2003(1853): p. 92-99.

[8]. Mu, F. and J.M. Vandenbossche, *Evaluation of the approach used for modeling the base under jointed plain concrete pavements in the AASHTO Pavement ME Design Guide.* International Journal of Pavement Research and Technology, 2016. **9**(4): p. 264-269.

[9]. Pradena, M. and L. Houben, *Uncracked joints in plain concrete pavements: causes, effects and possibilities of improvements.* Journal of Transport Literature, 2016. **10**(1): p. 40-44.

[10]. Uddin, W., et al., *Three-dimensional finite-element analysis of jointed concrete pavement with discontinuities.* Transportation Research Record, 1995. **1482**: p. 26-32.

[11]. Kim, S.-H., J.-Y. Park, and J.-H. Jeong, *Effect of temperature-induced load on airport concrete pavement behavior*. KSCE Journal of Civil Engineering, 2014. **18**(1): p. 182-187.

[12]. Kim, S., H. Ceylan, and K. Gopalakrishnan, *Finite element modeling of environmental effects on rigid pavement deformation.* Frontiers of Structural and Civil Engineering, 2014. **8**(2): p. 101-114.

[13]. Interactive, P. 2017 ; Available from: http://www.pavementinteractive.org/. [Accessed: April 2017]

[14]. FHWA. *Federal Highway Administration* 2017; Available from: https://www.fhwa.dot.gov/engineering/geotech/ ,[Accessed: June 2017].

[15]. Huang, Y.H., *Pavement analysis and design*. 1993. Prentice Hall Englewood Cliffs, NJ.

[16]. Porto, D.J., *Estado del Arte de los Pavimentos de Hormigón en Latino America* 2012: Argentina. Conference paper.

[17]. Eupave. *Eupave.eu*. 2017; Available from: http://www.eupave.eu/documents/home.xml?lang=en. [Accessed: April 2017].

[18]. Jofré, C., *The european standards on materials for concrete pavements,* Instituto Español del Cemento y sus Aplicaciones: Spain.

[19]. Sii, M.H.B., *Three-Dimensional Finite Element Analysis of Concrete Pavement on Weak Foundation*. 2014, Griffith University Gold Coast. PhD disertation.

[20]. Drivers. *Austroads.com.au*. 2016; Available from: http://www.austroads.com.au/. [Accessed: April 2017]

[21]. DNIT, *Manual de Pavimentos Rígidos*. 2005, Brasil Departamento Nacional de Infraestructura de Transporte.

[22]. Lamond, J.F. and J.H. Pielert. *Significance of tests and properties of concrete and concrete-making materials*. 2006. ASTM West Conshohocken, PA.

[23]. Wikipave. *Wikipave.org*. 2017; Available from: http://wikipave.org/index.php?title=Welcome_to_ACPA%27s_Concrete_Pavement_Wiki. [Accessed: April 2017].
[24]. Codot. *Colorado Department of Transportation*. 2017; Available from: https://www.codot.gov/. [Accessed: April 2017].
[25]. Davids, B., *EverFE theory manual.* 2003.
[26]. Fortunato, E., et al., *Estudo Laboratorial Sobre Agregados Aplicados Em Vias-Férreas Utilizando Ensaios De Carga Triaxial Cíclica Laboratorial Study On Unbound Granular Materials Applied In Rail Tracks Using Cyclic Triaxial Tests.*

A

A.1. PCA THICKNESS DESIGN

In this section, the thickness designs for data described in section 4.2 are carried out. The design consisted in determining the minimum slab thickness for a given k-value. The k-values were 35 MPa/m, 50 MPa/m, 80 MPa/m, 90 MPa/m, 110 MPa/m, 130 MPa/m, 150 MPa/m, and 180 MPa/m. It was considered both cases, with- and without concrete shoulders. The full worked worksheets are presented as follows:

a) With concrete Shoulders:

- Project: 4-LANE RURAL SECTION (1) = 35 MPa/m
- Project: 4-LANE RURAL SECTION (2) = 50 MPa/m
- Project: 4-LANE RURAL SECTION (3) = 80 MPa/m
- Project: 4-LANE RURAL SECTION (4) = 90 MPa/m
- Project: 4-LANE RURAL SECTION (5) = 110 MPa/m
- Project: 4-LANE RURAL SECTION (6) = 130 MPa/m
- Project: 4-LANE RURAL SECTION (7) = 150 MPa/m
- Project: 4-LANE RURAL SECTION (8) = 180 MPa/m

b) Without concrete Shoulders:

- Project: 4-LANE RURAL SECTION (9) = 35 MPa/m
- Project: 4-LANE RURAL SECTION (10) = 50 MPa/m
- Project: 4-LANE RURAL SECTION (11) = 80 MPa/m
- Project: 4-LANE RURAL SECTION (12) = 90 MPa/m
- Project: 4-LANE RURAL SECTION (13) = 110 MPa/m
- Project: 4-LANE RURAL SECTION (14) = 130 MPa/m
- Project: 4-LANE RURAL SECTION (15) = 150 MPa/m
- Project: 4-LANE RURAL SECTION (16) = 180 MPa/m

Calculation of Pavement Thickness

Project	4-LANE RURAL SECTION (1)			
Trial thickness	210	mm	Doweled Joints:	yes
Subbase-subgrade k	35	MPa/m	Concrete Shoulder:	yes
Modulus of rupture, MR	4.5	MPa	Design period [years]	20
Load safety factor, LSF	1.2			

Axel load, (kN)	Multiplied by LSF	Expected repetitions	Fatigue Analysis		Erosion Analysis	
			Allowable repetitions	Fatigue percent	Allowable repetitions	Fatigue percent
1	2	3	4	5	6	7
			8. Equivalent stress	1.42	10. Erosion factor	2.35
			9. Stress ratio factor	0.32		
Single Axles						
133	160	6310	21000	30.0	450000	1.4
125	150	14690	55000	26.7	950000	1.5
115	138	30140	180000	16.7	1600000	1.9
107	129	64410	700000	9.2	3000000	2.1
98	118	106900	9000000	1.2	10000000	1.1
89	107	235800	Unlimited	0.0	40000000	0.6
80	96	307200	Unlimited	0.0	Unlimited	0.0
			11. Equivalent stress	1.24	13. Erosion factor	2.50
			12. Stress ratio factor	0.28		
Tandem Axles						
231	278	21320	3000000	0.7	500000	4.3
213	256	42870	Unlimited	0.0	750000	5.7
195	234	124900	Unlimited	0.0	2000000	6.2
178	214	372900	Unlimited	0.0	3500000	10.7
160	192	885800	Unlimited	0.0	15000000	5.9
142	171	930700	Unlimited	0.0	Unlimited	0.0
125	150	1656000	Unlimited	0.0	Unlimited	0.0
			14. Equivalent stress	0.95	16. Erosion factor	2.60
			15. Stress ratio factor	0.21		
Tridem Axles						
240	96	250000	Unlimited	0.0	3000000	8.3
			Total	84.6	Total	49.8

Calculation of Pavement Thickness

Project	4-LANE RURAL SECTION (2)				
Trial thickness	200	mm		Doweled Joints:	yes
Subbase-subgrade k	50	MPa/m		Concrete Shoulder:	yes
Modulus of rupture, MR	4.5	MPa		Design period [years]	20
Load safety factor, LSF	1.2				

Axel load, (kN)	Multiplied by LSF	Expected repetitions	Fatigue Analysis		Erosion Analysis	
			Allowable repetitions	Fatigue percent	Allowable repetitions	Fatigue percent
1	2	3	4	5	6	7
			8. Equivalent stress	1.42	10. Erosion factor	2.39
			9. Stress ratio factor	0.32		
Single Axles						
133	160	6310	22000	28.7	400000	1.6
125	150	14690	55000	26.7	700000	2.1
115	138	30140	180000	16.7	1000000	3.0
107	129	64410	600000	10.7	1800000	3.6
98	118	106900	7000000	1.5	4000000	2.7
89	107	235800	Unlimited	0.0	15000000	1.6
80	96	307200	Unlimited	0.0	Unlimited	0.0
			11. Equivalent stress	1.22	13. Erosion factor	2.48
			12. Stress ratio factor	0.27		
Tandem Axles						
231	278	21320	10000000	0.2	550000	3.9
213	256	42870	Unlimited	0.0	900000	4.8
195	234	124900	Unlimited	0.0	2500000	5.0
178	214	372900	Unlimited	0.0	5000000	7.5
160	192	885800	Unlimited	0.0	20000000	4.4
142	171	930700	Unlimited	0.0	Unlimited	0.0
125	150	1656000	Unlimited	0.0	Unlimited	0.0
			14. Equivalent stress	0.95	16. Erosion factor	2.55
			15. Stress ratio factor	0.21		
Tridem Axles						
240	96	250000	Unlimited	0.0	50000000	0.5
			Total	84.6	Total	40.5

Calculation of Pavement Thickness

Project	4-LANE RURAL SECTION (3)			
Trial thickness	190	mm	Doweled Joints:	yes
Subbase-subgrade k	80	MPa/m	Concrete Shoulder:	yes
Modulus of rupture, MR	4.5	MPa	Design period [years]	20
Load safety factor, LSF	1.2			

Axel load, (kN)	Multiplied by LSF	Expected repetitions	Fatigue Analysis		Erosion Analysis	
			Allowable repetitions	Fatigue percent	Allowable repetitions	Fatigue percent
1	2	3	4	5	6	7
			8. Equivalent stress	1.40	10. Erosion factor	2.41
			9. Stress ratio factor	0.31		
Single Axles						
133	160	6310	36000	17.5	330000	1.9
125	150	14690	85000	17.3	600000	2.4
115	138	30140	260000	11.6	850000	3.5
107	129	64410	1000000	6.4	1600000	4.0
98	118	106900	Unlimited	0.0	3500000	3.1
89	107	235800	Unlimited	0.0	10000000	2.4
80	96	307200	Unlimited	0.0	100000000	0.3
			11. Equivalent stress	1.17	13. Erosion factor	2.44
			12. Stress ratio factor	0.26		
Tandem Axles						
231	278	21320	Unlimited	0.0	420000	5.1
213	256	42870	Unlimited	0.0	900000	4.8
195	234	124900	Unlimited	0.0	2900000	4.3
178	214	372900	Unlimited	0.0	5000000	7.5
160	192	885800	Unlimited	0.0	20000000	4.4
142	171	930700	Unlimited	0.0	Unlimited	0.0
125	150	1656000	Unlimited	0.0	Unlimited	0.0
			14. Equivalent stress	0.94	16. Erosion factor	2.48
			15. Stress ratio factor	0.21		
Tridem Axles						
240	96	250000	Unlimited	0.0	15000000	1.7
			Total	52.8	Total	45.4

Calculation of Pavement Thickness

Project	4-LANE RURAL SECTION (4)			
Trial thickness	190	mm	Doweled Joints:	yes
Subbase-subgrade k	90	MPa/m	Concrete Shoulder:	yes
Modulus of rupture, MR	4.5	MPa	Design period [years]	20
Load safety factor, LSF	1.2			

Axel load, (kN)	Multiplied by LSF	Expected repetitions	Fatigue Analysis		Erosion Analysis	
			Allowable repetitions	Fatigue percent	Allowable repetitions	Fatigue percent
1	2	3	4	5	6	7
			8. Equivalent stress	1.38	10. Erosion factor	2.40
			9. Stress ratio factor	0.31		
Single Axles						
133	160	6310	38000	16.6	400000	1.6
125	150	14690	85000	17.3	680000	2.2
115	138	30140	250000	12.1	1000000	3.0
107	129	64410	1400000	4.6	1900000	3.4
98	118	106900	Unlimited	0.0	4000000	2.7
89	107	235800	Unlimited	0.0	20000000	1.2
80	96	307200	Unlimited	0.0	Unlimited	0.0
			11. Equivalent stress	1.15	13. Erosion factor	2.42
			12. Stress ratio factor	0.26		
Tandem Axles						
231	278	21320	Unlimited	0.0	900000	2.4
213	256	42870	Unlimited	0.0	1500000	2.9
195	234	124900	Unlimited	0.0	4500000	2.8
178	214	372900	Unlimited	0.0	15000000	2.5
160	192	885800	Unlimited	0.0	40000000	2.2
142	171	930700	Unlimited	0.0	Unlimited	0.0
125	150	1656000	Unlimited	0.0	Unlimited	0.0
			14. Equivalent stress	0.93	16. Erosion factor	2.46
			15. Stress ratio factor	0.21		
Tridem Axles						
240	96	250000	Unlimited	0.0	11000000	2.3
			Total	50.5	Total	29.0

Calculation of Pavement Thickness

Project	4-LANE RURAL SECTION (5)			
Trial thickness	180	mm	Doweled Joints:	yes
Subbase-subgrade k	110	MPa/m	Concrete Shoulder:	yes
Modulus of rupture, MR	4.5	MPa	Design period [years]	20
Load safety factor, LSF	1.2			

Axel load, (kN)	Multiplied by LSF	Expected repetitions	Fatigue Analysis		Erosion Analysis	
			Allowable repetitions	Fatigue percent	Allowable repetitions	Fatigue percent
1	2	3	4	5	6	7
			8. Equivalent stress	1.44	10. Erosion factor	2.46
			9. Stress ratio factor	0.32		
Single Axles						
133	160	6310	21000	30.0	270000	2.3
125	150	14690	55000	26.7	450000	3.3
115	138	30140	180000	16.7	700000	4.3
107	129	64410	700000	9.2	1200000	5.4
98	118	106900	9000000	1.2	2600000	4.1
89	107	235800	Unlimited	0.0	8000000	2.9
80	96	307200	Unlimited	0.0	40000000	0.8
			11. Equivalent stress	1.20	13. Erosion factor	2.45
			12. Stress ratio factor	0.27		
Tandem Axles						
231	278	21320	Unlimited	0.0	700000	3.0
213	256	42870	Unlimited	0.0	1500000	2.9
195	234	124900	Unlimited	0.0	3500000	3.6
178	214	372900	Unlimited	0.0	8000000	4.7
160	192	885800	Unlimited	0.0	42000000	2.1
142	171	930700	Unlimited	0.0	Unlimited	0.0
125	150	1656000	Unlimited	0.0	Unlimited	0.0
			14. Equivalent stress	0.99	16. Erosion factor	2.47
			15. Stress ratio factor	0.22		
Tridem Axles						
240	96	250000	Unlimited	0.0	16000000	1.6
			Total	83.9	Total	40.9

Calculation of Pavement Thickness

Project	4-LANE RURAL SECTION (6)			
Trial thickness	170	mm	Doweled Joints:	yes
Subbase-subgrade k	130	MPa/m	Concrete Shoulder:	yes
Modulus of rupture, MR	4.5	MPa	Design period [years]	20
Load safety factor, LSF	1.2			

Axel load, (kN)	Multiplied by LSF	Expected repetitions	Fatigue Analysis		Erosion Analysis	
			Allowable repetitions	Fatigue percent	Allowable repetitions	Fatigue percent
1	2	3	4	5	6	7
			8. Equivalent stress	1.39	10. Erosion factor	2.45
			9. Stress ratio factor	0.31		
Single Axles						
133	160	6310	35000	18.0	280000	2.3
125	150	14690	85000	17.3	450000	3.3
115	138	30140	250000	12.1	700000	4.3
107	129	64410	1000000	6.4	1100000	5.9
98	118	106900	Unlimited	0.0	2900000	3.7
89	107	235800	Unlimited	0.0	8000000	2.9
80	96	307200	Unlimited	0.0	40000000	0.8
			11. Equivalent stress	1.17	13. Erosion factor	2.42
			12. Stress ratio factor	0.26		
Tandem Axles						
231	278	21320	Unlimited	0.0	1000000	2.1
213	256	42870	Unlimited	0.0	1600000	2.7
195	234	124900	Unlimited	0.0	2300000	5.4
178	214	372900	Unlimited	0.0	6000000	6.2
160	192	885800	Unlimited	0.0	90000000	1.0
142	171	930700	Unlimited	0.0	Unlimited	0.0
125	150	1656000	Unlimited	0.0	Unlimited	0.0
			14. Equivalent stress	0.97	16. Erosion factor	2.43
			15. Stress ratio factor	0.22		
Tridem Axles						
240	96	250000	Unlimited	0.0	70000000	0.4
			Total	53.8	Total	40.9

Calculation of Pavement Thickness

Project	4-LANE RURAL SECTION (7)				
Trial thickness	180	mm		Doweled Joints:	yes
Subbase-subgrade k	150	MPa/m		Concrete Shoulder:	yes
Modulus of rupture, MR	4.5	MPa		Design period [years]	20
Load safety factor, LSF	1.2				

Axel load, (kN)	Multiplied by LSF	Expected repetitions	Fatigue Analysis		Erosion Analysis	
			Allowable repetitions	Fatigue percent	Allowable repetitions	Fatigue percent
1	2	3	4	5	6	7
			8. Equivalent stress	1.36	10. Erosion factor	2.44
			9. Stress ratio factor	0.30		
Single Axles						
133	160	6310	50000	12.6	290000	2.2
125	150	14690	145000	10.1	450000	3.3
115	138	30140	500000	6.0	700000	4.3
107	129	64410	Unlimited	0.0	1300000	5.0
98	118	106900	Unlimited	0.0	2500000	4.3
89	107	235800	Unlimited	0.0	15000000	1.6
80	96	307200	Unlimited	0.0	30000000	1.0
			11. Equivalent stress	1.14	13. Erosion factor	2.40
			12. Stress ratio factor	0.25		
Tandem Axles						
231	278	21320	Unlimited	0.0	1000000	2.1
213	256	42870	Unlimited	0.0	1900000	2.3
195	234	124900	Unlimited	0.0	8000000	1.6
178	214	372900	Unlimited	0.0	20000000	1.9
160	192	885800	Unlimited	0.0	Unlimited	0.0
142	171	930700	Unlimited	0.0	Unlimited	0.0
125	150	1656000	Unlimited	0.0	Unlimited	0.0
			14. Equivalent stress	0.79	16. Erosion factor	2.45
			15. Stress ratio factor	0.18		
Tridem Axles						
240	96	250000	Unlimited	0.0	40000000	0.6
			Total	28.8	Total	30.0

Calculation of Pavement Thickness

Project	4-LANE RURAL SECTION (8)			
Trial thickness	170	mm	Doweled Joints:	yes
Subbase-subgrade k	180	MPa/m	Concrete Shoulder:	yes
Modulus of rupture, MR	4.5	MPa	Design period [years]	20
Load safety factor, LSF	1.2			

Axel load, (kN)	Multiplied by LSF	Expected repetitions	Fatigue Analysis		Erosion Analysis	
			Allowable repetitions	Fatigue percent	Allowable repetitions	Fatigue percent
1	2	3	4	5	6	7
			8. Equivalent stress	1.42	10. Erosion factor	2.49
			9. Stress ratio factor	0.32		
Single Axles						
133	160	6310	21000	30.0	290000	2.2
125	150	14690	55000	26.7	450000	3.3
115	138	30140	180000	16.7	700000	4.3
107	129	64410	700000	9.2	1300000	5.0
98	118	106900	9000000	1.2	2500000	4.3
89	107	235800	Unlimited	0.0	15000000	1.6
80	96	307200	Unlimited	0.0	30000000	1.0
			11. Equivalent stress	1.29	13. Erosion factor	2.43
			12. Stress ratio factor	0.29		
Tandem Axles						
231	278	21320	1000000	2.1	800000	2.7
213	256	42870	Unlimited	0.0	1700000	2.5
195	234	124900	Unlimited	0.0	5000000	2.5
178	214	372900	Unlimited	0.0	10000000	3.7
160	192	885800	Unlimited	0.0	90000000	1.0
142	171	930700	Unlimited	0.0	Unlimited	0.0
125	150	1656000	Unlimited	0.0	Unlimited	0.0
			14. Equivalent stress	1.03	16. Erosion factor	2.43
			15. Stress ratio factor	0.23		
Tridem Axles						
240	96	250000	Unlimited	0.0	80000000	0.3
			Total	86.0	Total	34.3

Calculation of Pavement Thickness

Project	4-LANE RURAL SECTION (9)			
Trial thickness	240	mm	Doweled Joints:	yes
Subbase-subgrade k	35	MPa/m	Concrete Shoulder:	no
Modulus of rupture, MR	4.5	MPa	Design period [years]	20
Load safety factor, LSF	1.2			

Axel load, (kN)	Multiplied by LSF	Expected repetitions	Fatigue Analysis		Erosion Analysis	
			Allowable repetitions	Fatigue percent	Allowable repetitions	Fatigue percent
1	2	3	4	5	6	7
			8. Equivalent stress	1.44	10. Erosion factor	2.62
			9. Stress ratio factor	0.32		
Single Axles						
133	160	6310	22000	28.7	1100000	0.6
125	150	14690	55000	26.7	1500000	1.0
115	138	30140	200000	15.1	3000000	1.0
107	129	64410	900000	7.2	3700000	1.7
98	118	106900	Unlimited	0.0	7500000	1.4
89	107	235800	Unlimited	0.0	15000000	1.6
80	96	307200	Unlimited	0.0	30000000	1.0
			11. Equivalent stress	1.35	13. Erosion factor	2.80
			12. Stress ratio factor	0.30		
Tandem Axles						
231	278	21320	700000	3.0	500000	4.3
213	256	42870	7000000	0.6	750000	5.7
195	234	124900	Unlimited	0.0	2000000	6.2
178	214	372900	Unlimited	0.0	3500000	10.7
160	192	885800	Unlimited	0.0	15000000	5.9
142	171	930700	Unlimited	0.0	Unlimited	0.0
125	150	1656000	Unlimited	0.0	Unlimited	0.0
			14. Equivalent stress	1.02	16. Erosion factor	2.96
			15. Stress ratio factor	0.23		
Tridem Axles						
240	96	250000	Unlimited	0.0	1900000	13.2
			Total	81.3	Total	54.3

Calculation of Pavement Thickness

Project	4-LANE RURAL SECTION (10)			
Trial thickness	230	mm	Doweled Joints:	yes
Subbase-subgrade k	50	MPa/m	Concrete Shoulder:	no
Modulus of rupture, MR	4.5	MPa	Design period [years]	20
Load safety factor, LSF	1.2			

Axel load, (kN)	Multiplied by LSF	Expected repetitions	Fatigue Analysis		Erosion Analysis	
			Allowable repetitions	Fatigue percent	Allowable repetitions	Fatigue percent
1	2	3	4	5	6	7

			8. Equivalent stress	1.43	10. Erosion factor	2.65
			9. Stress ratio factor	0.32		
Single Axles						
133	160	6310	22000	28.7	1100000	0.6
125	150	14690	55000	26.7	1500000	1.0
115	138	30140	200000	15.1	2500000	1.2
107	129	64410	900000	7.2	3700000	1.7
98	118	106900	Unlimited	0.0	7000000	1.5
89	107	235800	Unlimited	0.0	14000000	1.7
80	96	307200	Unlimited	0.0	Unlimited	0.0
			11. Equivalent stress	1.28	13. Erosion factor	2.80
			12. Stress ratio factor	0.28		
Tandem Axles						
231	278	21320	10000000	0.2	850000	2.5
213	256	42870	Unlimited	0.0	1400000	3.1
195	234	124900	Unlimited	0.0	2500000	5.0
178	214	372900	Unlimited	0.0	4000000	9.3
160	192	885800	Unlimited	0.0	8500000	10.4
142	171	930700	Unlimited	0.0	20000000	4.7
125	150	1656000	Unlimited	0.0	70000000	2.4
			14. Equivalent stress	0.97	16. Erosion factor	2.94
			15. Stress ratio factor	0.22		
Tridem Axles						
240	96	250000	Unlimited	0.0	6000000	4.2
			Total	77.8	Total	49.2

Calculation of Pavement Thickness

Project	4-LANE RURAL SECTION (11)			
Trial thickness	220	mm	Doweled Joints:	yes
Subbase-subgrade k	80	MPa/m	Concrete Shoulder:	no
Modulus of rupture, MR	4.5	MPa	Design period [years]	20
Load safety factor, LSF	1.2			

Axel load, (kN)	Multiplied by LSF	Expected repetitions	Fatigue Analysis		Erosion Analysis	
			Allowable repetitions	Fatigue percent	Allowable repetitions	Fatigue percent
1	2	3	4	5	6	7
			8. Equivalent stress	1.39	10. Erosion factor	2.69
			9. Stress ratio factor	0.31		
Single Axles						
133	160	6310	36000	17.5	750000	0.8
125	150	14690	85000	17.3	1100000	1.3
115	138	30140	260000	11.6	1900000	1.6
107	129	64410	1000000	6.4	2800000	2.3
98	118	106900	Unlimited	0.0	5000000	2.1
89	107	235800	Unlimited	0.0	9500000	2.5
80	96	307200	Unlimited	0.0	20000000	1.5
			11. Equivalent stress	1.18	13. Erosion factor	2.80
			12. Stress ratio factor	0.26		
Tandem Axles						
231	278	21320	Unlimited	0.0	850000	2.5
213	256	42870	Unlimited	0.0	1400000	3.1
195	234	124900	Unlimited	0.0	2500000	5.0
178	214	372900	Unlimited	0.0	4000000	9.3
160	192	885800	Unlimited	0.0	8500000	10.4
142	171	930700	Unlimited	0.0	20000000	4.7
125	150	1656000	Unlimited	0.0	70000000	2.4
			14. Equivalent stress	0.88	16. Erosion factor	2.90
			15. Stress ratio factor	0.20		
Tridem Axles						
240	96	250000	Unlimited	0.0	9000000	2.8
			Total	52.8	Total	52.3

Calculation of Pavement Thickness

Project	4-LANE RURAL SECTION (12)			
Trial thickness	210	mm	Doweled Joints:	yes
Subbase-subgrade k	90	MPa/m	Concrete Shoulder:	no
Modulus of rupture, MR	4.5	MPa	Design period [years]	20
Load safety factor, LSF	1.2			

Axel load, (kN)	Multiplied by LSF	Expected repetitions	Fatigue Analysis		Erosion Analysis	
			Allowable repetitions	Fatigue percent	Allowable repetitions	Fatigue percent
1	2	3	4	5	6	7

8. Equivalent stress	1.46	10. Erosion factor	2.75
9. Stress ratio factor	0.32		

Single Axles

133	160	6310	22000	28.7	540000	1.2
125	150	14690	55000	26.7	790000	1.9
115	138	30140	200000	15.1	1300000	2.3
107	129	64410	900000	7.2	1900000	3.4
98	118	106900	Unlimited	0.0	3500000	3.1
89	107	235800	Unlimited	0.0	6300000	3.7
80	96	307200	Unlimited	0.0	15000000	2.0

11. Equivalent stress	1.23	13. Erosion factor	2.85
12. Stress ratio factor	0.27		

Tandem Axles

231	278	21320	Unlimited	0.0	610000	3.5
213	256	42870	Unlimited	0.0	1000000	4.3
195	234	124900	Unlimited	0.0	1700000	7.3
178	214	372900	Unlimited	0.0	3000000	12.4
160	192	885800	Unlimited	0.0	6000000	14.8
142	171	930700	Unlimited	0.0	14000000	6.6
125	150	1656000	Unlimited	0.0	39000000	4.2

14. Equivalent stress	0.91	16. Erosion factor	2.93
15. Stress ratio factor	0.20		

Tridem Axles

240	96	250000	Unlimited	0.0	3000000	8.3

Total	77.6	Total	79.1

Calculation of Pavement Thickness

Project	4-LANE RURAL SECTION (13)			
Trial thickness	210	mm	Doweled Joints:	yes
Subbase-subgrade k	110	MPa/m	Concrete Shoulder:	no
Modulus of rupture, MR	4.5	MPa	Design period [years]	20
Load safety factor, LSF	1.2			

Axel load, (kN)	Multiplied by LSF	Expected repetitions	Fatigue Analysis		Erosion Analysis	
			Allowable repetitions	Fatigue percent	Allowable repetitions	Fatigue percent
1	2	3	4	5	6	7
			8. Equivalent stress	1.41	10. Erosion factor	2.74
			9. Stress ratio factor	0.31		
Single Axles						
133	160	6310	36000	17.5	540000	1.2
125	150	14690	85000	17.3	790000	1.9
115	138	30140	260000	11.6	1300000	2.3
107	129	64410	1000000	6.4	1900000	3.4
98	118	106900	Unlimited	0.0	3500000	3.1
89	107	235800	Unlimited	0.0	6300000	3.7
80	96	307200	Unlimited	0.0	15000000	2.0
			11. Equivalent stress	1.18	13. Erosion factor	2.84
			12. Stress ratio factor	0.26		
Tandem Axles						
231	278	21320	Unlimited	0.0	610000	3.5
213	256	42870	Unlimited	0.0	1000000	4.3
195	234	124900	Unlimited	0.0	1700000	7.3
178	214	372900	Unlimited	0.0	3000000	12.4
160	192	885800	Unlimited	0.0	6000000	14.8
142	171	930700	Unlimited	0.0	14000000	6.6
125	150	1656000	Unlimited	0.0	39000000	4.2
			14. Equivalent stress	0.88	16. Erosion factor	2.90
			15. Stress ratio factor	0.20		
Tridem Axles						
240	96	250000	Unlimited	0.0	3400000	7.4
			Total	52.8	Total	78.2

Calculation of Pavement Thickness

Project 4-LANE RURAL SECTION (14)

Trial thickness	200	mm	Doweled Joints:	yes
Subbase-subgrade k	130	MPa/m	Concrete Shoulder:	no
Modulus of rupture, MR	4.5	MPa	Design period [years]	20
Load safety factor, LSF	1.2			

Axel load, (kN)	Multiplied by LSF	Expected repetitions	Fatigue Analysis		Erosion Analysis	
			Allowable repetitions	Fatigue percent	Allowable repetitions	Fatigue percent
1	2	3	4	5	6	7
			8. Equivalent stress	1.46	10. Erosion factor	2.79
			9. Stress ratio factor	0.32		
Single Axles						
133	160	6310	22000	28.7	540000	1.2
125	150	14690	55000	26.7	790000	1.9
115	138	30140	200000	15.1	1300000	2.3
107	129	64410	900000	7.2	1900000	3.4
98	118	106900	Unlimited	0.0	3500000	3.1
89	107	235800	Unlimited	0.0	6300000	3.7
80	96	307200	Unlimited	0.0	15000000	2.0
			11. Equivalent stress	1.20	13. Erosion factor	2.88
			12. Stress ratio factor	0.27		
Tandem Axles						
231	278	21320	Unlimited	0.0	610000	3.5
213	256	42870	Unlimited	0.0	1000000	4.3
195	234	124900	Unlimited	0.0	1700000	7.3
178	214	372900	Unlimited	0.0	3000000	12.4
160	192	885800	Unlimited	0.0	6000000	14.8
142	171	930700	Unlimited	0.0	14000000	6.6
125	150	1656000	Unlimited	0.0	39000000	4.2
			14. Equivalent stress	0.91	16. Erosion factor	2.92
			15. Stress ratio factor	0.20		
Tridem Axles						
240	96	250000	Unlimited	0.0	4000000	6.3
			Total	77.6	Total	77.0

Calculation of Pavement Thickness

Project	4-LANE RURAL SECTION (15)			
Trial thickness	200	mm	Doweled Joints:	yes
Subbase-subgrade k	150	MPa/m	Concrete Shoulder:	no
Modulus of rupture, MR	4.5	MPa	Design period [years]	20
Load safety factor, LSF	1.2			

Axel load, (kN)	Multiplied by LSF	Expected repetitions	Fatigue Analysis		Erosion Analysis	
			Allowable repetitions	Fatigue percent	Allowable repetitions	Fatigue percent
1	2	3	4	5	6	7
			8. Equivalent stress	1.42	10. Erosion factor	2.79
			9. Stress ratio factor	0.32		
Single Axles						
133	160	6310	22000	28.7	400000	1.6
125	150	14690	55000	26.7	520000	2.8
115	138	30140	200000	15.1	900000	3.3
107	129	64410	900000	7.2	1300000	5.0
98	118	106900	Unlimited	0.0	2600000	4.1
89	107	235800	Unlimited	0.0	4000000	5.9
80	96	307200	Unlimited	0.0	17000000	1.8
			11. Equivalent stress	1.16	13. Erosion factor	2.87
			12. Stress ratio factor	0.26		
Tandem Axles						
231	278	21320	Unlimited	0.0	610000	3.5
213	256	42870	Unlimited	0.0	1000000	4.3
195	234	124900	Unlimited	0.0	1700000	7.3
178	214	372900	Unlimited	0.0	3000000	12.4
160	192	885800	Unlimited	0.0	6000000	14.8
142	171	930700	Unlimited	0.0	14000000	6.6
125	150	1656000	Unlimited	0.0	39000000	4.2
			14. Equivalent stress	0.88	16. Erosion factor	2.90
			15. Stress ratio factor	0.20		
Tridem Axles						
240	96	250000	Unlimited	0.0	9000000	2.8
			Total	77.6	Total	80.5

Calculation of Pavement Thickness

Project	4-LANE RURAL SECTION (16)			
Trial thickness	200	mm	Doweled Joints:	yes
Subbase-subgrade k	180	MPa/m	Concrete Shoulder:	no
Modulus of rupture, MR	4.5	MPa	Design period [years]	20
Load safety factor, LSF	1.2			

Axel load, (kN)	Multiplied by LSF	Expected repetitions	Fatigue Analysis		Erosion Analysis	
			Allowable repetitions	Fatigue percent	Allowable repetitions	Fatigue percent
1	2	3	4	5	6	7

8. Equivalent stress	1.37	10. Erosion factor	2.78
9. Stress ratio factor	0.30		

Single Axles

133	160	6310	60000	10.5	580000	1.1
125	150	14690	150000	9.8	700000	2.1
115	138	30140	700000	4.3	1200000	2.5
107	129	64410	3900000	1.7	1700000	3.8
98	118	106900	Unlimited	0.0	3000000	3.6
89	107	235800	Unlimited	0.0	5300000	4.4
80	96	307200	Unlimited	0.0	11000000	2.8

11. Equivalent stress	1.11	13. Erosion factor	2.85
12. Stress ratio factor	0.25		

Tandem Axles

231	278	21320	Unlimited	0.0	650000	3.3
213	256	42870	Unlimited	0.0	1000000	4.3
195	234	124900	Unlimited	0.0	1800000	6.9
178	214	372900	Unlimited	0.0	2800000	13.3
160	192	885800	Unlimited	0.0	6000000	14.8
142	171	930700	Unlimited	0.0	14000000	6.6
125	150	1656000	Unlimited	0.0	38000000	4.4

14. Equivalent stress	0.85	16. Erosion factor	2.88
15. Stress ratio factor	0.19		

Tridem Axles

240	96	250000	Unlimited	0.0	5000000	5.0

Total	26.3	Total	78.9

A.2. AASHTO THICKNESS DESIGN PARAMETERS

In this section, the parameters presented in the next table are determined.

Table A.2.1 – Design data for the AASHTO

Parameters	Assumed value
W_{18}	8000000
R (%)	85
S_0	0.35
p_i	4.5
p_t	2
E_c (psi)	4350000
MR (psi)	650
C_d	1
J	2.5 (shoulder), 3.6 (non-shoulder)
$K - value$	Variable

- Conversion of axle data to ESAL

In this section, the axle date used in PCA method is converted to equivalent single axle load (ESAL) to compute the slab thickness using the AASHTO method.

The ESAL equation for rigid pavement is

$$\frac{W_x}{W_{18}} = \left[\frac{L_{18} + L_{2s}}{L_x + L_{2x}}\right]^{4,62} \left[\frac{10^{G/\beta_x}}{10^{G/\beta_{18}}}\right] [L_{2x}]^{3,28}$$

Where:
W = axle applications inverse of equivalency factors (where W_{18} = number of 18,000 lb (80 kN) single axle loads)
L_x = axle load being evaluated (kips)
L_{18} = 18 (standard axle load in kips)
L_2 = code for axle configuration (where 1 = single axle, 2 = tandem axle, 3 = triple axle (added in the 1986 AASHTO *Guide*), x = axle load equivalency factor being evaluated, s = code for standard axle = 1 (single axle))
G = a function of the ratio of loss in serviceability at time, t, to the potential loss taken at a point where $P_t = 1,5$

$$G = \log\left(\frac{4,5 - P_t}{4,5 - 1,5}\right)$$

P_t = "terminal" serviceability index (point at which the pavement is considered to be at the end of its useful life). The terminal serviceability is assumed to be $P_t = 2,5$, such that

$$G = \log\left(\frac{4,5 - 2,5}{4,5 - 1,5}\right) = -0,176$$

β = function which determines the relationship between serviceability and axle load applications
D = Slab Depth in inches

$$\beta = 1 + \left(\frac{3{,}63(L_x + L_{2x})^{5{,}20}}{(D+1)^{8{,}46}{L_{2x}}^{3{,}52}}\right)$$

The β_{18} and $\frac{G}{\beta_{18}}$ values for the single, tandem and Tridem axles, respectively, are presented as follows:

$$\beta_{18} = 1 + \left(\frac{3{,}63(18+1)^{5{,}20}}{(7+1)^{8{,}46}1^{3{,}52}}\right) = 1{,}371 \qquad \frac{G}{\beta_{18}} = \frac{G}{1{,}371} = -0{,}128$$

$$\beta_{18} = 1 + \left(\frac{3{,}63(18+2)^{5{,}20}}{(7+1)^{8{,}46}2^{3{,}52}}\right) = 6{,}556 \qquad \frac{G}{\beta_{18}} = \frac{G}{6{,}556} = -0{,}027$$

$$\beta_{18} = 1 + \left(\frac{3{,}63(18+3)^{5{,}20}}{(7+1)^{8{,}46}3^{3{,}52}}\right) = 30{,}838 \qquad \frac{G}{\beta_{18}} = \frac{G}{30{,}838} = -0{,}006$$

Table A.2.2. Conversion of single axle data

W_x (kN)	W_x (kips)	L_x	β_x	$\frac{G}{\beta_x}$	$\frac{W_x}{W_{18}}$	LEF	Expected Repetitions	Subtotal
133	29925	29,93	5,67	-0,03	0,132	7,59	6310	47865,72
125	28125	28,13	4,42	-0,04	0,170	5,87	14690	86195,93
115	25875	25,88	3,25	-0,05	0,239	4,18	30140	126069,33
107	24075	24,08	2,57	-0,07	0,319	3,14	64410	202154,52
98	22050	22,05	2,01	-0,09	0,450	2,22	106900	237520,48
89	20025	20,03	1,63	-0,11	0,656	1,52	235800	359299,24
80	18000	18,00	1,37	-0,13	1,000	1,00	307200	307200,00

Table A.2.3. Conversion of tandem axle data

W_x (kN)	W_x (kips)	L_x	β_x	$\frac{G}{\beta_x}$	$\frac{W_x}{W_{18}}$	LEF	Expected Repetitions	Subtotal
231	51975	51,98	971,05	0,00	0,105	9,50	21320	202628,84
213	47925	47,93	647,61	0,00	0,151	6,63	42870	284221,92
195	43875	43,88	417,47	0,00	0,223	4,49	124900	560361,63
178	40050	40,05	265,83	0,00	0,333	3,00	372900	1119583,24
160	36000	36,00	157,41	0,00	0,531	1,88	885800	1667466,97
142	31950	31,95	88,05	0,00	0,892	1,12	930700	1043018,75
125	28125	28,13	47,75	0,00	1,544	0,65	1656000	1072490,68

Table A.2.4 - . Conversion of tridem axle data

W_x (kN)	W_x (kips)	L_x	β_x	$\frac{G}{\beta_x}$	$\frac{W_x}{W_{18}}$	LEF	Expected Repetitions	Subtotal
240	54000	54,00	5368,62	- 0,00003	0,369	2,71	250000	677319,56

Total ESALs 7,99E+06

- Reliability (R)

For a four-lane rural section design, a reliability of 85% from table 3.25 is assumed.

Table A.2.5 - Suggested Levels of Reliability for Various Functional Classifications [15]

Functional classification	Recommended level of reliability	
	Urban	Rural
Interstate and other freeways	85-99.9	80-99.9
Principal arterials	80—99	75—95
Collectors	80-95	75-95
Local	50-80	50-80

- Combined standard error of the traffic prediction and the performance prediction (So)

It is recommended values around 4.0 for rigid pavements. Since the traffic data is very detailed, a value of 3.5 was assumed.

- Initial serviceability (p_i)

After the AASHO road test, it was considered 4.5 as the initial serviceability for rigid pavements.

- Terminal serviceability (p_t)

A value of 2.0 is suggested as final serviceability for rigid pavements.

- Concrete material parameters (E_c and MR)

These values were assumed by the Autor, they correspond to the values presented in table 4.2, but in psi, instead of MPa.

- Drainage Coefficients (C_d)

Assuming good drainage conditions, a value of 1.0 is determined from table 3.29.

Table A.2.5 - Recommended Values of Drainage Coefficients C_d for Rigid Pavements [15]

Quality of drainage		Percentage of time pavement structure is exposed to moisture levels approaching saturation			
Rating	Water removed within	Less than 1%	1—5%	5—25%	Greater than 25%
Excellent	2 hours	1.25—1.20	1.20—1.15	1.15—1.10	1.1
Good	1 day	1.20—1.15	1.15—1.10	1.10—1.00	1.0
Fair	1 week	1.15—1.10	1.10—1.00	1.00—0.90	0.9
Poor	1 month	1.10—1.00	1.00—0.90	0.90—0.80	0.8
Very poor	Never drain	1.00—0.90	0.90—0.80	0.80—0.70	0.7

- Load Transfer Coefficient (J)

There was determined two Load Transfer Coefficient, one for the geometry with shoulder and one without shoulder, as shown in figure 3.28.

Table A.2.5 6 - Recommended Load Transfer Coefficient for Various Pavement Types and Design Conditions [15]

Type of shoulder	Asphalt		Tied PCC	
Load transfer devices	Yes	No	Yes	No
JPCP and JRCP	3.2	3.8—4.4	2.5—3.1	3.6—4.2
CRCP	2.9—3.2	N/A	2.3—2.9	N/A

B

B.1. SIMULATION RESULTS

In this section, maximum stress value at the slab bottom for the four geometries are summarized.

Table B.1.1. Maximum stress value at the slab bottom (Without shoulder, 100 mm subbase/subgrade)

Support	k-20	k-80	k-110	k-150	k-200
Non-Stabilized Subbase	5.1	4.33	4.46	4.36	4.49
Lime Stabilized Subgrade	4.53	4.33	4.46	4.35	4.47
Cement Stabilized Subgrade	4.59	4.34	4.45	4.34	4.43
Cement Treated Subbase	4.6	4.34	4.45	4.33	4.42
Lean Concrete Subbase	4.63	4.34	4.44	4.31	4.39

Table B.1.2. Maximum stress value at the slab bottom (Without shoulder, 200 mm subbase/subgrade)

Support	k-20	k-80	k-110	k-150	k-200
Non-Stabilized Subbase	4.55	4.34	4.48	4.38	4.5
Lime Stabilized Subgrade	4.56	4.34	4.47	4.37	4.48
Cement Stabilized Subgrade	4.64	4.28	4.36	4.24	4.29
Cement Treated Subbase	4.6	4.24	4.28	4.16	4.21
Lean Concrete Subbase	4.46	4.07	4.1	3.98	4.01

Table B.1.3. Maximum stress value at the slab bottom (With shoulder, 100 mm subbase/subgrade)

Support	k-20	k-80	k-110	k-150	k-200
Non-Stabilized Subbase	5.1	5.22	5.37	5.21	5.34
Lime Stabilized Subgrade	5.06	5.18	5.32	5.17	5.29
Cement Stabilized Subgrade	4.78	4.85	4.95	4.82	4.86
Cement Treated Subbase	4.72	4.78	4.88	4.73	4.77
Lean Concrete Subbase	4.58	4.6	4.69	4.54	4.64

Table B.1.4. Maximum stress value at the slab bottom (With shoulder, 200 mm subbase/subgrade)

Support	k-20	k-80	k-110	k-150	k-200
Non-Stabilized Subbase	4.92	5.07	5.22	5.09	5.22
Lime Stabilized Subgrade	4.86	4.99	5.13	4.99	5.11
Cement Stabilized Subgrade	4.26	4.27	4.33	4.24	4.28
Cement Treated Subbase	4.15	4.26	4.26	4.12	4.15
Lean Concrete Subbase	3.96	4.04	4.07	3.98	3.81